Journal of Materials Chemistry A

Solvate Ionic Liquids: Past, Present and Future

Journal:	*Journal of Materials Chemistry A*
Manuscript ID	TA-REV-02-2025-001406.R1
Article Type:	Review Article
Date Submitted by the Author:	20-Mar-2025
Complete List of Authors:	Henderson, Luke; Deakin University, Institute for frontier materials Dharmasiri, Bhagya; Deakin University, Institute for frontier materials Harte, Timothy; Deakin University, Institute for Frontier Materials Eyckens, Daniel; CSIRO, Manufacturing Simon, Žan; Deakin University, Institute for frontier materials Hayne, David; Deakin University, School of Life and Environmental Sciences

ARTICLE

Solvate Ionic Liquids: Past, Present and Future

Timothy Harte,[a,b] Bhagya Dharmasiri,*[,a] Žan Simon,[a] David J Hayne,[a] Daniel J. Eyckens,[b] and Luke C. Henderson.*[,a]

asReceived 00th January 20xx,
Accepted 00th January 20xx

DOI: 10.1039/x0xx00000x

Solvate ionic liquids (SILs) represent an expanding subclass of ionic liquids (ILs), formed through the chelation of the cationic species, typically by an oligoether, and an array of charge diffuse anions. Since their first report, SILs have garnered significant attention for their characteristic ionic liquid physicochemical properties, including high thermal stability, negligible vapour pressure, and tailored solvation dynamics, while being simple to synthesise and cost effective. These factors position SILs as promising candidates for next-generation energy storage applications, including lithium-ion (Li-ion), lithium-sulfur (Li-S), lithium-air (Li-air), lithium-redox, all-solid-state lithium batteries (ASLBs), as well as electric double layer transistors (EDLTs), thermoelectrochemical systems, piezoelectric generators and capacitor/supercapacitor devices. This review traces the evolution of SILs, from foundational studies on their structural and dynamic properties to contemporary advancements in their synthesis and application. SILs modular design potential, through ligand, cation, and anion modifications is evaluated. The multifaceted roles of SILs across various systems are explored, including their applications in electrodeposition and metal extraction, their function as reaction media in organic synthesis, their use as pharmaceutical delivery agents, and their role as constituents and curing catalysts in polymer composites. Furthermore, critical challenges such as optimising ion transport, understanding coordination dynamics, and mitigating environmental impacts are outlined. By integrating experimental insights with computational modeling, this review provides a comprehensive framework to guide future investigations, paving the way for the sustainable development of SILs across scientific and technological domains. SILs reported in the literature predominatly consist of oligoethers G3 (triglyme) or G4 (tetraglyme) chelating a lithium salt such as LiTFSI/LiTFSA/LiNTf$_2$, lithium bis(trifluoromethanesulphonyl)imide).

Introduction

Ionic liquids (ILs) are incredibly versatile, having found uses in a wide range of fields. For example, in materials science, they serve as electrolytes in energy storage, in synthetic chemistry as reaction solvents (Figure 1), and have even been shown to increase the biological activity of certain pharmaceuticals.[1,2, 3] The diverse applications of ILs is a function of their negligible vapor pressure, potent solubilising capabilities, conductivity, and capacity to incorporate specific functionalities (modifying physical state, hydro-philicity/phobicity).[4] The ability to tailor IL properties opens opportunities to extend IL use in drug delivery systems and biomedical analytics by tuning IL interactions with biological molecules via hydrogen bonding, hydrophobic interactions, or electrostatic attractions.[1, 5-9] Despite their versatility, conventional ILs often face limitations in achieving optimal ion transport properties and compatibility with solid-state systems, which has led to increased interest in the development of alternative IL-based electrolytes such as SILs.

Typically, ILs reported in the literature consist of quaternary amines, commonly as part of a heterocyclic system (e.g. imidazole, pyridine, etc) and large, charge diffuse anions. Imidazolium is an extremely common cationic unit for ILs, though pyridinic, piperidinic, and alkyl amines are also reported (Figure 2).

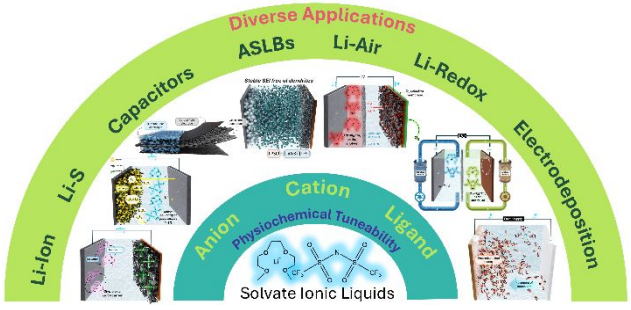

Figure 1 Optimisation possibilities leveraging the unique modular structures of SILs for diverse applications.

A key factor in the design of ILs is the concept of ion 'hardness', where the cationic and/or anionic charge is usually 'softened' via delocalisation of the charge over a large ionic volume and/or several atoms. For this reason, it is common to see ionic liquid components consist of resonance stabilised structures (e.g. imidazolium, sulphonimide, etc.) and/or ions with large radii (PF_6^-, BF_4^-, etc.).[10-12]

[a] Institute for Frontier Materials, Deakin University, Waurn Ponds, Victoria 3216, Australia
[b] Manufacturing, Commonwealth Scientific and Industrial Research Organisation, Clayton, Victoria 3168, Australia
† Footnotes relating to the title and/or authors should appear here.
Supplementary Information available: [details of any supplementary information available should be included here]. See DOI: 10.1039/x0xx00000x

Author biographies placeholder – supplied in separate document.

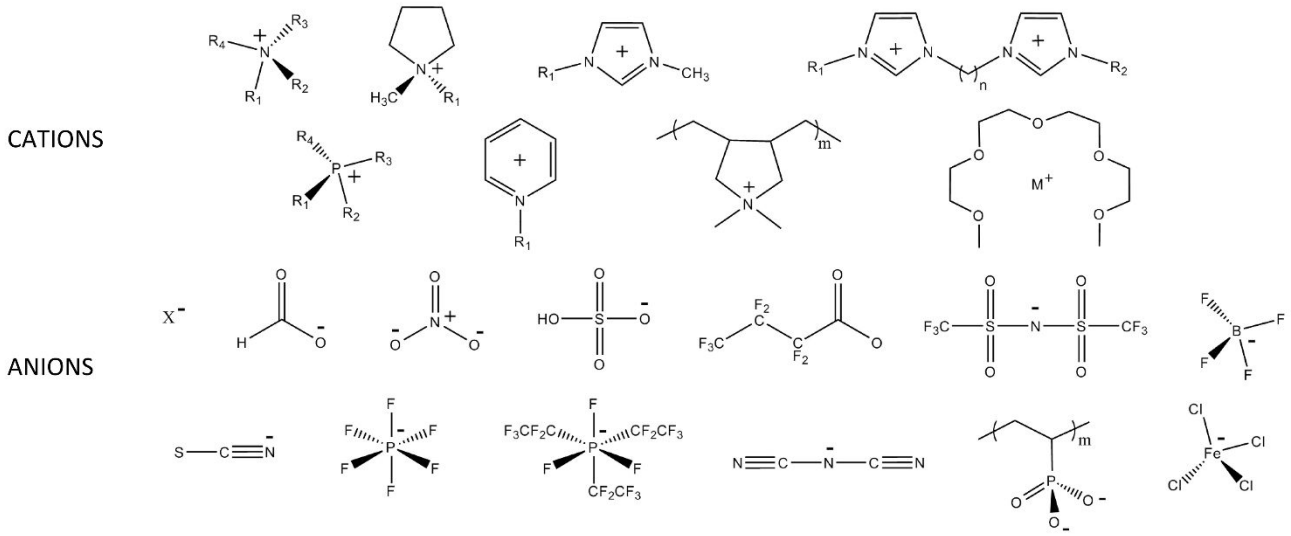

Figure 2 The chemical structures illustrate a variety of representative cations and anions commonly found in different types of ILs. The first row presents cations arranged from left to right, covering a broad spectrum, including ammonium, pyrrolidinium, 1-methyl-3-alkylimidazolium, and 1,3-bis[3-methylimidazolium-1-yl]alkane. The second row features additional cations such as phosphonium, pyridinium, poly(diallyldimethylammonium), and metal (M^+) tetraglyme complexes. The anions are displayed in the third and fourth rows, encompassing a diverse range from simple halides, formate, nitrate, and hydrogen sulphate to more complex species like heptafluorobutyrate, bis(perfluoromethylsulphonyl)imide, and tetrafluoroborate. The collection further extends to thiocyanate, hexafluorophosphate, tris(pentafluoroethyl)trifluorophosphate, dicyanamide, poly(phosphonic acid), and tetrachloroferrate, highlighting the structural diversity of anions used in IL formulations. Reprinted (adapted) with permission from Hayes, R., Warr, G.G. and Atkin, R., 2015. Structure and nanostructure in ionic liquids. Chemical reviews, 115(13), pp.6357-6426.[13]

As such, these ion pairs struggle to form ordered structures, instead sliding over each other and hence remaining as liquids at low temperatures, usually defined to be below 100 ˚C. Within this work, these ILs (e.g. imidazolium, pyridinic, etc.) will be referred to as 'traditional ILs' and reviews on their properties, synthesis, and applications have been extensively covered elsewhere.[10-12]

While ILs themselves remain a relatively new class of materials in their own right, solvate ionic liquids (SILs) are a more recently reported sub-class of ILs, defined by Tamura *et al*. in 2010.[10, 14] SILs consist of three components: a salt comprising a cation and anion, and a ligand molecule (typically an oligoether) coordinated to the cation.[10] SILs possess the same modular solvent properties as traditional ILs allowing for tuneable physicochemical characteristics by varying cations and anions, though for SILs the ligand for the cationic species provides an additional dimension for property tunability.[15-17] Utilised in various applications such as electrolytes in lithium ion batteries (LIBs),[18-21] components within bi-continuous electrolyte systems,[22, 23] reaction media,[2, 24] sizing agents for carbon fibre in structural composites,[25] and for their piezoelectric effects,[26] SILs have demonstrable versatility of application. Nevertheless, SILs remain relatively underutilised, and 'niche' compared to traditional ILs. This underutilisation stems from limited investigations into alternative ligand, cation & anion configurations, as well as a lack of comprehensive studies addressing their coordination dynamics and electrochemical stability in advanced applications.

The uniqueness of SILs becomes evident on inspection of the chelation of the hard Li^+ cation diffusing and dispersing the cationic charge over multiple atoms (row 2, far right, Figure 1). Glymes are a class of ethereal solvents, usually glycol dimethyl ethers, frequently employed for cation chelation. Conceptually, derived from the corresponding crown ethers, though not possessing the cyclic backbone. Their Lewis basicity facilitates the dissociation of salts and the cooperative solvation that occurs due to the polydentate glymes.[2, 27]

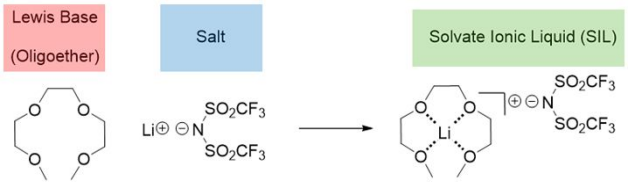

Figure 3 Schematic of SILs overall structure of ligand chelating a metal centre creating a charge diffuse cation. The TFSI anion used here is for simplicity and is the most common in the literature.

SILs (Figure 3) based on Li^+, Na^+, K^+, and Mg^{2+} exhibit good thermal stabilities (T_d 5% mass loss typically >180 °C), minimal volatility, and are non-flammable while maintaining acceptable ionic conductivity for battery and supercapacitor applications. The choice of metal ion (M^{n+}) was found to strongly influence SILs physicochemical properties and stabilities, and so is an important design consideration of SILs for specific applications.[28-35]

A significant advantage of SILs over traditional ILs is their straightforward preparation. For example, the dissolution of a readily available lithium salt, such as LiTFSI (Lithium bis(trifluoromethanesulphonyl)imide), in a stoichiometric quantity of glyme produces a SIL.

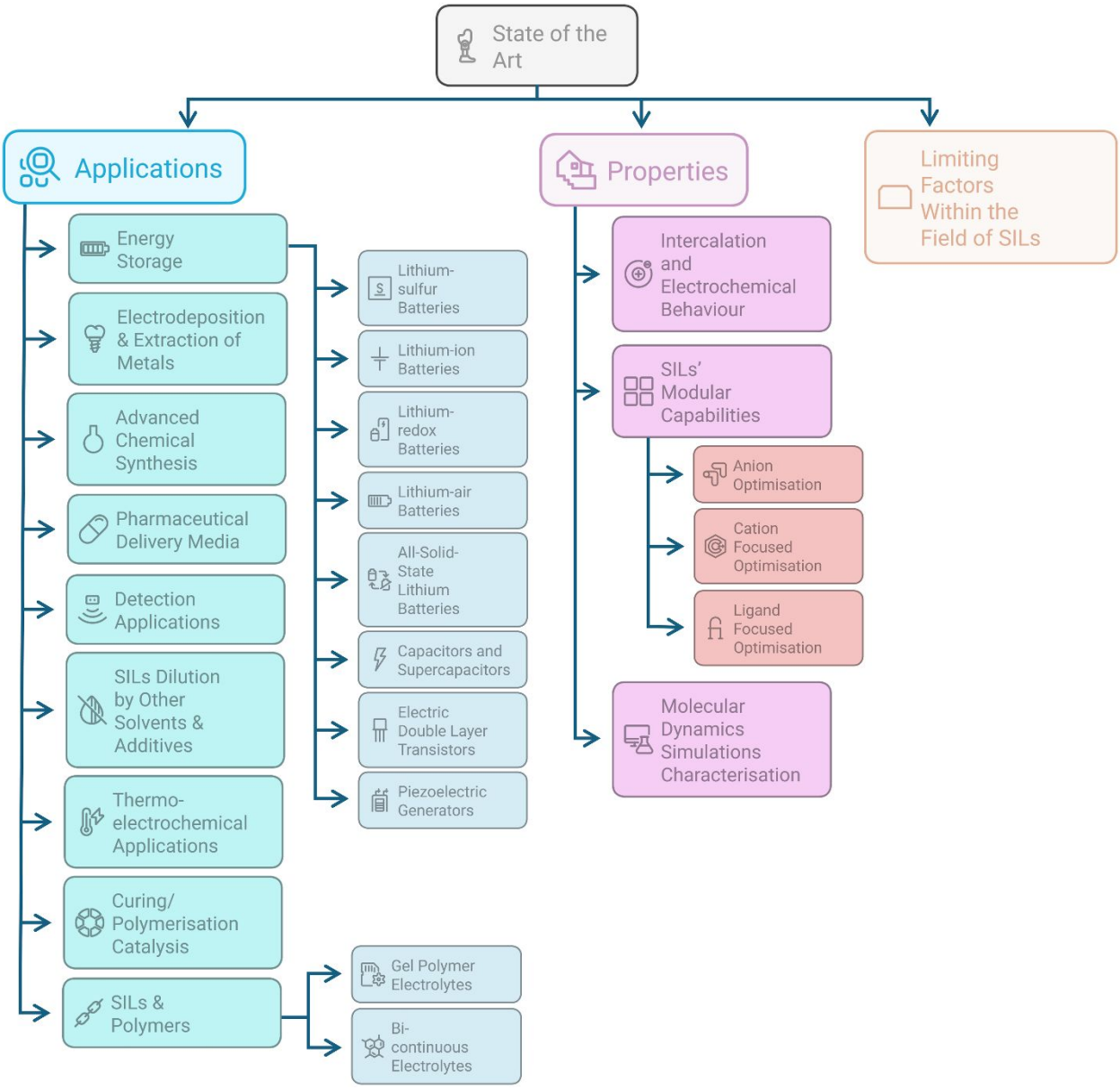

Figure 4 The structure of this review. The graphical representation listed left to right, top to bottom reflects the order of the headings and subheadings presented in the review.

In contrast, synthesising quaternary ammonium ILs entails the use of alkylating agents, subsequent product purification, and potential anion metathesis, each step incurring notable costs and introducing opportunities for contamination.[2, 36]

Additionally, traditional ILs' hygroscopic properties can promote the degradation of the ionic liquid by hydrolysis of the quaternary ammonium, often anecdotally observed as a yellow hue in the IL. While SILs exhibit some degree of hygroscopicity, any absorbed water interfering with the chelation of the lithium ion by the glymes is a reversible phenomenon and simply heating *in vacuo* (under vacuum) to remove any adventitious moisture regenerates the pristine SIL. Alternatively, storing SILs on activated molecular sieves, akin to common practice with organic solvents, extends their lifespan before requiring SIL regeneration.[2, 36]

Review scope, timeline and goals.

This review aims to provide an overview of the current state and potential of SILs since their first reporting in 2010 (Figure 5). SILs were first included in a general review article about ILs in 2012, '*Ionic Liquids: Past, present and future*' by Angell *et al*.[10] and have since been the focus of four reviews, '*Criteria for solvate ionic liquids*' by Mandai *et al*.[12] in 2014, '*From Ionic Liquids to Solvate Ionic Liquids: Challenges and Opportunities for Next Generation Battery Electrolytes*' by Watanabe *et al*.[37] in 2018, '*A Review of Solvate Ionic Liquids: Physical Parameters and Synthetic Applications*' by Eyckens *et al*.[38] in 2019, and '*Solvate Ionic Liquids for Li, Na, K, and Mg Batteries*' by Mandai *et al*.[11]

in 2019. In this report, we hope to update developments since the most recent review and identify areas that are critical to the development of these unique materials in the future. Specifically, this review aims to identify gaps in the current literature, such as challenges in achieving optimised ion transport, the need for broader structural diversification of SIL ligands, and their applicability in next-generation electrochemical systems.

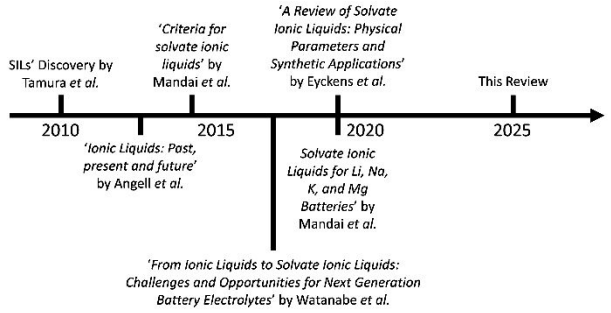

Figure 5 A timeline of reviews focused on SILs.

Herein (Figure 4), we will present the reports of SILs grouped by application (e.g. energy storage, reaction media, etc.), including SILs incorporated into polymer composites to produce new multifunctional materials. The goal is to highlight the unique properties of SILs that provide significant benefits over traditional solvent systems, e.g. the ability of SILs to suppress sulphur migration in Li-S batteries. While every effort has been made to include all relevant work, some omissions may have been inadvertently made, and for this, the authors apologise.

State of the art

Initially reported in the literature in 2010,[14, 39] the focus of early studies primarily centred on elucidating the fundamental properties and structural characteristics of SILs. These studies aimed to comprehensively understand the unique solvent-solute interactions and the influence of different solvating agents on the properties of the resulting SILs. This was required to determine if the SILs were indeed 'true' ILs or if they were just concentration solutions with exacerbated colligative properties.[40] The outcomes of these studies was that, indeed, the SILs were not just concentrated solutions but were a coordinated ion of lithium with the associated anion, and thus did justifying classification as an IL. A significant shift occurred from around 2014 onwards, marking a turning point in SIL research. During this period, there was a substantial increase in the number of publications highlighting the utilisation of SILs in diverse applications, ranging from materials science to biomedicine. This shift underscores the growing recognition of SILs as versatile and promising candidates for various practical applications. By 2014, articles focusing on SIL applications formed approximately 50% of the total SIL publications, indicating a significant expansion beyond the initial characterisation efforts. This trend continued to gain momentum, with most articles published by 2025 exploring the multifaceted applications of SILs. These applications span a wide spectrum, including catalysis,[41, 42] reaction media,[2, 24, 43, 44] electrochemistry,[22, 23, 45] and pharmaceuticals.[46] Such a pronounced shift in focus reflects the increasing confidence in the potential of SILs to address complex challenges across different disciplines. This underscores the growing importance of applied research in harnessing the unique properties of SILs for practical use.[10-12, 37, 38]

A major driving force for ionic liquid research, including SILs, is optimising electrolytes and enhancing their performance in electrochemical systems as this is crucial for increasing the availability of cost-competitive renewable electricity in the pursuit of challenging conventional energy production and consumption methods.[47] Such optimisation will enhance battery storage capacity,[22, 48] safety, longevity and stability of LIBs. IL-based electrolytes can significantly enhance both the safety and energy density of lithium metal batteries, addressing critical limitations of conventional liquid electrolytes.[49] Compared to traditional ILs, SILs as electrolytes in these systems have demonstrated potential to offer superior thermal and electrochemical stability, flame retardant properties, and tuneable solvation characteristics. These aspects ultimately address the concerns related to safety and stability in LIBs while offering potential electrochemical device life-span improvements.[50]

SILs can be considered modular systems as optimisation strategies commonly involve changing the constituent ions in pursuit of more desirable physicochemical properties.[15-17] Unlike traditional ILs, the requirement of a ligand for metal chelation in these systems offers another dimension for optimisation and exploration of structure-activity relationships unavailable to traditional ILs.[51]

The literature for SILs since their first report and characterisation in 2010 is shown in Figure 6a. Articles published annually on SILs peaked at 33 in 2024, with these later manuscripts largely examining ligand modification (Figure 6b). However, it should be noted that most of these ligand optimisation papers solely focused on superficial variations to molecular structure or stoichiometric changes using G3 (triglyme) and G4 (tetraglyme) ligands. Little-to-no examination of other ligands or modified G3/G4 ligands are typically undertaken. Therefore, there remains ample opportunity for investigating other simple ethereal scaffolds which may imbue the system with other functionality.

Applications

SILs have found versatile applications across diverse fields, showcasing their intrinsic value in addressing challenges and enhancing performance in various systems. In the realm of energy storage, SILs have been utilised as precursors for gel polymer electrolytes in lithium-ion batteries (LIBs), improving safety and cycle stability.[52] SILs have been explored in flexible electrolytes for sodium-ion batteries, exhibiting exceptional properties.[53, 54]

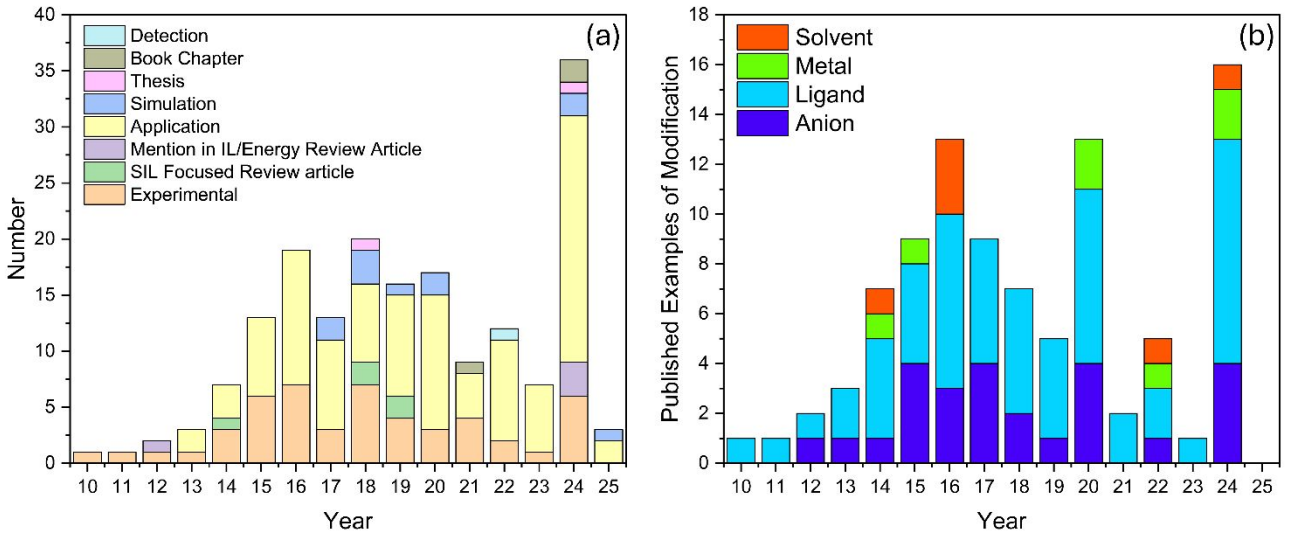

Figure 6 (a) Plot showing the literature base of SILs from 2010 to 2025 and its breakdown into articles focused on: the detection of SILs using analytical techniques, non-peer reviewed thesis's & book chapters, simulation, experimental characterisation, SIL focused reviews, mentions in general IL or energy focused reviews and applications involving SILs. (b) A plot showing the frequency of published SIL optimisation by type (anion, ligand, metal centre or solvent dilution) since the first report of SILs in 201

The incorporation of SILs into epoxy-based vitrimers showcased improved stress-relaxation properties, enabling applications in flexible hybrid electronics.[55] Flexible zinc–air battery systems have applied ILs to achieve ampere-hour capacities and wide-temperature adaptability, reinforcing the viability of IL-based electrolytes in next-generation energy storage devices.[56] In lithium-rich disordered rocksalt cathodes SILs demonstrated enhanced capacity retention by avoiding electrolyte decomposition.[57] The application of SILs in solid-state batteries resulted in outstanding electrochemical properties.[58] Beyond energy storage, SILs have been employed in diverse fields, such as polymer synthesis,[59, 60] corrosion-resistant coatings,[61], and flexible magnesium-ion conducting gel polymer electrolytes.[62] These studies collectively underscore the adaptability and value of SILs across a spectrum of applications, ranging from advanced batteries to materials science, highlighting their potential to address multifaceted challenges in different industries.[2, 18-20, 22, 24, 37, 38, 41, 46, 52, 53, 55, 57-125]

Energy Storage

A large body of SIL literature examines their use in energy storage systems (batteries, supercapacitors, etc.) due to their high ionic conductivity and ease of preparation. A large portion of these works focus on Lithium-sulphur batteries, and as such, they will be covered first, and then non-sulphur systems will be discussed.

Lithium-sulphur (Li-S) batteries

Lithium-sulphur (Li-S) batteries (Figure 7) are an emerging class of rechargeable batteries that use sulphur as the cathode and lithium metal as the anode. A summary of SILs application within Li-S systems is provided in Table 1. Battery discharge involves the forming and dissolution of lithium ions from the anode which then form alkali metal polysulphide salts with sulphur from the cathode. This process reverses during charging, with deposition of lithium and sulphur at the anode and cathode, respectively. Li-S batteries have attracted attention due to their high theoretical energy density, potentially enabling longer-lasting and lighter energy storage systems compared to LIBs, but they face challenges related to sulphur's insulating nature, volumetric expansion, and the dissolution of polysulphide intermediates impacting overall performance and cycle life.[20, 63, 75, 77, 82, 108, 122]

Li–S batteries operate through the conversion of elemental sulphur into lithium polysulphides (Li_2S_8 to Li_2S) during discharge, and the reverse process during charge. The dissolution and diffusion of intermediate polysulphides in traditional organic electrolytes contribute to the well-known 'shuttle effect,' leading to self-discharge and capacity fade.

The dissolution of polysulphide salts, Li_2S_m ($2 \leq m \leq 8$), by conventional organic solvents leads to a redox shuttle, where the shuttle accepts electrons from the anode before diffusing and donating electrons directly to the cathode increasing self-discharge.[63, 126] Additionally, dissolved Li_2S_m can diffuse and react directly with the Li metal anode supressing coulombic efficiencies, cycle stability, and rate capabilities. The inclusion of SILs as electrolytes in Li-S batteries has shown a lower solubility for lithium polysulphide salts, and with minimal compromise to ionic conductivity.[63, 122] Further suppression of Li_2S_m solubility in Li-S batteries has been achieved with polyfluorinated additives, such as the non-flammable 1,1,2,2–tetrafluoroethyl 2,2,3,3–tetrafluoropropyl ether (HFE) and 1,1,2,2-tetrafluoroethyl 2,2,2-trifluoroethyl ether (TFTFE). These co-solvents provide additional benefits, such as improved diffusion coefficients, via decreasing SIL viscosity, without disrupting the Li-glyme solvate structure. This coincides with increasing discharge capacity and rate capability along with high cycling reversibility and cycle stability.[77] Attempts to improve cathode compatibility with SILs have led to investigations into different binders (e.g. poly(ethylene oxide), PEO, and poly(vinyl

alcohol), PVA). The compatibility of polymer binders with SILs varies significantly, with PEO exhibiting high compatibility but promoting lithium polysulphide dissolution, while PVA's compatibility improves with reduced saponification, enabling partial swelling and enhanced electrolyte uptake, whereas fully saponified PVA (PVA-100) and PVAc (poly(vinyl acetate)) exhibit limited or no compatibility.

Electrochemical reactions within Li-S cells using [Li(G4)][TFSI] SIL as an electrolyte showed that the SIL was only compatible (i.e., formed a single phase) with polyvinyl acetate (PVA) binders that possessed hydrolysed side chains (20% or more). While the exact reason is not explicitly stated, it is likely due to hydrogen bonding effects and polarity changes induced by partial PVA hydrolysis.[20] Other SIL approaches to reduce solubilised lithium-polysulphide salts have focused on the solid electrode interface (SEI). The SEI layer forms on the electrode surface of lithium-ion batteries during the initial charging and discharging cycles. It acts as a protective film, facilitating ion transport while preventing further electrolyte decomposition and side reactions.[120]

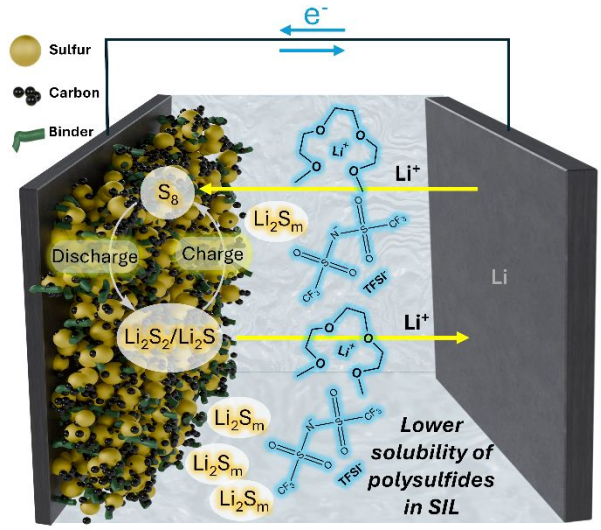

Figure 7 A Li-S battery, with a cathode comprised of sulphur, carbon black and binder and anode comprised of lithium metal. The suppression of polysulphide salt dissolution using [Li(G4)][TFSI] SILs as electrolytes is depicted.

The dissolution of lithium polysulphides was addressed using [Li(G4)][TFSI] and various carbon supports, with an emphasis on the role of carbon pore structure. This approach utilised a similar PVA support, as above, and successfully employed the SIL to replace $LiNO_3$ as a sacrificial additive, improving SEI formation.[82] The [Li(G4)][TFSI] SIL facilitates stable SEI formation on the lithium metal anode, reducing lithium dendrite growth and improving Coulombic efficiency. Unlike conventional electrolytes, SILs can enhance the formation of a more uniform, inorganic-rich SEI, preventing side reactions and prolonging battery life.[82] Lithium nitrate ($LiNO_3$) was used as a sacrificial additive in lithium metal batteries to promote the formation of a stable, inorganic-rich SEI, improving lithium deposition morphology, enhancing Coulombic efficiency, and extending cycle life by gradually being consumed during the charge cycling process.[127] Neat and HFE-diluted [Li(G4)][TFSI] SILs in Li-S batteries have also been investigated, focusing on addressing challenges associated with lithium anodes, such as the formation of dendrites that can lead to short circuits, the generation of 'dead' lithium that reduces capacity, and the safety hazards posed by lithium's reactivity in liquid electrolytes. These issues have hindered the commercial viability of lithium metal anodes in Li-S systems, emphasising the need for innovative electrolyte formulations and electrode designs to enhance stability and performance.[75] To this end, the chemical stability of oxysulphide $(70Li_2S\cdot(30\text{-}x)P_2S_5\cdot xP_2O_5$, x = 0, 2, 5, 10) solid-state electrolytes (SSEs) in $[Li(G3)_x][TFSI]$ SILs (x = 1, 2, 3, 4) has been investigated. Increasing oxygen content in the oxysulphide SSEs improved their stability in SILs, highlighting the potential of oxysulphide SSE + SIL systems for future semi-solid state battery designs.[128] The electrochemical reactions in polysulphide-insoluble lithium-sulphur batteries using SILs (Li-glyme, of unspecified anion and glyme size) compared to sulpholane-based super-concentrated electrolyte solutions (SL-based SCES) has been investigated and compared.

Table 1 A summary of the key 'focus areas' investigated for SILs applied as electrolytes within Li-S battery systems and the influence of SILs on these factors.

Focus Area	SILs Influence
SEI Formation[63]	SILs contribute to stable SEI layers, reducing lithium dendrite growth and improving Coulombic efficiency.
Solvation Effects[75]	SILs enhance lithium-ion transport by forming stable solvation structures, mitigating polysulfide dissolution.
Interfacial Stabilisation[77]	SILs prevent direct contact between discharge intermediates and lithium metal anode, reducing self-discharge.
Porosity Influence[82]	SIL-electrolytes interact with carbon supports to optimise pore volume and pore size, improving sulphur utilisation.
Polymer Binder Compatibility[20]	SILs affect the adhesion and electrochemical stability of polymer binders, impacting cycling performance.
Electrolyte Interphase[108]	SILs modify the SEI by stabilising lithium deposition and minimising side reactions.
Artificial SEI[120]	Incorporation of perfluorinated ionomers in SILs enhances SEI uniformity, improving lithium compatibility.
Discharge Behaviour[122]	SILs control discharge kinetics, affecting sulphur reduction pathways and lithium polysulfide precipitation.
Oxysulfide Stability[128]	SILs enhance the compatibility of oxysulfide solid electrolytes, reducing degradation under cycling.
Electrochemical Impedance[129]	SILs influence impedance characteristics, facilitating polysulfide-inhibited charge transfer dynamics.
Li Polysulfide Structure[130]	SILs modify polysulfide solubility and ionic conductivity, affecting redox shuttle effects.
Al-LLZO Solid Electrolyte[131]	SILs work synergistically with solid electrolytes to prevent sulphur dissolution and enhance cycle life.

While both electrolytes exhibited distinct discharge behaviours, the SL-based SCES demonstrated better battery performance, with multi-step reactions occurring during the discharge process (though minimal information about the SIL performance was provided).[129] A SIL comprised of 1.0 M LiTFSI in 1,3-dioxolane (DOL)/dimethoxyethane (DME) 1:1 volume mixture was investigated for its performance as a solid-state electrolyte (SSE) in Bi_2Se_3-doped $Li_8P_2S_9$ in lithium-sulphur battery systems. The SIL significantly enhanced electrode-electrolyte contact, reducing internal resistance, and

contributed to improved electrochemical stability and capacity retention.[132] The structure and physicochemical properties of solutions of lithium disulphide, tetrasulphide, and octasulphide in a lithium perchlorate solvated by sulpholane (pseudo SILs) have been explored for their potential as electrolytes for lithium-sulphur batteries. Higher concentrations and longer-chain polysulphides increased clustering and decreased ionic conductivity and diffusion coefficients, significantly influencing electrolyte performance.[130] Similarly, [Li(G4)][TFSI] and [Li(SL, sulpholane)$_2$][TFSI] were shown to lower solubility of discharge intermediates and improve battery performance. Additionally, this system showed suppression of sulphur cathode self-discharge, especially when combined with an Al-LLZO ($Li_{6.25}Al_{0.25}La_3Zr_2O_{13}$) solid electrolyte separator.[131]

Molten solvates with longer ligands, such as [Li(G2)$_{1.3}$][TFSI] and [Li(G3)$_1$][TFSI], are effective in suppressing the redox shuttle mechanism in Li-S cells, further enhancing cycle stability and Coulombic efficiency. These studies collectively underscore the substantial impact of SILs on the performance and stability of Li-S batteries, by modulating electrolyte interactions with composite cathodes and support solvents, the intricate interplay between SILs and SEI dynamics deliver enhanced Li-S battery performance.[108] Additionally, *in situ* EIS studies have shed light on the crucial role of SILs in the formation of the SEI and the discharge reaction dynamics in Li-S batteries, on copper and lithium metallic anodes.[108, 122]

SIL-based electrolytes have been explored as a promising solution to mitigate polysulphide dissolution while maintaining high ionic conductivity. By coordinating lithium ions within an ether-solvated structure, SILs suppress polysulphide solubility and shuttle effects, enhancing cycling stability. By addressing polysulphide solubility, improving lithium deposition, and reducing electrolyte volatility, SILs represent a unique electrolyte class with distinct advantages for next-generation Li–S batteries.

Lithium-ion (Li-ion) batteries

Lithium-ion (Li-ion) batteries using sulphur-free electrodes are widely used for numerous electronic devices and electric vehicles making them a cornerstone for modern life. Several studies have explored the use of SILs as electrolytes in Li-ion batteries, showcasing their potential to enhance stability and performance. A summary of SILs application within Li-ion systems is provided in Table 2.

Investigations into the impact of SILs in Li–$LiCoO_2$ cells have highlighted the role of chelation in enhancing the stability of the cationic lithium complex, improving cycle stability, and increasing Coulombic efficiency. However, their low ionic conductivity and high viscosity can be addressed by adding non polar solvents to improve performance.[67] Investigations into optimising the composition ratio of [Li(G3)$_n$][TFSI] has revealed that deviations from 1:1 stoichiometry affect electrochemical stability and cycle life. In one report, three concentrations of G3:LiTFSI were examined: a 1:1 mixture, a 25% molar excess of glyme, and a 25% molar excess of lithium salt. Super-stoichiometric lithium salt concentrations were associated with reduced interfacial resistance degradation, resulting in longer cycle life and improved discharge capacities. However, internal resistance increased with cycling, indicating a need for further optimisation based on battery design and operating conditions. Conversely, excess glyme concentrations were found to promote oxidative instability at high voltages, which can accelerate interfacial degradation and capacity loss.[81]

Table 2 A summary of the influence of SILs on key factors within Li-ion systems.

SILs' Influence	Details
Electrochemical Stability[133]	Branched glyme-based SILs enhance oxidative stability up to 5V vs Li^+/Li, allowing stable high-voltage cycling.
Ionic Conductivity[133]	Branched glymes maintain ionic conductivity between 10^{-1} to 10 mS/cm at 25°C, essential for ion transport in Li-metal batteries.
Interfacial Stabilisation[133]	Fluorinated SILs form stable electrolyte/electrode interfaces, reducing degradation and improving long-term cycling stability.
SEI Formation[110]	Redox-active SILs contribute to uniform and reversible SEI formation, preventing dendrite growth and capacity fading in semi-liquid lithium batteries.
Solvation Effects[110]	Tetrahalogenoferrate anions influence solvation structures, modifying Li+ coordination and enhancing charge transfer kinetics.
Charge Storage[110]	Redox-active anions ($[FeX]^-$) store charge, enabling dual-function electrolytes that facilitate both Li^+ transport and redox reactions.
Interfacial Structure[92]	SILs maintain Li+ coordination at electrified interfaces, preventing solvent decomposition and ensuring stable charge transfer.
Electrochemical Reduction[92]	Li^+ solvation distortion in SILs enhances electrochemical reduction kinetics at negative electrodes, aiding Li deposition in lithium-metal batteries.
Battery Cycle Life[133]	Li/NMC622 cells with SILs demonstrate stable cycling with high Coulombic efficiency (~100%) over extended cycles.
Catholyte Stability[110]	SILs in redox-active systems maintain liquid-phase stability at room temperature, increasing catholyte lifespan in semi-liquid batteries.
Dendrite Suppression[133]	Branched glyme-based SILs contribute to homogeneous Li plating, reducing dendritic growth and improving safety in Li-metal batteries.
High-Voltage Stability[110]	[Li(G3)][$FeCl_4$] SIL exhibits the lowest melting point (28°C), enabling stable operation at high voltages in semi-liquid lithium batteries.

The nanostructure behaviour of [Li(G3)][TFSI] in Li-ion batteries has been explored through molecular dynamics simulations, suggesting potential enhancements in battery performance through the manipulation of SIL nanostructures. At negative electrodes, the lithium-glyme coordination sphere shifts from in-plane to out-of-plane as charge density increases, indicating that SIL behaviour at cathode surfaces may deviate from typical ionic-liquid properties. This structural distortion of the lithium-glyme complex could also weaken the interaction between Li^+

and G3, potentially influencing the reduction of Li^+ during charging processes.[92] SILs comprised of LiTFSI with four branched glymes, TEP (1,2,3-Trimethoxypropane), ME-TOD (Methoxyethoxytrimethoxysilane), F-ME-F (Fluorinated Methoxy-Ethyl-Fluoromethane), and F-ME-ME (Fluorinated Methoxy-Ethyl-Methoxy), were also investigated, showing high ionic conductivity, excellent stability at elevated voltages (up to 4.5V vs. Li^+/Li), and long cycling performance in lithium-metal batteries. Notably, F-ME-ME showed superior oxidation stability and interfacial compatibility.[133]

A series of glyme-based SILs have been investigated as catholytes for semi-liquid lithium secondary batteries (Figure 8). Of primary importance are effects of their molecular structures on thermal and electrochemical properties. The SILs, particularly [Li(G3)][$FeCl_4$] (Figure 8), proved beneficial due to their high Li-ion conductivity, low melting point, and ability to support redox reactions, resulting in improved battery capacity, those SILs exhibit desirable properties, such as scalability. Further discussion on flow battery applications will be covered in the next section.[110]

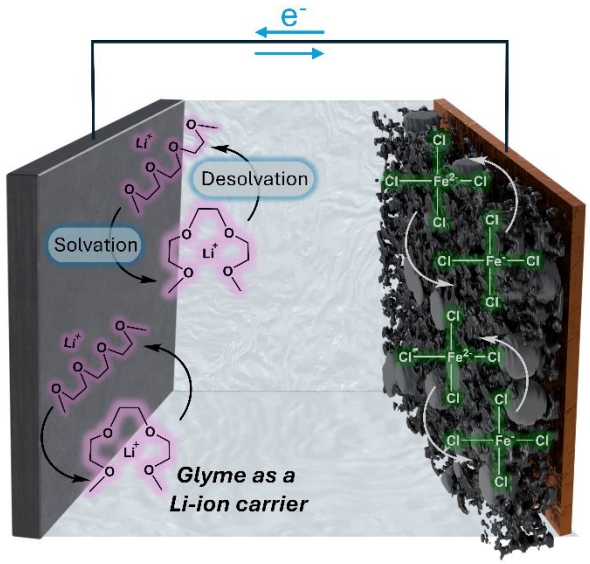

Figure 8 [Li(G3)][TFSI] SILs with tetrahalogenoferrate(III) complex anions as electrolytes in Li-ion batteries. A lithium metal anode is depicted on the left and a porous carbon cathode is shown on the right.

Lithium (Li) redox batteries

The use of SILs in lithium (Li) redox batteries, an alternative battery configuration often referred to as a lithium 'flow battery' or lithium 'redox flow battery', has also been investigated. Here, the battery is rechargeable and employs a redox reaction of lithium ions between two liquid electrolytes contained in separate tanks. Unlike traditional lithium-ion batteries where the electrodes store and release lithium ions, in a lithium redox battery, the electroactive species are dissolved in the liquid electrolytes, referred to as a catholyte and anolyte.[134-136] A summary of SILs application within Li-redox systems is provided in Table 3.

During the battery's operation, lithium ions shuttle between the two electrolyte solutions, and the redox reactions at the electrodes generate electrical energy. One advantage of lithium redox batteries is their potential for scalability and flexibility, making them suitable for large-scale energy storage applications. Flow batteries, in general, are known for their ability to decouple power and energy, allowing for better customisation to meet specific needs. Lithium redox batteries are an area of active research with a focus on improving their energy density, efficiency, and overall performance for various applications, including grid energy storage and renewable energy integration.[134-136]

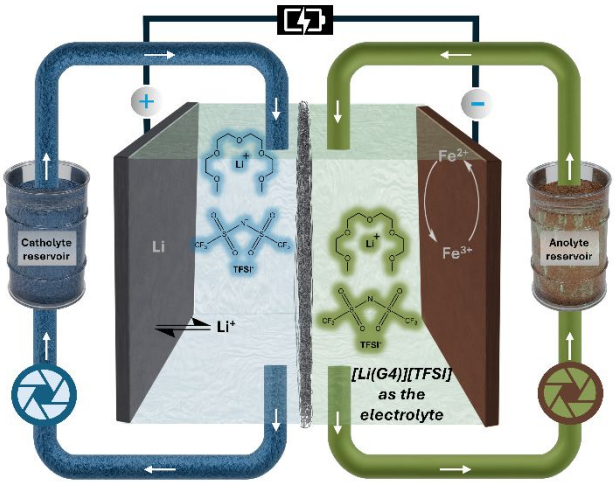

Figure 9 Schematic of a Li-redox battery utilising [Li(G4)][TFSI] SILs as an electrolyte. The cathode consists of the redox reaction of an iron complex and the anode redox reaction consists of lithium dissolution and deposition.

Table 3 A summary of the influence of SILs on key factors within Li-redox battery systems.

Key Mechanism	Influence of SILs
SEI Formation[68, 83]	SILs contribute to the formation of stable and uniform SEI layers, reducing side reactions and enhancing cycle life. The presence of solvate structures impacts ion transport across the interface.
Solvation Effects[68, 83]	SILs enable a unique solvation structure that minimises free solvent molecules, thereby improving electrochemical stability. The interactions between Li^+ and solvate ionic species enhance ionic conductivity.
Interfacial Stabilisation[68, 83]	SILs facilitate improved interfacial compatibility between electrodes and electrolytes, mitigating dendrite growth and ensuring stable electrochemical performance in lithium redox systems.

The development of a lithium-redox battery utilising the redox reaction of an iron complex for the cathode (Figure 9), lithium dissolution and deposition for the anode, and [Li(G4)][TFSI] SIL as the electrolyte has been investigated. The tris(2,2'-bipyridine)iron(II) complex ($[Fe(bpy)_2]^{2+}$) demonstrated solubility and stability in the SIL, and its redox reaction is reversible. The resulting redox battery exhibited over 95% Coulombic efficiency and reversible charge-discharge cycling for 30 cycles, with an average cell voltage of 3.9 V.[83] Further investigations have been conducted into supercooled liquid SIL comprised of 4-methoxy-2,2,6,6-tetramethylpiperidine 1-oxyl

(MT) was applied as a redox compound with LiTFSI as a supporting salt, due to the TFSI anion's plasticising effect at molar ratios of 1:1 MT:LiTFSI up to 20:1. Ratios in the 1:1 to 20:1 range yielded orange-coloured liquids at RT. They were examined for their melting mechanisms, structural characteristics, and ion-conducting properties of MT:LiTFSI catholytes, which demonstrated excellent electrochemical stability, high energy density, and scalability suitable for flow battery applications.[68] While SILS showed encouraging results in this application, their use has not been explored extensively and remains an area of potential application.

Lithium-air (Li-Air) batteries

Another rechargeable form of battery is in a lithium-air (Li-Air) or lithium-oxygen configuration. In this instance, atmospheric oxygen acts as the cathode material, providing a significant advantage to the air and moisture sensitivity of traditional LIBs. During discharge, lithium ions react with oxygen, forming lithium oxide and releasing electrical energy. Li-Air batteries have garnered interest for their high theoretical energy density, offering the potential for extended range in electric vehicles, but they face challenges related to stability, efficiency, and the management of reaction byproducts. One of the major limitations of Li-Air batteries is the instability caused by parasitic reactions and the accumulation of byproducts. These degrade the electrode and electrolyte over time; the use of SILs has emerged as a promising solution to mitigate these issues by enhancing the reversibility of the oxygen reduction–oxygen evolution reaction (ORR–OER) and reducing the formation of undesired side products. In Li–O_2 batteries, the ORR during discharge leads to the formation of lithium peroxide (Li_2O_2) at the cathode, while the OER during charging decomposes Li_2O_2 back into lithium ions and oxygen gas, completing the cycle.[64, 84, 103] A summary of SILs application within Li-Air systems is provided in Table 4.

The utilisation of SILs as electrolytes in lithium-air (Li-air) batteries has been investigated for their impact on the reversible oxygen reduction–oxygen evolution reaction (ORR–OER). Using $[Li(G3)_1][TFSI]$ SIL as a non-volatile electrolyte has been shown to support reversible ORR–OER reactions in a rechargeable Li–O_2 battery, with the reversibility influenced by the reduction limit of ORR. This highlights the importance of discharge depth in battery performance, discharge depth being the extent to which the negative potential is extended during the discharge process, which significantly impacts the reversibility of the oxygen reduction-oxygen evolution reaction (ORR-OER) in lithium-air batteries by influencing the formation of side products and the retention of discharge capacity.[64] A comparison of [Li(G3)][TFSI] SIL with conventional organic solvent electrolytes for Li–O_2 batteries revealed improved stability, distinct charging curve shapes, and O_2 evolution behaviour, highlighting the benefits of the SIL due to its oxidative stability. The voltage profiles observed during the charging process of Li–O_2 batteries using $[Li(G3)_1][TFSI]$ SIL differed compared to that of a conventional organic solvent electrolyte $[Li(G3)_4][TFSI]$. The SIL exhibited a gradual voltage increase throughout the charge, in contrast to the conventional electrolyte, which showed an initial high overpotential followed by a plateau near 4.2 V. This difference is attributed to the distinct morphology of the lithium peroxide (Li_2O_2) discharge products, which are influenced by the solubility of the superoxide intermediate. In the SIL, the reduced solubility of the intermediate leads to a surface-based growth mechanism, forming a film-like morphology, whereas the conventional system facilitates a solution-based mechanism, resulting in a needle-like structure. The O_2 evolution in this system remained below the ideal value, with the Li_2O_2 discharge product exhibiting a film-like morphology, unlike the needle-like structures typical of traditional systems. This difference, attributed to the SIL electrolyte ($[Li(G3)_1][TFSI]$), stems from its low intermediate solubility and surface-based growth mechanism. While the film-like morphology enhances reversibility and reduces side reactions, the suboptimal O_2 evolution indicates persistent inefficiencies.[84] SILs provide a highly stable electrochemical environment that mitigates undesired side reactions, such as the formation of lithium carbonate (Li_2CO_3), by limiting the solubility of reactive oxygen species. The low volatility and strong coordination ability of SILs reduce the nucleation of large Li_2O_2 particles, instead promoting a film-like morphology that improves reversibility.[84] The effectiveness of specific SILs, such as [Li(G4)][FSI] (Figure 10), in suppressing lithium dendrite formation and achieving stable performance in aqueous lithium–oxygen cells has been demonstrated, and attributed to SILs high salt concentration, lithium-ion transference number, and compatibility with aqueous systems, further highlighting the promise of SILs for advanced energy storage applications.[70]

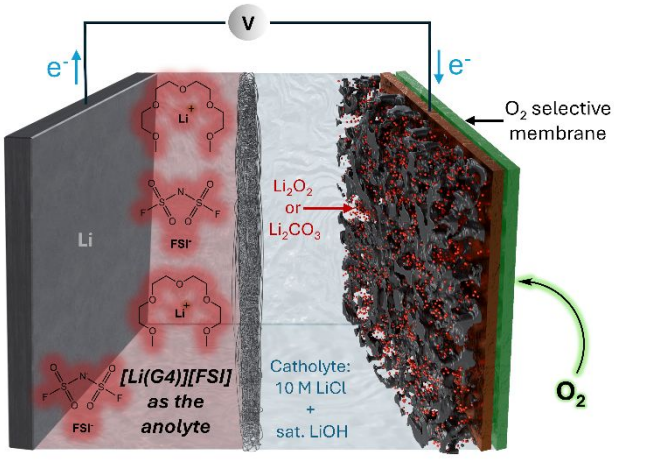

Figure 10 A Li-Air battery depicting [Li(G4)][FSI] SIL used as an anolyte. A lithium metal anode is used in this battery, the porous separator is depicted in the middle of the diagram, and a porous carbon cathode with a O_2 selective membrane backing is used as the cathode.

A 4.0 M $LiNO_3$/DMSO *pseudo*-SIL, as the lithium cation is not sequestered by an oligoether but by DMSO, was explored for lithium-oxygen batteries, demonstrating a low charging voltage and preventing side products on a cathode surface.[103] These findings suggest the potential applicability of SILs with redox mediators to enhance Li-air cell performance. This may be different for a more 'conventional' SIL as was investigated in other works,[64, 84, 103] that highlighted the pivotal role of SILs in improving the performance and reversibility of lithium-air (Li-

air) batteries. Unlike conventional organic electrolytes, which facilitate side reactions leading to electrode passivation and capacity fade, SILs enhance the reversibility of Li–O_2 batteries by reducing superoxide radical mobility and stabilising intermediate species. This leads to lower overpotentials during charging and discharging, improving energy efficiency and cycle life.

Table 4 A summary of the influence of SILs on key factors within Li-air battery systems.

Key Mechanism	Influence of SILs
Electrolyte Stability & Volatility[64, 70, 84]	SILs exhibit high oxidative stability and negligible volatility, which enhances the long-term stability of Li-air cells compared to conventional electrolytes.
SEI Formation[70, 103]	SILs help form a more stable SEI layer, reducing undesired lithium dendrite growth and improving lithium-metal anode protection.
Solvation Effects & Ionic Transport[64, 84]	SILs control solvation structure, limiting free solvent molecules, thus reducing solvent decomposition and improving lithium-ion transport efficiency.
Interfacial Stabilisation & Redox Mediation[103]	SILs incorporating lithium nitrate act as redox mediators, facilitating Li_2O_2 decomposition at lower overpotentials and improving interfacial stability.
Charge/Discharge Efficiency & Cycle Life[64, 84, 103]	SILs reduce charging overvoltages, leading to better cycle stability and increased round-trip efficiency in Li-air batteries.
Reduction of Side Reactions & Decomposition[64, 84, 103]	SILs limit the solubility of reactive intermediates (e.g., LiO_2), reducing the formation of insulating by-products like Li2CO3 and improving reversibility.

All-Solid-State Lithium Batteries (ASLBs)

All-solid-state lithium batteries (ASLBs) are an advanced type of lithium-ion battery that replaces traditional liquid electrolytes with solid-state electrolytes, typically ceramic materials. This design enhances safety, reduces the risk of dendrite formation, and allows for higher energy density and potential improvements in battery performance.[137] A summary of SILs application within ASLBs is provided in Table 5.

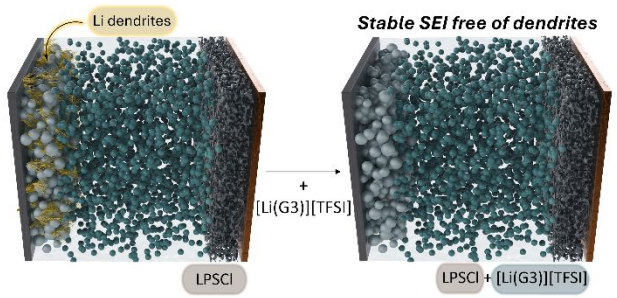

Figure 11 An All-solid-state Lithium-ion Battery (ASLB) comprised of 2D structured argyrodite Li_6PS_5Cl (LPSCl) solid electrolyte, porous carbon as the cathode material and Li metal as the anode. On the right a stable solid electrolyte interphase (SEI) occurs, suppressing Li dendrite formation, when [Li(G3)][TFSI] is used in conjunction with the LPSCl solid electrolyte.

The pivotal role of SILs in enhancing the performance of ASLBs is underscored by multiple studies (Figure 11).[69, 104, 123, 125] One study demonstrated the excellent stability of sulphide solid electrolytes when combined with [Li(G3)][TFSI], showcasing their utility in high-performance ASLBs and highlighting capacity increase achieved through the introduction of [Li(G3)][TFSI].[125] Another study extended this work to address challenges in the wet-slurry process for sulphide solid electrolytes, achieving significantly improved electrochemical performance in ASLB electrodes with the use of [Li(G3)][TFSI]-based polymeric binders.[104]

Table 5 A summary of the influence of SILs on key factors within ASLB systems.

Role of SILs	Key Mechanisms
Enhancing Ionic Contacts[69]	Improved interface compatibility with sulphide solid electrolytes, reducing interfacial resistance.
Boosting Interface Kinetics[104]	Enhances Li4Ti5O12 anode performance by promoting interfacial Li^+ transport.
SEI Formation[123]	Facilitates robust SEI development for lithium metal stability.
Conductive Polymeric Binders[125]	Improves slurry-fabricable binders, enabling practical high-conductivity polymer electrodes.
Functionalised Dry Electrodes[138]	Enhances electrochemical stability and rate performance of dry electrode structures.
Separator-Free Ionogel Electrolytes[139]	Improves interfacial compatibility and mechanical integrity via in situ polymerisation.
Electrode/Ceramic Electrolyte Interface Optimisation[140]	Enhances Li^+ solvation, stabilises interfaces, and improves Li^+ transport kinetics in NASICON-based solid electrolytes.

The [Li(G3)][TFSI] SIL enhanced the electrochemical performance by improving the compatibility and ionic conductivity at the interfaces, forming a compact, stable microstructure within composite electrodes and electrolyte interfaces, which facilitated efficient Li-ion transfer and suppressed detrimental reactions.[104] Lastly, the inclusion of [Li(G3)][TFSI] in all-solid-state lithium metal batteries facilitated the development of a durable SEI layer and effectively restrained lithium dendrite growth, thereby advancing the development of high-energy ASLBs.[123] [Li(G4)][TFSI] SIL has been investigated in functionalised dry electrodes (FDEs) for ASLBs. The incorporation of SIL-infiltrated ethyl cellulose as a ASLB binder significantly enhanced lithium-ion conductivity, resulting in improved electrochemical performance, including high reversible capacity and stable cycling, even at high areal capacities.[138] An in situ polymerised separator-free ionogel electrolyte has been developed for ASLBs, using the [Li(G4)][TFSI] SIL as the electrolyte base. The in situ preparation significantly improved interfacial compatibility and mechanical strength, leading to enhanced cycle stability (94.32% capacity retention at 0.5C after 300 cycles) and rate performance compared to conventional ex situ methods.[139] [Li(G3)][TFSI] SIL has been investigated to optimise the interface between ceramic electrolytes and electrodes in ASLBs. SIL served as a high-concentration lithium carrier, facilitating enhanced lithium-ion transport and providing a stable interfacial modification layer in the PEO-based polymer electrolyte. The incorporation of SIL into a high-

concentration PEO-based polymer layer significantly improved ionic conductivity (up to 0.94 mS cm^{-1} at room temperature), thermal stability, and electrochemical performance, leading to robust cycling stability and wide-temperature operability for NASICON-based lithium metal batteries.[140]

The incorporation of SILs as electrolytes in ASLBs emerges as a crucial advancement, offering enhanced stability, safety, and performance over traditional liquid electrolytes. The studies on SILs within ASLBs,[69, 104, 123, 125] collectively demonstrate the transformative impact of SILs on sulphide solid electrolytes, electrode fabrication, and interface mediation, showcasing their potential to accelerate the development of high-energy ASLBs with improved electrochemical performance and cycling stability. The addition of [Li(G3)][TFSI] not only showcases its compatibility with various solid electrolytes but also highlights its role in creating additional ionic pathways, addressing challenges in electrode fabrication, and advancing the industrialisation of ASLBs.[69, 104, 123, 125, 141]

Capacitors and Supercapacitors

A capacitor is an electronic device that stores and releases electrical energy at fast rates, typically used to manage voltage and power flow in circuits. Supercapacitors enhance this functionality by offering much higher capacitance values, enabling them to store significant amounts of energy and discharge it rapidly. Both types of capacitors rely on electrolytes to facilitate ion movement between their electrodes, crucial for their function. A recent branch of energy storage is that in 'structural' capacitors, the electrolyte not only plays a key role in energy storage but also contributes to the mechanical properties of the material, allowing for lightweight and efficient energy storage solutions in diverse applications. The choice and design of the electrolyte are therefore vital for optimising performance, enhancing energy density, and improving overall efficiency.[22, 45, 142-145] A summary of SILs application within capacitors is provided in Table 6.

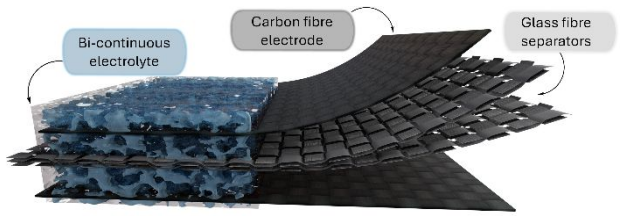

Figure 12 A diagram of a carbon fibre structural supercapacitor that utilises a bicontinuous electrolyte comprised of epoxy resin (30% wt.) and [Li(G3)][TFSI] SIL (70% wt.).

Solid polymer electrolytes (SPEs) containing [Li(G3)][TFSI] SILs (Figure 12), [22, 23, 45] and [Li(G4)][TFSI] SILs,[23] have been applied in carbon fibre structural supercapacitors in numerous published works.[22, 23, 45] [Li(G3)][TFSI] was used as an electrolyte to achieve a 45-fold improvement in specific capacitance due to carbon fibre surface modification compared to control devices, resulting in a specific capacitance of 1439 mFg^{-1} at 0.5 mAg^{-1}. The high amount (70%) of SIL within the epoxy resin created conductive channels, allowing the device to be flexible without compromising performance. This electrolyte was later applied as an electrolyte in MXene-coated carbon fibre capacitors.[45] [Li(G4)][TFSI] when applied within carbon fibre capacitor devices was found to exhibit a 22% higher specific capacitance than when the [Li(G3)][TFSI] SIL was used in prototype capacitors.[23]

The interfacial behaviour and charge storage mechanisms has been investigated within graphene-based nonaqueous electrochemical capacitors at the graphene/SIL [Li(G4)][FSI (bis(fluorosulfonyl)imide)] interface using a gap-enhanced Raman spectroscopy strategy. The charge storage mechanism depends on the number of graphene layers, with single-layer graphene predominantly using co-ion desorption and few-layer graphene employing ion exchange, leading to an increase in area-specific capacitance from 64 to 145 μF cm^{-2}.[146]

Table 6 A summary of the influence of SILs on key factors within capacitor systems.

Key Mechanism	Influence of SILs
SEI Formation[146]	SILs influence SEI composition by promoting anion-derived SEI layers, leading to enhanced stability and reduced impedance.
Solvation Effects[146]	SILs alter the coordination structure of Li^+ with glymes, affecting ion transport and charge separation.
Interfacial Stabilisation[146]	SILs enhance interfacial stability by reducing side reactions and stabilising the electrical double layer.
Electrode Compatibility[146]	Graphene-based electrodes interact with SILs differently based on layer thickness; thicker graphene layers benefit from improved charge transfer efficiency.
Capacitance Enhancement[146]	SILs influence the capacitance by modifying ion packing at the electrode/electrolyte interface.
Electrochemical Stability[146]	SILs increase electrochemical stability by suppressing electrolyte decomposition and extending operational voltage windows.
Cycling Stability[23]	Bicontinuous SIL-based electrolytes exhibit high capacitance retention over 5000 cycles, improving supercapacitor lifespan.
Charging Mechanism Influence[146]	Single-layer graphene favours co-ion desorption, while few-layer graphene follows an ion-exchange mechanism due to SIL interactions.

Despite significant advancements in applying SIL containing SPEs in carbon fibre structural supercapacitors, there remain gaps in fully understanding the long-term stability, mechanical-electrical integration, and scalability of these electrolytes, particularly in the optimisation of electrolyte composition for maximising both energy storage and structural functionality. The SILs tend to act as catalysts for epoxy curing reactions due to their Lewis acidity, which can activate the oxirane rings in epoxy monomers. This catalytic effect significantly accelerates the curing process but may narrow the polymer processing window and increase void formation, potentially impacting the mechanical properties of the resulting polymer matrix.[23, 41] Further research is needed to explore new electrolyte designs that balance mechanical performance and flexibility with enhanced electrochemical performance and to address

challenges related to their commercial viability in diverse applications.

Electric Double Layer Transistors (EDLTs)

Electric double layer transistors (EDLTs) (Figure 13) are field-effect transistors where the electrical double layer formed at the interface of a semiconductor and an electrolyte serves as the gate dielectric. The gate voltage controls the carrier concentration in the semiconductor channel, leading to the modulation of electrical conductivity. EDLTs offer tuneable electronic properties, enabling applications in flexible and transparent electronics and facilitating studies of novel electronic phases in materials.[147, 148] High-density Li^+ cations play a crucial role in enhancing the performance of EDLTs by significantly increasing charge carrier density at the interface.[147] The application of [Li(G4)][TFSI] as a gate dielectric in $SrTiO_3$-based EDLTs was investigated through EIS measurements that found the electric double layer capacitance of the SIL increased significantly with more negative polarisation of the working electrode, surpassing that of conventional ILs. Using the SIL as the gate dielectric in $SrTiO_3$-based EDLTs resulted in improved transfer characteristics, notably with larger drain currents. The consistent findings between EIS measurements and electronic transport in the semiconductor channel of EDLTs suggest the SIL's potential for effective carrier accumulation on the electrode surfaces. The approach of involving high-density Li^+ cations in the electric double layer through desolvation, particularly with glyme molecules, presents a promising strategy for iontronics research, offering opportunities to explore novel functionalities in semiconductor materials and devices.[113]

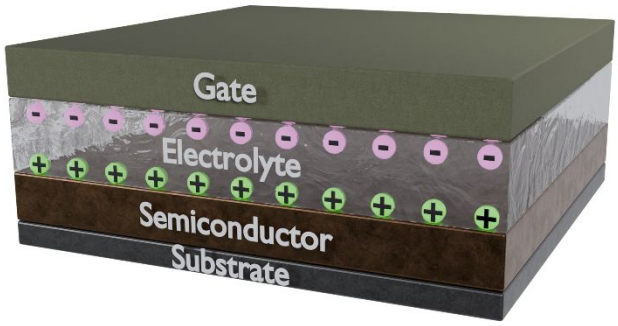

Figure 13 A schematic diagram showing the structure of an electric double layer transistors (EDLT).

SILs have been explored in only a single published study regarding their application in EDLTs, highlighting a significant opportunity for further research in this area.

Piezoelectric Generators

Piezoelectric generators are a promising avenue in energy harvesting, relying on materials that generate an electric charge in response to applied mechanical stress. This phenomenon, pivotal for developing multifunctional energy systems, has recently been extended to ionic liquids,[149, 150] including SILs. A 2024 study explored the piezoelectric behaviour of [Li(G3)][TFSI] SIL, at 1:1.5 glyme:LiTFSI super stoichiometric ratios of Li, in both its pure form and as part of a bicontinuous solid polymer electrolyte (SPE) composite (70% SIL:30% epoxy resin, by weight) (Figure 14).

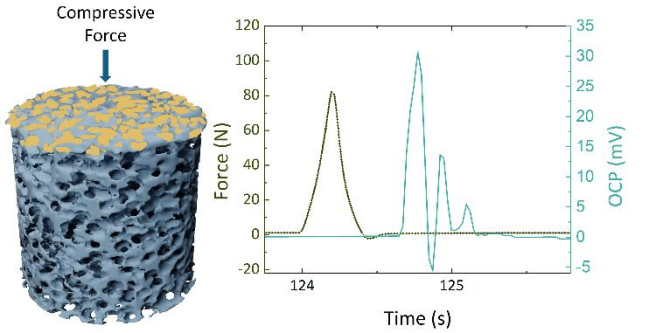

Figure 14 A schematic illustrating the confinement of [Li(G3)][TFSI] SIL within the porous, bicontinuous epoxy resin framework at a 1:1.5 glyme:LiTFSI stoichiometric ratio, undergoing compression during piezoelectric testing. The plot on the right illustrates the relationship between the applied force on the bicontinuous epoxy resin framework and the open-circuit potential (OCP) current generated by the piezoelectric SIL under compression.

Results indicated that mechanical pressure induced a liquid-to-crystalline phase transition in the SIL, generating a bulk potential difference of up to 150 mV in its pure state and around 30 mV within the SPE due to reduced SIL content at the interface. These findings not only validate the potential of SILs as piezoelectric materials but also suggest innovative applications in structural energy systems where materials simultaneously bear mechanical loads and harvest energy, such as in aerospace or renewable energy sectors.[26]

Electrodeposition & Extraction of Metals

Electrodeposition, an electrochemical process wherein metal ions in a solution are reduced and deposited onto a conductive substrate, forming a solid metal layer. A summary of SILs use in electrodeposition & extraction applications is provided in Table 7. During electrodeposition, an electric current is applied, causing the reduction of metal ions at the cathode, leading to the formation of a metallic coating or layer on the electrode surface. This technique is widely employed for various applications, including electroplating, battery manufacturing, and the fabrication of electronic components.[151]

Metals such as lithium, aluminium, magnesium, silver, neodymium, and tantalum have been electrodeposited using various SILs and solvent-containing SILs. These processes encompass low-temperature electrochemical deposition, alloy formation, and unique coatings. Investigations emphasise the advantageous characteristics of these SILs, including tunability, cost-effectiveness, and substantial dissolution capacity, making them applicable in a diverse range of contexts, from lithium-ion battery electrolytes to environmentally friendly silver-plating baths and the creation of corrosion-resistant coatings.[61, 73, 93, 94, 101, 107, 109, 111, 116, 117, 152, 153]

The electrodeposition properties of lithium-containing SILs, $[Li(L)_n][X]$, have been investigated, where ligands L included G1 and G2 with varying n (1, 2, or 3), and anions X including $TFSI^-$, Br^-, or I^-. Halides as anions resulted in significantly lower Coulombic efficiency during reduction–oxidation cycles compared to SILs containing $TFSI^-$, which was attributed to poor SEI formation or extensive dendrite growth. High current densities were achieved without stirring; however, cyclic voltammetry revealed incomplete reversibility due to electrolyte decomposition and SEI formation, as confirmed by electrochemical quartz microbalance and Auger electron

spectroscopy. Copper was selected as the working electrode material due to its superior efficiencies, and lithium deposits from $[Li(G1)_2][TFSI]$ on copper electrodes exhibited a rough but well-covered surface, as observed through SEM microscopy.[152]

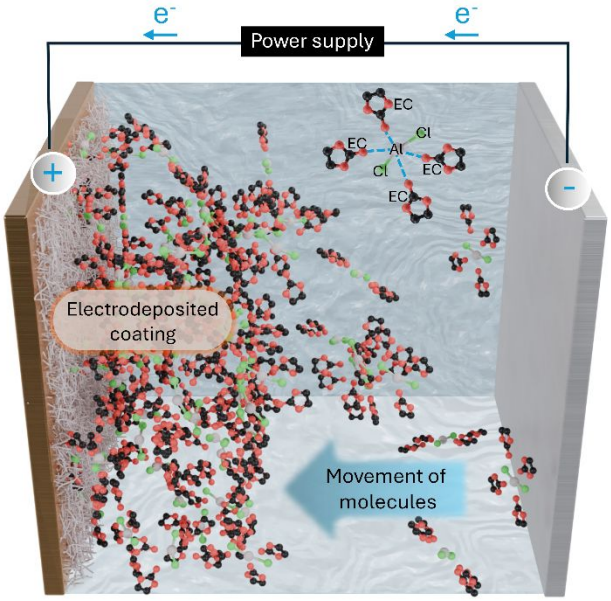

Figure 15 The electrodeposition of aluminium metal from a solution of [Al(ethylene carbonate)][Cl_2] SIL.

The deposition and dissolution of lithium on a nickel (Ni) electrode coated with a lithium phosphorus oxynitride (LiPON) thin film in [Li(G3)][TFSI] SIL have been investigated. The LiPON thin film effectively prevented the decomposition of the [Li(G3)][TFSI] SIL over a wide potential range (0–6 V vs. Li/Li(I)). Lithium deposition and dissolution were observed through the LiPON thin film, and coating the Ni electrode with LiPON improved the Coulombic efficiency for these processes, indicating that the LiPON thin film acts as an artificial SEI film. Those findings suggest that artificial SEI films could be valuable for understanding the properties of SEI films formed in different electrolytes.[73]

Investigations into the low-temperature electrochemical extraction of lithium from its oxides, a process historically challenging in traditional ILs, have utilised [Al(EC, ethylene carbonate)][Cl_2] SIL (Figure 15). Li_2O was used as a precursor for lithium, successfully dissolving in an electrochemically stable aluminium-containing SIL. Potentiostatic deposition at a relatively low temperature (80 °C) led to the formation of both lithium and nanoscale Al–Li intermetallic structures on an aluminium surface. The dissolution mechanism involving $[AlCl_2(EC)_4]^+ + Li_2O \rightleftharpoons [(Li_2O)_xAlCl_2(EC)_{4-x}]^+$ was identified, emphasising the significance of strong Lewis acid species in acidifying oxides. Aluminium-containing SILs are considered more practical for applications in SIL electrodeposition or low-temperature electrometallurgy, particularly for active metal extraction, due to their higher tunability, cost-effectiveness, substantial dissolution capacity, and other advantages over traditional ILs.[94]

A novel aluminium-containing SIL, composed of a 2:1 (mol/mol) mixture of ethylene carbonate (EC) and $AlCl_3$, has been extensively investigated for its potential in low-temperature electrochemical deposition of aluminium and alloys. This system forms various coordination compounds, including $[AlCl_4]^-$, $[AlCl_3(EC)_2]$, and a novel $[AlCl_2(EC)_4]^+$ complex, which arises from the asymmetric cleavage of a halide-bridged dimer and the strong interactions between aluminium and carbonyl oxygen atoms. Classified as an SIL, it exhibits IL-like properties such as low vapor pressure and high ionic conductivity, attributed to the solvate octahedral geometry of the aluminium-containing cations. Successful potentiostatic electrodeposition of aluminium has been achieved using this SIL, revealing electroactive species and outlining an electrochemical mechanism. Moreover, this SIL has proven effective for ambient condition electrodeposition of lithium and the formation of an Al-Li alloy through co-deposition. Expanding its applications, a similar EC/$AlCl_3$ mixture was utilised for the electrochemical co-deposition of an Al-Nd alloy near room temperature, facilitating the dissolution of $NdCl_3$. The dissolution mechanism is represented as $3[AlCl_2(EC)_n]^+ + 2NdCl_3 \leftrightarrows 2Nd(III) + 3[AlCl_4]^- + 3nEC$, leading to the successful deposition of a thermally stable Al_2Nd alloy. Cyclic voltammetry indicated that Nd deposition occurs through a direct one-step process, while aluminium deposition originates from the Al-containing cations $[AlCl_2(EC)_n]^+$, underscoring the versatility and potential of this SIL for diverse electrochemical applications. [93, 101]

The physicochemical properties of three novel SILs, $[Mg(G1)_3][TFSI]_2$, $[Mg(G2)_2][TFSI]_2$ and $[Mg(G3)_2][TFSI]_2$, were investigated for applications in the reversible electrodeposition and stripping of magnesium using mixtures of SILs and tetra-n-butylammonium chloride. Mixing $[Mg(G1)_3][TFSI]_2$ and $[Mg(G3)_2][TFSI]_2$ with tetrabutylammonium chloride produced highly concentrated non-volatile electrolytes, facilitating the electrodeposition and stripping of magnesium metal at elevated current densities (>1.0 A dm^{-2}). While chloride anions had no significant impact on the magnesium deposition process, they played a crucial role in the stripping process by reducing stripping overpotential and enhancing reversibility.[107]

The electrochemical reduction mechanism of Ta(V) in an ethylene carbonate and aluminium chloride (EC–$AlCl_3$) SIL was investigated using cyclic voltammetry (CV), X-ray photoelectron spectroscopy, scanning electron microscopy, and energy-dispersive spectroscopy. In the EC–$AlCl_3$ (molar ratio 1:0.2) system, the CV displayed two reduction peaks at 0.53 and −0.75 V (vs Al), indicating the underpotential deposition of aluminium and the subsequent deposition of bulk aluminium. Meanwhile, the EC–$AlCl_3$–$TaCl_5$ (molar ratio 1:0.2:0.003) SIL exhibited three reduction peaks at −0.55, −0.72, and −1.12 V (vs Al), corresponding to the reduction stages of Ta(V) to Ta(IV), Ta(IV) to Ta(III), and Ta(III) to tantalum metal, respectively. The reduction of Ta(III) to tantalum metal was identified as an irreversible diffusion-controlled reaction, with the diffusion coefficient showing a temperature-dependent increase. Electrodeposition experiments further confirmed the composition of tantalum and tantalum oxides in the deposits obtained under specific conditions.[109] Investigations into silver SIL baths comprised of G2, G3, G4, or G5 with AgTFSI focused

on replacing conventional cyanide-containing baths for silver electrodeposition. The [Ag(G5)][TFSI] demonstrated liquid-state characteristics at room temperature, with distinct redox waves observed in cyclic voltammogram experiments, indicating its potential as an electroactive species for silver plating. Galvanostatic electrodeposition at 0.08 mA cm^{-2} resulted in dense and smooth silver deposits from [Ag(G5)][TFSI], in contrast to the coarse and faceted deposits obtained from a diluted AgTFSI-G5 solution. The study highlighted the importance of both high silver ion concentration and specific solvent properties in achieving highly smooth silver deposits, providing valuable insights for designing efficient and environmentally friendly silver plating baths.[111]

The use of an aluminium-containing SIL, DMI (1,3-dimethyl-2-imidazolidinone)–$AlCl_3$ (1 M)–$MgCl_2$ (0.5 M), as an electrolyte for magnesium electrodeposition was investigated through Raman spectroscopy, ^{27}Al nuclear magnetic resonance, X-ray dispersive energy spectrometry (EDS), and X-ray diffraction (XRD) analysis. At 298 K (24.85 °C), the combination of DMI and $AlCl_3$ produced a well-dispersed solution, as confirmed by Raman spectrometry and ^{27}Al NMR, that detected $[AlCl_4]^-$ anions and $[AlCl_2(DMI)_4]^+$ cations, thus meeting the criteria defining SILs. The addition of $MgCl_2$ (with an $AlCl_3/MgCl_2$ molar ratio of 2) as a precursor for Mg led to oxidation-reduction reactions studied through cyclic voltammetry at 323 K. The deposition mechanisms for aluminium and magnesium were observed, resulting in dense deposits without dendrites, predominantly composed of aluminium, as confirmed by XRD and EDS analyses.[116]

The development of a cost-effective SIL containing neodymium (Nd III), 1,3-dimethyl-2-imidazolidinone (DMI), and OTf^- (trifluoromethanesulphonate) was also investigated for the purpose of electrodeposition. A feasible approach was presented for obtaining metallic neodymium (Nd) at low temperatures, utilising $Nd(OTf)_3$ as an inexpensive and highly soluble precursor. The addition of $Nd(OTf)_3$ to DMI resulted in the formation of a Nd-containing cationic SIL, $[Nd(DMI)_4]^{3+}[(OTf)_3]^{3-}$. Electrochemical investigations revealed that Nd(0) could not be electrodeposited from this liquid until $LiNO_3$ was added, which facilitated a single-step reduction of Nd(III) to Nd(0). Nd(0) could not be electrodeposited from the liquid until $LiNO_3$ was added because the nitrate ions in $LiNO_3$ disrupted the strong coordination complex between Nd(III) and DMI, reducing the solvation number and enabling the generation of electroactive Nd species, which facilitated their discharge. The study demonstrated the feasibility of Nd potentiostatic electrodeposition on aluminium substrates, confirming the cost-effective electrodeposition of Nd and providing a practical method for the low-temperature electrochemical extraction of easily coordinated elements from soluble precursors.[117] A digital holographic microscope was used to investigate the Li^+ concentration profile during the electrodeposition and electrochemical dissolution of Li metal in [Li(G4)][TFSI]. At the cathodic side, a decreasing Li^+ concentration and viscosity, along with transient Raman spectra, suggested the desolvation of G4 from the solvation structure due to Li electrodeposition. Li_2O-rich SEI formation was observed at the electrodeposited Li surface. On the anodic side, an increasing Li^+ concentration and viscosity impeded natural convection effects during Li dissolution. Raman spectroscopy revealed the formation of contact ion pairs (CIPs) and aggregates near the anode, consistent with the increased electrolyte viscosity. A sharp decrease in free G4 molecules was noted, which could potentially influence the anode potential during Li dissolution.[153] The formation of a solid-electrolyte interphase (SEI) during lithium (Li) deposition/stripping in [Li(G3)][TFSI], [Li(G4)][TFSI], [Li(G3)][FSI] and [Li(G4)][FSI] SILs has been investigated. LiFSI-based SILs formed thinner, effective SEIs that suppressed electrolyte decomposition and enabled stable, reversible Li cycling, whereas LiTFSI-based SILs exhibited thicker SEIs and continuous electrolyte decomposition.[154] The electrochemical properties and electrodeposition behaviour of SILs comprised of DMI (1,3-dimethyl-2-imidazolidone) with samarium Sm(III) triflate and Sm(III) nitrate hexahydrate. Sm(III) coordinates with the carbonyl group of DMI, with distinct reduction potentials for Sm(III)/Sm(II) and Sm(II)/Sm(0), and electrodeposition on a copper substrate produced compact deposits from triflate-DMI and granular deposits from nitrate-DMI solutions.[155] The effect of electrolyte concentration on lithium morphology during deposition-dissolution reactions has been investigated in [Li(G4)][TFSI] SILs at varying electrolyte concentrations ranging from 2.52 to 3.89 mol/L (LiFSI/G4 ratio = 0.7, 0.85, 1.0, 1.15, and 1.3). The morphology and thickness of lithium deposits were strongly influenced by the solute-solvent molar ratio, with an equimolar ratio (MLiFSI/G4 = 1.0) yielding the most efficient and compact deposition behaviour, making it optimal for anode-free batteries.[156]

The electrodeposition of a Zn–Ta coating from a DMI (1,3-Dimethyl-2-imidazolidinone)–$ZnCl_2$–$TaCl_5$ SIL was investigated using CV and potentiostatic analysis. Tantalum electrodeposition from DMI with $TaCl_5$ was challenging; however, co-deposition of zinc and tantalum was successfully achieved in DMI with both $ZnCl_2$ and $TaCl_5$. The resulting coating, obtained under specific electrodeposition conditions, demonstrated higher corrosion resistance compared to pure zinc coatings, exhibiting a corrosion current density of 1.83×10^{-1} mA cm^{-2}.[61] The effect of magnesium chloride ($MgCl_2$) as an additive on zinc electrodeposition in a 1,3-dimethyl-2-imidazolidinone (DMI) and $ZnCl_2$ SIL system has been investigated. The addition of $MgCl_2$ improved zinc deposition by reducing the overpotential, enhancing the smoothness and uniformity of zinc coatings, and significantly increasing corrosion resistance, particularly at an optimal concentration of 0.1 mol/L $MgCl_2$.[157] These works stand apart from the other electrodeposition investigations utilising SILs, as the electrodeposited coating was evaluated for corrosion resistance.

In summary, these studies collectively demonstrate the versatility of SILs in enabling electrodeposition of a wide range of metals, showcasing their potential for applications such as low-temperature electrochemical deposition, alloy formation, and environmentally friendly coatings. These applications are key and emphasise SILs advantageous properties such as

tunability, cost-effectiveness, and substantial dissolution capacity in comparison to traditional ILs. The systematic exploration of these SILs contributes valuable insights to the development of efficient and tailored processes for various electrochemical applications. There is an opportunity to expand further on SILs use in electrodeposition, particularly in the evaluation of corrosion resistant electrodeposited coatings utilising SILs.

Table 7 A summary of the influence of SILs on electrodeposition of various metals.

Metal(s) Studied	SIL Influence	Key Mechanisms
Zn, Ta[61]	Enhanced solubility of $TaCl_5$ and $ZnCl_2$	Solvation effects improved electrodeposition kinetics
Li[73]	Facilitated Li transport through LIPON	Interfacial stabilisation for improved lithium deposition
Al, Li[93]	Stabilisation of Al and Li species in solution	Controlled electrodeposition via complexation
Li[94]	Stabilised Li^+ ions enabling direct deposition	Reduction of overpotential and enhanced nucleation
Al, Nd[101]	Low-temperature stabilisation of Al-Nd alloy	Improved co-deposition efficiency via solvation
Mg[107]	Enhanced Mg electrodeposition and stripping	Electrolyte stabilisation via complex formation
Ta[109]	Improved Ta electrochemical stability	Electrode surface passivation and controlled dissolution
Ag[111]	Enhanced Ag deposition uniformity	Interfacial stabilisation preventing dendrite formation
Al, Mg[116]	Room temperature co-deposition	Altered electrochemical window facilitating deposition
Nd[117]	Selective Nd deposition with $LiNO_3$ support	Complex formation aiding Nd extraction
Li[152]	Improved Li electrodeposition morphology	Solid-electrolyte interface stabilisation
Li[153]	Controlled Li ion transport and solvation effects	Ionic mass transfer regulation during electrodeposition

Advanced Chemical Synthesis

The use of ionic liquids as reaction media, as a replacement for traditional organic solvents, has seen extensive use and is one of the key applications of traditional ILs. This is due to their ability to be tailored in terms of polarity, to stabilise or destabilise transition states, and thus favour reaction outcomes and enhance reaction rates. They also serve as outstanding microwave energy absorbers so have been used to great effect in microwave assisted syntheses.

There are some limitations though, when using traditional ILs as a reaction media, such as the reaction of the C-H at the 2 position of imidazolium group with strong base, which initiates α-elimination and the formation of N-heterocyclic carbenes. Also, ILs are not suited to use at low temperatures (in some cases 0 °C) due to viscosity increase or freezing at these temperatures. Therefore, the use of SILs, lacking acidic protons, their innate Lewis acidity and their consistent liquid state across a broad range of temperatures offers a potential avenue of reactions, unable to be carried out in traditional ILs, able to be conducted in SILs. In this section, advanced chemical synthesis refers to the sophisticated and precise methods employed in the creation of complex molecules through regio- or stereo-selective reactions. The full spectrum of reported organic reactions utilising SILs as catalysts is depicted in Figure 16.

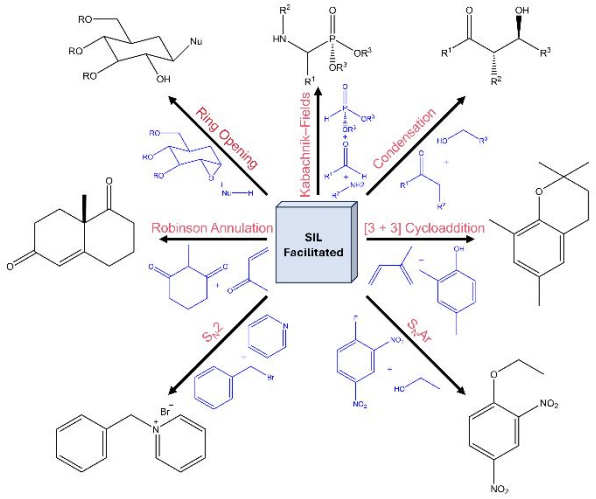

Figure 16 A diagram showing the diversity of SIL facilitated organic reactions. Condensation reaction – reported as a stereoselective asymmetric aldol reaction.[85] Kabachnik–Fields reaction – reported for synthesising diverse α-aminophosphonates.[24] Ring opening reaction – reported as the regio- and stereoselective ring opening of α-Gluco Carbasugar 1,2-Epoxides.[102] Nucleophilic aromatic substitution (S_NAr) and nucleophilic substitution (S_N2) – reported between S_NAr ethanol and 1-fluoro-2,4-dinitrobenzene to yield the phenetole and S_N2 pyridine and benzyl bromide yielding the pyridinium salt.[99] Robinson annulation – reported as a enantioselective Robinson annulation catalysed by (S)-proline.[158] [3 + 3] cycloaddition reaction – reported between 2,4-dimethylphenol and isoprene yielding the picture product as the main product.[42]

[Li(G3)][TFSI] and [Li(G4)][TFSI] SILs possess mild Lewis acidity, making them versatile solvents for various organic transformations.[2] The use of SILs in combination with (*S*)-proline and water (Figure 17) has been shown to significantly enhance the reactivity and selectivity of (*S*)-proline in stereoselective asymmetric aldol reactions by forming a crucial supramolecular ensemble involving electrostatic interactions with glyme-coordinated lithium.[85]

Additionally, [Li(G3)][TFSI] and [Li(G4)][TFSI] SILs have demonstrated efficacy as reaction media for the Kabachnik–Fields reaction, swiftly synthesising diverse α-aminophosphonates within 5 minutes, a significantly faster reaction than typical molecular liquid systems, where reaction times generally range from 30 minutes to over an hour for similar yields.[24] This reaction has been further applied to synthesise α-aminophosphonate derivatives for enhancing flame-retardant properties of epoxy resins.[43, 44] The utility of [Li(G3)][TFSI] and [Li(G4)][TFSI] SILs in stereo- and regioselective reactions was further highlighted, particularly in the opening of α-gluco carbasugar 1,2-epoxides, with [Li(G4)][TFSI] proving to

be an efficient solvent for synthesising carbasaccharides or pseudodisaccharides with β-gluco configuration.[102]

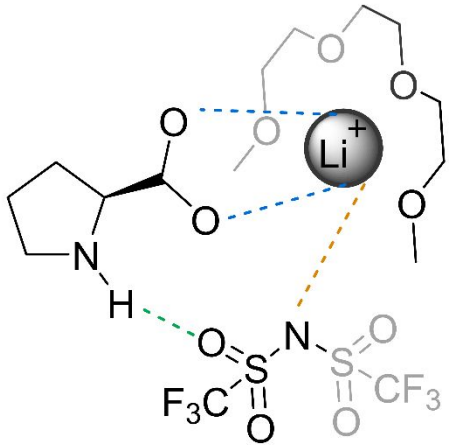

Figure 17 The supramolecular ensemble involving electrostatic interactions between [Li(G3)][TFSI] SIL and (*S*)-proline in stereoselective asymmetric aldol reactions.

SILs have also impacted nucleophilic aromatic substitution (S_NAr) and nucleophilic substitution (S_N2) reactions, where decreased rate constants in S_N2 reactions compared to acetonitrile may be beneficial for suppressing such reactions, while S_NAr reactions exhibited predictable solvent effects, with a cautionary note on solvent reactivity at high SIL proportions.[99] The enantioselective Robinson annulation catalysed by (S)-proline under mechanochemical conditions, focusing on the influence of [Li(G3)][ClO_4], [Li(G4)][ClO_4], [Li(G3)][TFSI] and [Li(G4)][TFSI] SILs have also been investigated. [Li(G4)][TFSI] improved enantioselectivity significantly and reduced reaction time from three days to 90 minutes, demonstrating its potential to enhance sustainable mechanochemical processes.[158] A summary of SILs polarity and Kamlet-Taft parameters is provided in Table 8.

Table 8 Polarity (E^N_T) and Kamlet–Taft Parameters; α (hydrogen bond donor ability), *B* (hydrogen bond acceptor ability), π^* (polarity/polarizability); for SILs, G3/G4 ethereal solvents and [Bmim][TFSI]. Normalised against methanol (*a*) and DMSO (*b*). Data from various sources.[38, 159-161]

Solvent	E^N_T	α^a	B^b	π^*
[Li(G3)][TFSI] [38, 159]	1.028	1.32	0.31	0.94
[Li(G4)][TFSI] [38, 159]	1.033	1.35	0.28	0.91
[Li(G3)][BETI] [38, 159]	n.d.	0.88	0.32	0.84
[Li(G4)][BETI] [38, 159]	n.d.	0.8	0.36	0.86
G3[38, 159]	0.301	0.1	0.62	0.74
G4[38, 159]	0.284	0.03	0.72	0.68
[Bmim][TFSI] [160]	0.59	0.55	0.22	0.97
Water[160]	1	1.05	0.76	1

Aluminium(III) and gallium(III) triflate SILs, consisting of [M(G3)][$TFSI_3$], have been explored as recyclable Lewis acidic catalysts. Both Al-SILs and Ga-SILs were fully soluble and catalytically active in a [3 + 3] cycloaddition reaction, with Ga-SILs exhibiting higher Lewis acidity and superior catalytic performance compared to their aluminium counterparts.[42] This underscores the versatility and effectiveness of SILs in enhancing synthetic processes across various chemical transformations.

Pharmaceutical Delivery Media

Pharmaceutical delivery media play a crucial role in enhancing the bioavailability and efficacy of drugs by facilitating their absorption and distribution within the body. Solvents like dimethyl sulphoxide (DMSO) are commonly used in low aqueous concentrations to improve drug solubility in cell media and membrane permeation in cellular assays, but alternative delivery systems are being explored to optimise these processes while minimising side effects.[162] SILs, such as [Li(G3)][TFSI] and [Li(G4)][TFSI], have demonstrated potential as alternatives to traditional solvents like DMSO for pharmaceutical delivery. They effectively solubilise small molecular therapeutics while offering advantages like reduced compound degradation during prolonged storage and prevention of freeze-thaw cycle issues, particularly since [Li(G4)][TFSI] remains in a liquid state at -20 °C. SILs have also shown comparable or slightly superior performance in delivering compounds such as DEAB and SU5402 to zebrafish embryos. DEAB (N,N-diethylaminobenzaldehyde) is a retinoic acid synthesis inhibitor that blocks the activity of retinaldehyde dehydrogenases, crucial for embryonic development, while SU5402 is a pan-fibroblast growth factor receptor (FGFR) inhibitor used to study FGFR signalling, affecting processes like cranial neural crest development and organogenesis. Furthermore, SILs enable drug delivery with full penetrance in experimental models, reinforcing their suitability as viable replacements for DMSO in drug delivery applications.[46] [Li(G3)][TFSI] and [Li(G4)][TFSI] SILs, exhibit low toxicity *in vivo*, as demonstrated by minimal apoptosis and developmental abnormalities in zebrafish embryos at concentrations up to 50 µM, making them a promising alternative to traditional solvents like DMSO for biological applications.[163]

Detection Applications

The detection applications of SILs reported in the literature involve their use, such as G3/G4 trinitrobenzene substituted SILs, for chemoselective detection of amine gases on a quartz crystal microbalance. These ionic liquids offer a straightforward and cost-effective synthesis with potential applications in portable gas analysis and as invisible ink.[88]

The utility of SILs, specifically G3, G4, G3/G4 trinitrobenzene substituted, G4 3-nitrobenzene substituted, and G4 1,3-nitrobenzene substituted, was investigated for the chemoselective detection of amine gases on a quartz crystal microbalance (QCM). The detection process involved nucleophilic aromatic additions with G3/G4 trinitrobenzene substituted SIL thin coated on quartz chips. A notable advantage was the straightforward, cost-effective synthesis of G3/G4 trinitrobenzene substituted SILs using a short-step synthetic approach, in contrast to common imidazolium traditional ILs. G3/G4 trinitrobenzene substituted SILs proved ideal for chemoselective amine gas detection due to the simple and

label-free analysis of nucleophilic aromatic addition reactions by QCM, along with their potential applications in portable gas analysis and as invisible ink.[88]

The application of SILs in detecting amine gases demonstrates a promising approach for chemoselective detection using SILs, offering cost-effective synthesis and potential applications in portable gas analysis and as invisible ink. Further research is needed to explore SILs performance in detecting a broader range of volatile organic compounds and to evaluate the long-term stability and reliability of these detection systems under varied environmental conditions.

SILs Dilution by Other Solvents & Additives

Diluting SILs with other solvents and additives can significantly enhance their performance and properties, making them more effective for various applications. Typical additives include molecular solvents like glymes (e.g., G3 and G4), fluoroethylene carbonate (FEC), and propylene carbonate (PC), as well as diluents such as hexafluoropropylene oxide dimers (HFE) and acetone. These additions improve solvation of polymers, modify ion coordination structures, and optimise ionic conductivity. While dilution may seem to challenge the definition of a SIL, the resulting systems often retain key SIL characteristics, such as preserved Li-ion solvation structures and strong polymer coordination. These changes ultimately lead to better thermal stability, safety, and cycling performance in lithium-ion batteries and other energy storage systems.

Conformation and solvent qualities in SILs were investigated using small angle neutron scattering (SANS) and rheology to explore the behaviour of poly(ethylene oxide) (PEO) in different SILs. In [Li(G4)][TFSI], PEO dissolved through coordinate bonds with lithium, exhibiting behaviour similar to PEO dilution in conventional ILs. The Flory exponent values and viscosity behaviour indicated that the three SILs provided moderate solvation qualities for PEO. The solvation of PEO in SILs involved competition for Li^+ coordination sites with anions and glymes. Poorer solvent quality for PEO was observed in SILs with stronger coordination between Li^+ and the anion or glyme, leading to the conclusion that weakly coordinating anions in SILs are more effective solvents for PEO.[71, 80] The local Li^+ structure in [Li(G4)][TFSI] SILs was investigated using Raman spectroscopy and high-energy X-ray total scattering (HEXT) experiments. This indicated that G4 strongly solvates Li^+ at its central and middle oxygen atoms, with terminal oxygen atoms dynamically coordinating in both neat and HFE-diluted SILs. Additionally, the thermophysical and transport properties of [Li(G4)][TFSI] blended with [mEtMeIm (1-(2-methoxyethyl)-3-methylimidazolium)][TFSI] were examined, revealing a nearly ideal inverse relationship between conductivity and viscosity. This suggests strong Li^+ coordination in the blended SIL, making it suitable for various applications requiring elevated temperatures.[74 87] The improvement of cycle performance in Si-flake-powder (Si Leaf Powder, Si-LP) negative electrodes within [Li(G4)][TFSI] SIL diluted by HFE was investigated, resulting in an emphasis on the importance of effective pre-films for Si-S batteries to achieve a stable SEI layer. Practical methods were highlighted, such as pre-cycling Si-LP electrodes in specific electrolytes. Additionally, the transport and SEI-modifying properties of [Li(G4)][TFSI] SIL diluted with fluoroethylene carbonate (FEC) were explored, revealing that FEC acted as a viscosity-reducing agent. This enhancement in Li ion transport led to the formation of a more stable SEI film, ultimately improving the performance of Si composite electrodes.[95 105]

The effects of dilution on SILs has also been explored with using non-stoichiometric amounts of the lithium salt, for example $[Li_{1.25}(G4)_1][TFSI_{1.25}]$ and $[Li1(G4)_1][TFSI_1]$ with HFE (mole fractions 0.25 to 8) and with propylene carbonate (PC) and HFE on [Li(G4)][TFSI]. It was found that dilution with specific solvents preserved the Li-ion solvation structure and improved Li^+ transference numbers, showcasing the importance of solvent choice in optimising SIL properties.[164, 165] Diluted G3/G4 LiTFSI SILs were investigated using various amounts of solvents, such as G3, G4, water, acetonitrile (AN), propylene carbonate (PC), acetone, diethyl carbonate (DEC), HFE, toluene and hexane content. Observations of Li^+ solvation in SILs diluted with various molecular solvents indicated competitive solvation between glyme and the diluents, which affected the stability of glyme–Li complex cations.[166] Ion transport properties in high concentration electrolytes (HCEs) and localised high concentration electrolytes (LHCEs) have been investigated in SILs comprised of LiFSI in dimethyl carbonate (DMC) with and without tetrafluoroethyl ether (TTE) as a diluent at 1.23:0.62:1 (DMC:TTE:LiFSI) 9.0M and 2:1:1 (DMC:TTE:LiFSI) 5.55M concentrations. HCEs exhibited high lithium transference numbers due to concerted ion-hopping mechanisms, while LHCEs, despite reduced viscosity, displayed lower transference numbers and disrupted cation-hopping mechanisms. [167]

The comprehensive investigations discussed above collectively underscore the dynamic changes in the properties of SILs as they undergo dilution with various solvents and additives. These studies reveal nuanced alterations in SIL behaviour, such as enhanced effectiveness in coordinating with polymers, shifts in Li^+ coordination structures, changes in solvent quality, and improvements in ionic conductivity and cycling performance. These findings highlight the versatile nature of SILs, showcasing their potential in tailoring electrolyte properties for diverse applications, including lithium-ion batteries and silicon electrode systems. While the investigations have provided valuable insights into the effects of dilution on various properties of SILs, there remains a gap in understanding the long-term stability and degradation mechanisms of diluted SILs under operational conditions. Exploring these aspects could further enhance the design of more resilient electrolyte systems for advanced energy storage applications.

Thermoelectrochemical Applications

Thermoelectrochemical applications of SILs (Figure 18a) involve utilising these SILs in thermoelectric devices (Figure 18b) to generate electrical power from temperature gradients. Thermoelectrochemical applications of SILs have garnered attention due to their unique properties and potential contributions to enhancing energy conversion efficiency. SILs, such as those incorporating glyme ligands and $TFSI^-$ anions, exhibit favourable thermal and electrochemical stability.

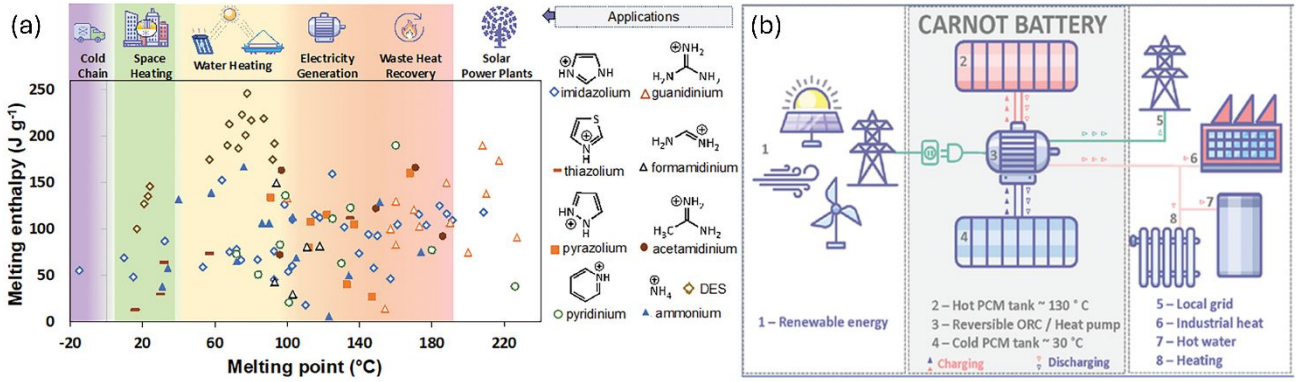

Figure 18 (a) A diagram from Matuszek *et al*. (2024)[3] of thermal properties of various IL phase change material cation families. Melting enthalpy (J g^{-1}) is plotted against melting temperature (°C). Icons above the graph indicate the primary applications of phase change materials across different temperature ranges. (b) is a illustration from Piper *et al*. (2023) [168] of a phase change material (PCM)-based Carnot thermal battery. During the charging phase, surplus renewable energy powers a heat pump to transfer heat (depicted by upward red and blue arrows) from a cold reservoir to melt a PCM in a hot reservoir. In the discharge phase, the system functions in reverse as an organic Rankine cycle engine, utilizing the stored thermal energy (represented by downward red and blue arrows) to produce electricity while releasing heat for various applications. For maximum efficiency, the PCM should store energy within the 100–220 °C range.

(a) Reprinted (adapted) with permission from Matuszek, K., Piper, S.L., Brzęczek-Szafran, A., Roy, B., Saher, S., Pringle, J.M. and MacFarlane, D.R., 2024. Unexpected energy applications of ionic liquids. *Advanced Materials*, p.2313023. and (b) reprinted (adapted) with permission from Piper, S.L., Forsyth, C.M., Kar, M., Gassner, C., Vijayaraghavan, R., Mahadevan, S., Matuszek, K., Pringle, J.M. and MacFarlane, D.R., 2023. Sustainable materials for renewable energy storage in the thermal battery. *RSC Sustainability*, *1*(3), pp.470-480

These attributes make them promising candidates for advanced devices, where the interplay of temperature gradients and electrochemical processes can be harnessed to generate electrical power. These attributes make them promising candidates for advanced thermoelectrochemical devices, where the interplay of temperature gradients and electrochemical processes can be harnessed to generate electrical power.

The thermoelectrochemical properties of [Li(G4)][TFSI] SIL for the direct conversion of waste heat into electricity were investigated and resulted in notable findings. The complexation of G4 molecules with lithium cations led to an entropy-driven release during the thermoelectrochemical process, yielding favourable Seebeck coefficients ranging from approximately +0.9 to +1.4 mVK^{-1}. The most efficient power generation occurred at a ~1:4 stoichiometry of Li[TFSI] and G4; higher ratios increased viscosity and reduced the availability of uncomplexed G4 molecules. Additionally, the porous nature of electrodeposited lithium enhanced performance over repeated use by increasing electrode surface area. However, despite low thermal conductivity, the overall performance and efficiency of the thermoelectrochemical cells were limited by relatively low conductivity values.[78] While the single investigation into SILs' thermoelectrochemical properties has provided significant insights into the thermoelectrochemical properties of SILs, there is still a lack of understanding regarding the long-term stability and performance degradation of these systems under varying operational conditions. Addressing these aspects could enhance the reliability and efficiency of thermoelectric devices in practical applications.

Curing/Polymerisation Catalysis

The curing and polymerisation catalysis applications of SILs involve their unique role as effective catalyst additives in radical polymerisation processes, as demonstrated by the SIL catalysed cationic polymerisation of isobutyl vinyl ether.[59] SILs have been applied, with various ligands and metal centres, to achieve ultrafast curing times in epoxy resin systems for high-volume manufacturing of fibre-reinforced composites.[41] The Lewis acidic nature of SILs enhances the cure rate by activating the epoxide moiety, showcasing their potential advantages over conventional polymerisation methods (Figure 19), as was eluded to above when examining bi-continuous electrolyte epoxy systems.[23, 55]

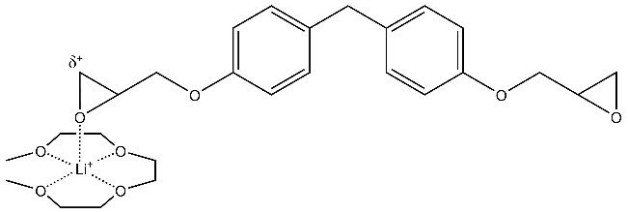

Figure 19 The proposed curing catalysis mechanism involves the interaction of the metal atom within the SIL chelate, which activates the epoxide group through Lewis acid activation. This process enhances the reactivity of the epoxide, facilitating subsequent chemical transformations.

The use of SILs in polymerisation processes was investigated for different applications. One study focused on the radical polymerisation of isobutyl vinyl ether (IBVE) with lithium cations (Li^+) using LiTFSI and ester compounds to form SILs, revealing a unique cationic polymerisation mechanism. Successful polymerisation occurred at high temperatures (60°C to 100°C), while low temperatures (0°C) inhibited the process, due to the decreased mobility of cationic species in the SIL at low temperatures, which limited the stabilisation and propagation of the reactive cations essential for the polymerisation mechanism. The addition of Lewis bases (4-propylpyridine, dipropylsulphide, urea, and other amide series) were found to stabilise propagating cations through interactions with SILs, contributing to this mechanism.[59] Another investigation examined SILs as catalysts for ultrafast curing in epoxy systems, with findings indicating that cure rate enhancement depended on the selection of metal centres, ligands, and counter anions in

SILs. The Lewis acidic nature of SILs facilitated rapid reactions with nucleophiles, activating the epoxide moiety and improving curing rates.[41] The impact of LiTFSI concentration within [Li(G3)][TFSI] and [Li(G4)][TFSI] on curing kinetics in bicontinuous SPEs was assessed, revealing that increased LiTFSI content led to a significant reduction in curing time, suggesting a catalytic effect on the epoxy resin curing process. This rapid curing enhanced mechanical properties but also raised concerns about potential void formation in the resin samples as the handling time of the systems is dramatically reduced.[23]

The integration of SILs such as $Zn(OAc)_2$, [Li(G3)][TFSI], [Li(G3)][OTf], $[Mg_{0.5}(G4)][TFSI]$, and $[Zn_{0.5}(G4)][TFSI]$ into epoxy-based vinylogous urethane (VU) vitrimers has been shown to enhance curing efficiency by accelerating epoxy ring-opening and amine-addition reactions. This acceleration, attributed to the increased Lewis acidity of Zn^{2+} and Mg^{2+} cations, reduces both onset and gel times during curing. SILs also form complexes with epoxides, as indicated by IR analysis, further facilitating the curing process. Post-curing, SILs lower enthalpic barriers for nucleophilic reactions in cross-linked epoxy networks. Mechanical tests confirmed that SIL-containing samples retain strength while improving elongation at break.[55]

Overall, these findings highlight the potential of SILs to accelerate polymerisation and curing processes, while emphasising the need for careful consideration to balance rapid curing with mechanical performance in manufacturing applications. However, the long-term stability and durability of the cured materials when using SILs as catalysts have not been thoroughly investigated, leaving a gap in understanding their performance in real-world applications.

SILs & Polymers

Gel Polymer Electrolytes (Including Ionogels)

Gel polymer electrolytes (GPEs) are hybrid materials that combine a polymer matrix with a liquid electrolyte, forming a gel where the polymer acts as a host structure and the liquid component, such as ILs or organic solvents, provides ionic conductivity. These materials are widely used in batteries and fuel cells, offering a flexible and mechanically stable medium for ion conduction while minimising leakage risks in the event of rupture. Ionogels, in contrast, incorporate ILs directly into a solid-like matrix, which can be organic (e.g., polymers), inorganic (e.g., silica), or a combination of both. The ILs are immobilised within the matrix, contributing to unique properties such as high thermal stability, low volatility, and negligible vapor pressure, making ionogels suitable for various electrochemical devices. Unlike GPEs, where the liquid electrolyte is added as a secondary phase, ionogels inherently integrate the IL during synthesis, resulting in distinct performance advantages. [169, 170] The incorporation of polymer and ionic liquid cross-linking strategies has been shown to enhance the electrochemical performance of gel polymer electrolytes, making them viable candidates for flexible solid-state supercapacitors.[171]

The integration of SILs within GPEs and ionogels has emerged as a versatile and impactful strategy for advancing various electrochemical applications. Polymer electrolytes leveraging the self-assembly of ABA-triblock copolymers, polystyrene-b-poly(methyl methacrylate)-b-polystyrene (PSt-b-PMMA-b-PSt, SMS), have been explored in recent studies. One study focused on a novel class of polymer electrolytes using SIL and ABA-triblock copolymer, revealing the formation of ion gels with micelle structures transitioning into polymer networks. Another employed poly(lithium acrylate-r-acrylic acid)-b-poly(methyl methacrylate)-b-poly(lithium acrylate-r-acrylic acid) (LML) as a host matrix and found that the LML/[Li(G4)][TFSI] ion gel demonstrated superior tensile properties and ionic conductivity due to strong ion-ion interactions and compatibility between LML and [Li(G4)][TFSI].[18, 65, 172] Further studies expanded on this theme by investigating various ABA-triblock copolymers in SILs for enhanced ionic conductivity and thermal stability. One promising finding was the PSt-b-PMMA-b-PSt-based (polystyrene-b-poly(methyl methacrylate)-b-polystyrene) electrolyte that exhibited an electrochemical window exceeding 4.2 V and stable Li-ion secondary battery operation at elevated temperatures. Additionally, research into zwitterionic polymer scaffold-supported solvate ionogels revealed room temperature Li^+ conductivity and self-healing capabilities, demonstrating potential for flexible solid-state Li-based batteries.[90, 97]

Investigations into the mechanical and structural properties of ionogels has demonstrated significant progress. For example, high-conductivity solid ionogel electrolytes based on [Li(G4)][TFSI] SIL in methyl cellulose have shown impressive ionic conductivity and mechanical strength.[98] Additionally, ionogels for lithium metal batteries synthesised through UV radiation-induced chemically crosslinked polymerisation in [Li(G4)][TFSI] SIL have achieved superior ionic conductivities and anodic oxidation stability surpassing 5.06 V (electrochemical stability window determined by linear sweep voltammetry (LSV) using lithium foil and stainless steel as the counter/reference and working electrodes).[119]

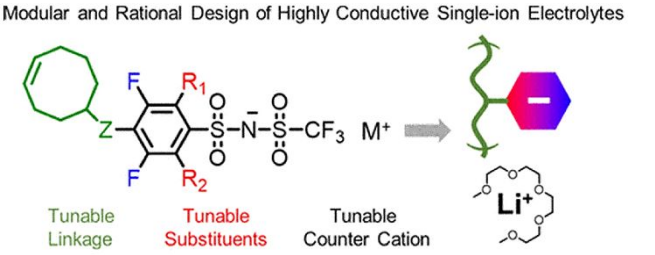

Figure 20 Graphical abstract from Zhang *et al*. 2021[115] depicting polyFAST salts.

Reprinted (adapted) with permission from Zhang, W., Feng, S., Huang, M., Qiao, B., Shigenobu, K., Giordano, L., Lopez, J., Tatara, R., Ueno, K., Dokko, K. and Watanabe, M., 2021. Molecularly tuneable polyanions for single-ion conductors and poly (solvate ionic liquids). *Chemistry of Materials*, *33*(2), pp.524-534. Copyright 2021 American Chemical Society.

A new class of polymer electrolytes, polyFAST salts (Figure 20) (fluorinated aryl sulphonimide tagged anions as side chains with [Li(G4)][TFSI] as an electrolyte), have been introduced, showcasing improved ionic conductivity and electrochemical stability. The impact of side chain substitution patterns on these properties was highlighted. Additionally, research has focused on enhancing the safety of lithium-ion batteries using SIL-based

GPEs with low flammability, while demonstrating high thermal and cycle stability in LIBs.[52, 115]

Studies have explored tailored electrolytes for specific battery types. In one instance, a flexible SIL-GPE for quasi-solid-state sodium-ion batteries was developed, demonstrating high ionic conductivity and electrochemical stability. Another investigation employed mesoporous silica MCM-41 (Mobil Composition of Matter No. 41) to immobilise SILs, expanding the electrochemical window and achieving high ionic conductivity for improved lithium-ion battery performance.[53, 58] Investigations into the cationic homopolymerisation of a biomass-derived monomer (trans-4-methoxy-β-methylstyrene, commonly known as trans-anethole) revealed successful polymerisation with solubility variations depending on the solvent choice. This study utilised SILs and Lewis bases, including ethyl acetate (EtOAc), diisopropyl ether (iPr_2O), methyl ethyl ketone (MEK), 1,2-dimethoxyethane (DME), tri-n-butyl phosphate (TBP), and N,N-dimethylacetamide (DMAc), as a key components of the polymerisation system. SILs provided a unique environment that stabilised the propagating cations, enabling successful polymerisation of trans-anethole under low-temperature conditions. This approach not only improved polymer yield but also influenced the molecular weight and stereoregularity of the resulting polymer, highlighting the critical role of SILs in enhancing polymerisation efficiency and tailoring polymer properties.[60] Additionally, interface resistance challenges in solid-state batteries were addressed through the development of a gel polymer electrolyte interlayer, which stabilised the Li|LAGP ($Li_{1.5}Al_{0.5}Ge_{1.5}P_3O_{12}$, a NASICON-type sodium superionic conductor ceramic electrolyte) interface and enhanced battery cycling stability.[121] Magnesium-ion conducting GPEs using SIL and a magnesium salt were explored, identifying an optimal molar ratio of 1:0.5 G2/$Mg(ClO_4)_2$ for high room temperature ionic conductivity (~3.15×10^{-3} S cm^{-1}) and wide electrochemical and good thermal stability. These findings position these electrolytes as promising candidates in magnesium-ion batteries, with stable Mg-stripping/plating behaviour validated for practical applications.[62]

A GPE for LIBs was developed using an imidazolium-functionalised copolymer supported by a equimolar [Li(G4)][TFSI] SIL. The GPE demonstrated impressive room-temperature ionic conductivity, high lithium-ion transference numbers, and excellent electrochemical stability, highlighting its potential for safer and more efficient lithium-ion battery applications.[173] [Li(G4)][TFSI] SIL has been applied as a plasticiser in a poly(ethylene oxide)-based SPE to improve ionic conductivity and lithium compatibility. Incorporating the SIL significantly reduced PEO crystallinity, enhanced ionic conductivity, and contributed to stable lithium plating/stripping performance, enabling high-capacity and long-life operation of lithium metal batteries at room temperature.[174] GPE membranes combining [Li(G4)][TFSI] SIL, with crosslinked network polymers featuring different main chains, have been investigated, with the aim of enhancing ion conductivity and stability for LIBs. The GPE membrane based on poly(TTT-PEMP)/[Li(G4)][TFSI], TTT being 1,3,5-trially-1,3,5triazine-2,4,6-trione and PEMP being pentaerythritol tetrakis (3-mercaptopropionate), exhibited the best performance, achieving high ion conductivity (up to 3.13×10^{-3} S cm^{-1} at 90°C), excellent electrochemical stability (>5 V vs. Li/Li^+), and superior long-cycle durability.[175] GPEs have been developed that incorporate SILs comprised of NaTFSI di(propylene glycol) dimethyl ether (DPGDME) in varying molar ratios (0.1:1 to 0.8:1 NaTFSI:DPGDME). The optimised GPE demonstrated high ionic conductivity (~1.1 mS cm^{-1}), Na^+ transport number (~0.67), and oxidative stability (~5.2 V vs Na/Na^+), confirming its potential applicability in quasi-solid-state sodium-ion batteries.[176] A free-standing, single-ion conducting semi-solid polymer electrolyte (PBSIL) has been developed using a [Li(G4)][TFSI] SIL and anion acceptor (borate ester) to enhance lithium-ion transport while immobilising anions. The PBSIL demonstrated improved ionic conductivity (8.0×10^{-4} S cm^{-1} at 25°C), a high lithium-ion transference number (0.75), and excellent long-term cycling performance, highlighting its potential for high-voltage lithium metal battery applications. The SIL played a critical role in the PBSIL electrolyte by promoting the dissociation of lithium salts, thereby facilitating lithium ion (Li^+) transport while maintaining anion immobilisation.[177] A quasi-SPE (QSPE) system has been investigated in which poly(ethylene glycol) diacrylate (PEGDA) was cross-linked with SILs containing tetraethylene glycol dimethyl ether (TEGDME), LiTFSI, and 1-ethyl-3-methylimidazolium bis(trifluoromethylsulphonyl)imide (EMIM-TFSI). The SIL-based QSPE exhibited a nanoscale branched network structure with enhanced ionic conductivity (1.8 mS cm^{-1} at 298 K), dielectric constant (125 at 298 K), and mechanical flexibility, outperforming systems based on single-component ionic liquids.[178]

In summary, the comprehensive exploration of SILs in diverse polymer electrolyte and ionogel systems, as discussed above, collectively underscores the versatility and potential of SILs in enhancing electrochemical performance, safety, and flexibility across a range of battery technologies. However, the specific interactions and compatibility between various SILs and different polymer matrices in GPEs and ionogels remain largely unexplored, presenting an opportunity for further investigation to optimise performance and develop novel formulations.

Bi-continuous Electrolytes

Bi-continuous electrolytes (Figure 21) are conductive materials characterised by a network structure where two distinct phases coexist: a liquid electrolyte phase and a solid polymer phase. Typically, ILs are used as the liquid phase due to their high ionic conductivity, broad electrochemical window, and thermal stability. Recent advancements have demonstrated the use of SILs as an alternative liquid phase. The bi-continuous architecture facilitates efficient ionic transport through the liquid phase while leveraging the mechanical robustness of the solid epoxy resin phase, making these materials promising candidates for multifunctional structural electrolytes.[179, 180]

A novel approach to developing fast lithium-conducting polymer electrolytes was investigated using polymer solutions in a glyme-Li salt SIL, $[Li(G4)_1][TFSI]$, comprising an equimolar mixture of [Li(G3)][TFSI]. Different polymers (PEO, poly(ethylene oxide), PMMA, poly(methyl methacrylate), and PBA, poly(butyl acrylate)) were added to explore the impact of

polymer structure on thermal stability, ionic transport, and electrochemical properties. Variable stability of $[Li(G4)_1]^+$ complex cations was observed, with $[Li(G4)_1]^+$ being stable in PMMA- and PBA-based solutions but undergoing ligand exchange in PEO-based solutions. The stability of ligand exchange correlated with thermal and electrochemical stability, influencing the ionic conduction mechanism. It was found polymer electrolytes, utilising low-melting SILs, can achieve rapid Li^+ ion transport along with high thermal and electrochemical oxidative stabilities. PBA-based matrices displayed superior lithium transport properties due to a lower glass transition temperature and low affinity for Li^+ ions, while PMMA-based solutions showed enhanced thermal and oxidative stability.[19]

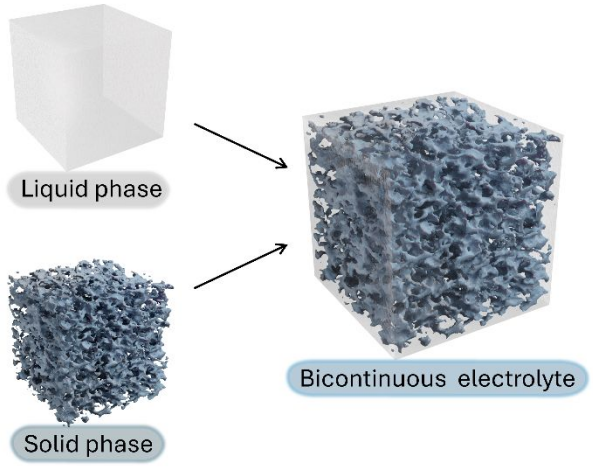

Figure 21 Representative bi-continuous electrolyte, consisting of solid phase (blue) and liquid electrolyte phase (clear).

The incorporation of Zn(OAc (acetoxy))$_2$, [Li(G3)][TFSI], [Li(G3)][OTf], [$Mg_{0.5}$(G4)][TFSI] and [$Zn_{0.5}$(G4)][TFSI] SILs into commercial epoxy-based vinylogous urethane (VU) vitrimers was investigated to enhance their stress-relaxation properties. The addition of these species resulted in accelerated epoxy ring-opening and amine-addition reactions during curing, which reduced both onset and gel times, presumably to the increase Lewis acidity of the Zn and Mg cations. The catalytic performance varied with SIL dosage, and IR analysis indicated complex formation between SILs and epoxides, enhancing the curing process. After full curing, the SILs significantly accelerated nucleophilic reactions in model compounds and cross-linked epoxy networks, reducing enthalpic barriers. Tensile tests revealed that SIL-containing samples retained mechanical strength and exhibited higher elongation at break, making them suitable for various applications where high strength is not critical. Incorporating SILs into vitrimer epoxies retained over 70% of the original mechanical strength and increased elongation at break (EoB) by 5–40%, depending on the type and dosage of SIL. Additionally, a SIL-loaded epoxy vitrimer was successfully applied to fabricate a flexible hybrid electronics package, addressing challenges in manufacturing industries while offering potential advantages in stress relaxation, formability, rework ability, compatibility, and adhesion performance.[55] A bi-continuous electrolyte with [Li(G3)][TFSI] SILs and epoxy resin was applied for carbon fibre (CF) supercapacitors. A 45-fold improvement in specific capacitance was achieved due to CF surface modification compared to control devices, with a specific capacitance of 1439 mFg^{-1} at 0.5 mAg^{-1}. The high amount (70%) of SIL within the epoxy resin created conductive channels, allowing the device to be flexible without compromising electrochemical performance.[22] This system was also later applied as an electrolyte in MXene coated CF supercapacitors,[45] and investigated for its piezo-electric effect both neat as a neat SIL and within a bicontinuous polymer system.[26, 181] Investigations into bicontinuous solid polymer electrolytes (SPEs) with SILs for supercapacitors resulted in findings that ionic conductivity was approximately double in [Li(G4)][TFSI] epoxy resin samples compared to [Li(G3)][TFSI] (Figure 22), with [Li(G4)][TFSI] samples exhibiting a 22% higher specific capacitance than [Li(G3)][TFSI] in prototype capacitors. Although there was a reduction in mechanical strength, due to rapid curing leading to potential void formation and minimal cross-linking from dilution, the thermal stability remained above 210 °C, making it suitable for most civilian high-temperature applications. The findings highlighted optimising SPEs by balancing ionic conductivity and mechanical properties for supercapacitor development.[23]

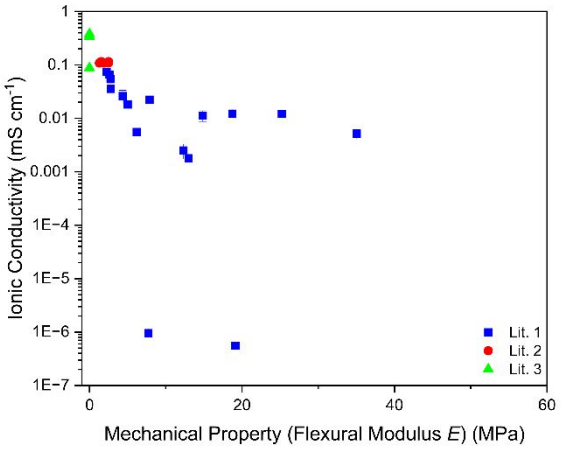

Figure 22 Literature values of mechanical flexural and electrochemical properties of SPEs comprised of SILs at room temperature. Lit. 1.23, Lit. 2.182 & Lit. 3.19 Note the mechanical properties for Lit. 3.19 were not reported and hence have been plotted as a zero value.

Bicontinuous epoxy resin and SIL systems have also been emphasised for their basic physical design being highly suitable for electrolyte recycling and recovery from SPEs. High recovery rates of SILs were achieved, with up to 92.8% recovered from epoxy-based bicontinuous SPEs. The recovered SILs maintained comparable electrochemical and mechanical properties to pristine SILs. Additionally, the recycling process significantly reduced manufacturing costs by 66.51% over 5 cycles.[182]

The comprehensive exploration of SILs in diverse polymer electrolyte and ionogel systems, as discussed above, collectively underscores the versatility and potential of SILs in enhancing electrochemical performance, safety, and flexibility across a range of battery technologies and applications. However, the specific effects of varying SIL concentrations and their

interactions with different polymer matrices on the long-term stability and performance of bi-continuous electrolytes remain underexplored, highlighting a critical area for future research.

Properties

The physicochemical properties of SILs are fundamentally shaped by the interactions between their constituent cations, anions, and ligands, influencing key characteristics such as ionicity, viscosity, and electrochemical stability. A summary of SILs properties compared to ILs is provided in Table 9 and a summary of SILs physical properties is provided in Table 10.
Understanding these properties is crucial for tailoring SILs to specific applications, including energy storage systems, where their modular capabilities allow for fine-tuning of thermal stability, ionic conductivity, and solvation dynamics.[23, 183] A table summarising the broad trend of physiochemical properties of SILs, compared with traditional ILs, is provided below. For more detailed information the ESI table 2 compares quantitative values for 4 SILs with 4 ILs.

Table 9 A summary table comparing the properties of SILs as a class to traditional ILs.

Property	SILs	Conventional ILs
Electrical Conductivity (S/cm)	Higher than ILs due to the presence of coordinating solvents improving ion mobility[37, 38]	Highly variable; some are excellent conductors while others have high viscosities reducing ion transport[10, 184]
Thermal Stability (°C)	Typically lower than ILs, limited by solvent decomposition rather than cation-anion interactions[11, 37]	Generally high, with some ILs stable up to 400°C due to strong ion pairing[185, 186]
Melting Point (T_m) (°C)	Lower melting points due to solvation effects reducing lattice energy[12, 37]	Wide range from -10°C to 300°C depending on cation-anion combination[185, 186]
Glass Transition Temperature (T_g) (°C)	Generally lower due to flexible coordination environment[12, 37]	Varies widely based on structure, typically higher than SILs[185, 186]
Toxicity	Less studied, but can be more toxic due to potential solvent toxicity[37]	Varies; some ILs show low toxicity while others have environmental concerns[184, 187]

Intercalation and Electrochemical Behaviour

The intercalation and electrochemical behaviour of SILs involve phenomena such as Li^+ co-intercalation and graphite exfoliation in $[Li(G3)_x][TFSI]$ electrolytes.
Intercalation mechanisms and electrochemical behaviours have been explored in different electrolyte systems.[66] The Li^+ intercalation into graphite electrodes was investigated using $[Li(G3)_x][TFSI]$ electrolytes, discovering co-intercalation of G3 and Li^+ in $[Li(G3)_x][TFSI]$ electrolytes with excess G3 ($x > 1$). The reversible electrochemical intercalation of solvate $[Li(G3)_1]^+$ cations into graphite occurred within the 1.2–0.4 V range (vs Li/Li^+).[66] The electrochemical deposition and dissolution of lithium metal on a carbon fibre composite electrode was investigated in [Li(G4)][TFSI] SIL, demonstrating the use of a porous vapor-grown carbon fibre (VGCF®-H) network for Li metal storage, with deposited Li primarily located within the voids of the modified Cu electrode.[89] Investigations into the interfacial structure and stability of SILs have been conducted with different focuses. The [Li(G4)][TFSI]/Au electrode interface was investigated using SEIRAS (surface enhanced infrared absorption spectroscopy), revealing partial desolvation of $[Li(G4)]^+$ near the electrode at a potential close to the point of zero charge. This partial desolvation was attributed to the disruption of the isotropic dielectric environment at the interface.[118] The implications for rechargeable batteries are significant, with findings highlighting the competing characteristics necessary for achieving safe and durable SIL-based batteries. The modification of solvate stabilities at the interface and the dual characteristics of solvate cations contribute to understanding how to balance stability in the bulk with rapid desolvation on the electrode surface for optimal performance.[118]

Table 10 A summary of SILs physical parameters such as melting point (T_m), density (ρ), solvent polarity ($E_T(30)$) and normalised polarity (E^N_T), compared to values for G3, G4, water and a IL.[159]

Solvent	T_m (°C)	ρ (g/mL)	$E_T(30)$ (kcal/mol)	E^N_T
[Li(G3)][TFSI]	23	1.42	64	1.028
[Li(G3)][FSI]	56	1.36		
[Li(G3)][Otf]	35	1.3		
$[Li(G3)][NO_3]$	27	1.18		
[Li(G3)]]TFA]		1.2		
[Li(G4)]]TFSI]		1.4	64.2	1.033
[Li(G4)]]CTFSI]	28	1.4		
[Li(G4)]]FSI]	23	1.32		
[Li(G4)]]BETI]	23	1.46		
$[Li(G4)]]ClO_4]$	28	1.27		
$[Li(G4)]]BF_4]$	39	1.22		
$[Li(G4)]]NO_3]$		1.17		
[Li(G4)]]TFA]		1.19		
Water	0		63.1	1
G3			40.4	0.301
G4			39.9	0.284
[Bmim]]TFSI]			49.8	0.59

With only three studies on this topic, significant gaps remain in understanding the full scope of intercalation mechanisms and electrochemical behaviours in SIL systems. In particular, how solvate stability and Li^+ desolvation processes at the electrode interface influence long-term performance and safety in rechargeable batteries. Further research is needed to clarify the competing factors of stability in the bulk electrolyte and rapid desolvation at the electrode for optimised performance in these systems.

SILs' Modular Capabilities

By modifying the chemical structures of cations and/or anions, the thermal and physicochemical properties of traditional ILs have been customised, and indeed this third component of SILs compared to traditional ILs provides a unique ability to tune chemical, physical, and electrical properties.[188-190] For example, it has been reported that the melting point, glass transition temperature, and viscosity of ionic liquids can be reduced through the incorporation of an asymmetric structure into the cation and/or anion within the SILs.[191-193] Within SILs the three components of the SIL system can be interchanged in a modular manner (Figure 23).

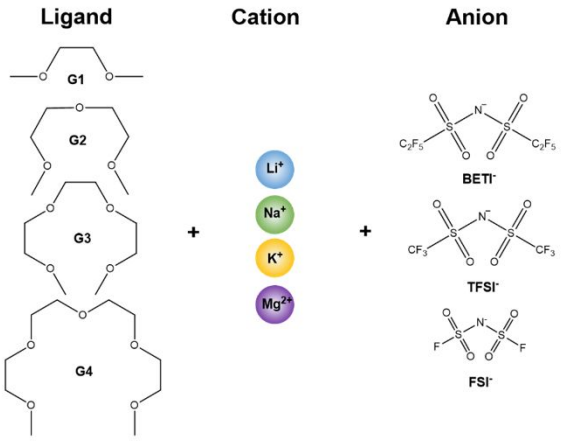

Figure 23 The modularity of SILs demonstrated by some of the interchangeable ligand, cation and anion options available to researchers. Note all these different combinations have different properties making them more or less desirable for specific applications.

Within glyme-based SILs, it is essential to account for the competitive interactions involving Li^+ ions and counter anions, along with those between Li^+ ions and glymes. Given that glyme molecules are anticipated to exhibit a preference for interacting with Li^+ ions.[2, 38] The varying strengths of interactions between Li^+ ions and glymes, as opposed to those between Li^+ ions and anions, serve as direct indicators of the states of the mixtures.[2, 38, 194] The Lewis basicity, a donor property of the anions, is well correlated with the relevant physicochemical properties and coordinating structure of [Li(Glyme)][Anion].[12] The spectrum of anions based on their Lewis basicity (Figure 24), anions with strong Lewis basic characteristics establish relatively robust interactions with metal cations (M^+) when compared to the interactions between metal cations and glyme molecules. This suggests that the strength of the M^+-anion interaction is notably influenced by the Lewis basicity of the anions, with stronger Lewis basic anions fostering more pronounced and durable associations with the metal cations.[40] Stronger metal-anion interactions hinder the formation of SILs because the anions compete more effectively with glyme molecules for coordination with metal cations, reducing the extent of dissociation necessary for SIL formation. [40]

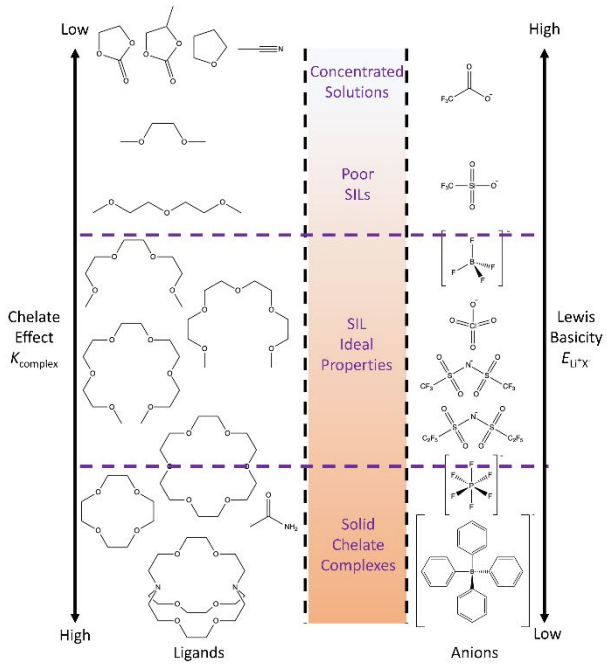

Figure 24 A spectrum of comparison of solid chelate complexes through to concentrated solutions, with SILs positioned with attributes between these two categories.

Anion Optimisation

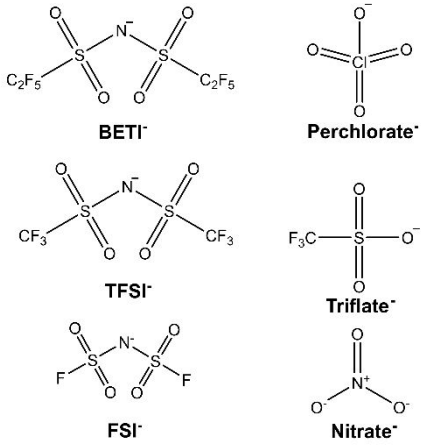

Figure 25 Anions applied in SILs reported in the literature.

This section explores the optimisation of SILs through the interchanging of anion components, as reported in the literature. The research landscape on SILs has seen significant exploration in recent years, with various studies shedding light on their physicochemical properties, nanostructures, and applications in energy storage devices.[21, 30, 40, 164, 195-205] These collective efforts provide a comprehensive understanding of SILs, paving the way for their optimised design and broader application in advanced energy storage systems.

The anionic structure of [Li(glyme)]X and its influence on ionicity has been extensively studied and from these works the IL systems can be categorised into two groups based on the competitive interactions between glymes, counter anions, and

Li^+ cations. SILs with weak Lewis basic anions, such as $TFSI^-$ and ClO_4^-, exhibit behaviour similar to traditional ILs.[40, 198] These systems form long-lived and stable $[Li(glyme)]^+$ complex cations due to the weak basicity of the anions, leading to properties typical of ILs, such as high ionicity, high lithium transference numbers, and minimal free solvent, distinguishing them from concentrated solutions. In contrast, SILs with strong Lewis basic anions display low ionicity, resembling concentrated solutions. This distinction is further supported by solvation studies, where the concentration of free glyme in [Li(glyme)]X affects the Li/Li^+ electrode potential, suggesting energetically unstable Li^+ solvation environments in SILs.[198]

The electrochemical properties and performance of SILs in Li-S batteries such as [Li(G4)][bis(pentafluoroethanesulphonyl)imide ($BETI^-$)] and [Li(G3/G4)][$TFSI^-$], are exemplified by their high electrochemical stability, effective suppression of polysulphide dissolution, and impressive overall performance in Li-S batteries.[21, 195] Physicochemical properties such as Kamlet–Taft parameters, density, viscosity, and thermal stability of various SILs with alternated anions, $TFSI^-$, $BETI^-$, OTf^- (triflate), NO_3^-, TFA^- (Figure 25) and $[FeBr_4]^-$, have been investigated.[200, 206] Nanostructure investigations of [Li(G4)][TFSI] and [Li(G4)][NO_3] SILs using AFM have revealed layers of ions near the interface.[195] A Multimode 9 AFM in contact mode, with silicon cantilevers calibrated via the thermal noise method was used. Force measurements were performed using an electrochemical cell with HOPG and Au(111) electrodes, under varying potentials to analyse normal force-distance curves and interfacial ionic layer structures.[195] Additional research into SIL–electrode interfaces emphasises the influence of anion species and glyme length on the interfacial structure and friction behaviour.[201, 207] Fluoride-based SILs have been developed, through the combination of 1-butyl-3-methylimidazolium or 1-ethyl-3-methylimidazolium, silver fluoride (AgF), and ethylene glycol (EG) in dry methanol, resulting in anhydrous SILs $[C_4C_1im]F{\cdot}EG$ and $[C_2C_1im]F{\cdot}EG$, showcasing low vapor pressure and melting points that could facilitate surfactant self-assembly.[202] [Li(G4)][TFSI], [Li(G4)][A(pentafluorophenyl anion)], [Li(G4)][A-SO_2iPrF_4] and [Li(G4)][A-$SiPrF_4$] SILs were investigated with a finding that enhanced thermal and oxidative stability resulted from introducing S-substituted fluorinated aryl sulphonamide-tagged anions. The three different S-containing anion substituents (sulphides, sulphoxides, and sulphones) in combination with electron-withdrawing fluorine substituents, exhibited high electrochemical stability, low Lewis basicity, and high ion conductivity, as confirmed by both DFT calculations and experimental measurements. This modification resulted in high electrochemical stability and low Lewis basicity, broadening SILs' application range in battery devices.[208]

Despite the extensive research into the anionic structure of [Li(glyme)]X and its influence on ionicity, significant gaps remain in understanding the precise relationship between anion structure, glyme length, and interfacial behaviours in SILs, particularly at higher Li-salt concentrations. Further exploration is needed on how these factors influence electrochemical stability and performance, especially in emerging battery technologies like Li-S systems, as well as the impact of novel anion modifications on long-term stability and device integration.

The modification of anions in SIL systems plays a crucial role in improving properties and optimising SILs, as highlighted above by various studies. By altering the chemical structures of cations and/or anions, researchers have successfully customised the thermal and physicochemical properties of conventional ILs. The incorporation of asymmetric structures into the cation and/or anion within ILs has been reported to reduce the melting point, glass transition temperature, and viscosity. In glyme-based SILs, it becomes essential to consider competitive interactions involving Li^+ ions, counter anions, and glyme molecules. The strength of interactions between Li^+ ions and glymes, compared to those with anions, directly indicates the state of the mixtures. Lewis basicity, a property of the anions, correlates well with relevant physicochemical properties, emphasising its importance in coordinating structures. Anions with strong Lewis basic characteristics establish robust interactions with metal cations, influencing the strength of M^+-anion interactions. The classification of SILs based on Lewis basicity further guides the understanding of their behaviour.[2, 12, 21, 30, 38, 40, 152, 153, 164, 165, 188-218]

Cation Focused Optimisation

The chelation of the cation in SILs is a fundamental aspect of their chemical identity, thus changing the cation within SILs significantly impacts their properties, particularly regarding stability and electrochemical performance.[11] The stability of SILs is influenced by the charge density of the cation, with divalent cations like Mg^{2+} providing greater thermal and electrochemical stability than monovalent cations such as Li^+ and Na^+. This enhancement is due to stronger electrostatic interactions with solvent molecules, leading to more stable complex formations.[31, 35, 219] Additionally, the choice of cation affects the melting point of SILs; for example, Mg-based SILs generally have higher melting points (10–20°C), though incorporating ligands with flexible asymmetric termination groups like G3Bu, where the terminal methyl ethers are replaced by large tertiary butyl groups, can reduce these melting points, enabling the development of room-temperature SILs.[11, 220] Different cations also influence the electrochemical stability windows of SILs; Mg-based SILs can achieve anodic stabilities up to 4.5 V vs. Li^+/Li, making them suitable for high-voltage applications, while Na-based SILs show compatibility with various electrode materials, supporting stable cycling.[32, 221] The compatibility of Na-based SILs with various electrode materials, such as hard carbon (HC) and $Na_{0.44}MnO_2$, stems from their ability to form stable electrode-electrolyte interfaces, as evidenced by stable cycling and negligible capacity fade over extended cycles. This behaviour is closely linked to the unique coordination and transport properties of the Na^+ complexes, which are specific to SILs and not universally applicable to all Na salts.[32, 221] Furthermore, the type of cation affects the reductive stability of the anions in the SIL; certain anions like $[TFSI]^-$ may react undesirably with deposited metal (e.g. Li^+, Na^+, and K^+, which are commonly used in battery and energy storage systems),

reducing Coulombic efficiency, while substituting these anions with more stable alternatives can enhance performance.[32]

The mobility and dissociative behaviour of ions in SILs are also dependent on the anion, with the introduction of $[FSA]^-$ ions in Na-based SILs improving ionic conductivity and electrochemical stability compared to $[TFSI]^-$.[31] Lastly, the cation type impacts the compatibility of SILs with various positive and negative electrode materials, ultimately affecting overall battery performance.[32] Altering the cation in SILs can lead to significant changes in thermal stability, electrochemical performance, and compatibility with battery materials, highlighting the importance of cation selection in designing effective electrolytes for energy storage systems.

A hydronium (H_3O^+) SIL solvated by 18-crown-6-ether, denoted as $[H_3O^+{\cdot}18C6][TFSI^-]$, has been investigated, providing strong acidity without the levelling effect of unprotonated water.[203, 205] The leveling effect refers to the phenomenon in which the acidity of strong acids in a particular solvent (like water) is limited or "levelled" to the strength of the solvated proton (H_3O^+ in water), because stronger acids completely dissociate, resulting in the same effective proton donor, H_3O^+.[203, 205] Additionally, the first example of an ammonium (NH_4^+) SIL, $[NH_4^+{\cdot}18C6][TFSI^-]$, demonstrated impressive ionic conductivity and thermal stability.[217] The physicochemical characteristics of G5–Na[TFSI] have been investigated revealing the formation of a low-melting solvate complex in the equimolar combination of G5 and Na[TFSI].[30] The complex cation $[Na(G5)_1]^+$, created through sodium-glyme chelation, analogous to the lithium centre, exhibited a remarkably long lifetime (> 10^{-4} s) in concentrated mixtures. The molten solvate $[Na(G5)_1][TFSI]$ demonstrated high ionic conductivity (0.61 mS cm^{-1}) at 30 °C, promoting the dissociation into $[Na(G5)_1]^+$ and $[TFSI]^-$. When employed as an electrolyte, $[Na(G5)_1][TFSI]$ exhibited enhanced oxidative stability with increasing Na[TFSI] concentration, enabling stable charge/discharge cycles in a Na cell within the voltage range of 2.0–4.0 V (vs. Li metal soaked in $[Li(G4)_1][TFSA]$ as a reference electrode). The resulting cell displayed good cycle stability, providing a capacity of approximately 100 mA h g^{-1} for 50 cycles.[30] G3, G4 and G5 were investigated with Li, Na and K metal centres and the $TFSI^-$anion. It was found the formation of certain complexes depended on both glyme length and M^+ ion, revealing a discernible trend in glyme complexation behaviour with various M[TFSI] complexes. Proposed criteria for achieving stable glyme−M[TFSI]-based complexes, characterised as good SILs, were primarily based on the coordination number of each metal ion. Na[TFSI] parent salts in SILs exhibited higher thermal stabilities than Li[TFSI] and K[TFSI] salts, with a balance among competitive interactions identified as a determinant of SIL stabilities when considering ion radii effects.[28] The transference numbers of alternative cations (Na^+, K^+, and Mg^{2+}) in [Na(G3)][TFSI], [K(G3)][TFSI] and $[Mg(G3)][TFSI]_2$ SILs at 1:1 and 2:1 (G3:salt) ratios and within polymer electrolytes has been investigated using electrophoretic NMR (eNMR) and electro impedance spectroscopy (EIS). Cationic transference numbers were around 0.4 for SILs and lower values (0.14–0.2) for polymer electrolytes, with Mg^{2+} showing a relatively higher transference number (T ≈ 0.3) due to unique ion coordination effects.[222]

While significant progress has been made in understanding how cation choices in SILs affect stability and performance, gaps remain in exploring novel cations and the mechanisms behind their ionic conductivity and thermal stability. Research is needed to identify more stable anions, investigate the effects of cation and anion combinations on thermal stability, and assess long-term performance and safety. Comprehensive studies focusing on ionic conductivity, compatibility with various electrodes, and the potential of multivalent cation systems will help advance SIL technology for energy storage applications. A significant challenge in exploring SILs utilising different metal centres is that not all cation/anion pairs are soluble in G3/G4 ether solvents and hence the cation is not suitably dissolved to be freely available for chelation by the ether and formation of a SIL.

Ligand Focused Optimisation

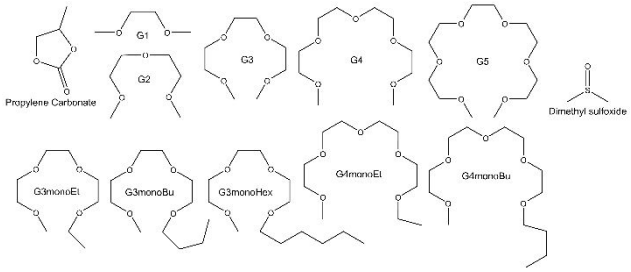

Figure 26 Ligands applied in SILs reported in the literature. Note G is short for glyme, e.g. triglyme is G3.

Remarkable changes in the physicochemical properties of glyme–Li salt complexes can be achieved through the modification of the chemical structure of glyme/chelating group, with the introduction of non-symmetric molecules facilitated by altering a glyme terminal alkyl group.[14, 37, 38] The substitution of a different alkyl group for one of the terminal methyl groups in glyme allows for a reduction in the melting point and/or glass transition temperature, consequently expanding the liquid temperature range.[14, 37, 38] Fixing one terminal as the methyl group and varying the length of the other terminal alkyl chain results in the viscosity attaining a minimum value at the ethyl termination. The decrease in viscosity is ascribed to the interplay between columbic and van der Waals interactions in longer terminal alkyl chain lengths. As the alkyl chain length increases, there is a decrease in the ionic concentration within the liquid, causing the relaxation of the coulombic interaction among the ionic species.[192, 223] Similar to the strategy applied to conventional ILs, the modification of ligand structures proves effective in precisely tailoring the physicochemical properties of SILs.[12, 37, 183, 224, 225]

The creation of enduring and sturdy complexes between Li^+ ions and ligands, even in a liquid state, ensures a consistent diffusion coefficient between Li^+ ions and ligands as they move together.[12, 40, 183] The results from the propylene carbonate (PC) complexes with Li reveal that the stability of the solvate $[Li(PC)_4]^+$, featuring the monodentate ligand PC, is significantly lower compared to that of $[Li(G3/G4)]^+$ with the multidentate

chelating ligand. This discrepancy leads to a shorter lifespan of the solvates in Li-PC mixtures. In contrast to the scenario with [Li(G3/G4)][TFSI], where glymes and Li^+ ions form stable solvate ions and move together, the diffusion coefficients of PC ligand molecules in the $[Li(PC)_4][TFSI]$ mixture, and even in the more concentrated $[Li(PC)_3][TFSI]$ mixture, exceed those of the Li^+ ions.[15, 226-232]

The complex formation constant, $K_{complex}$, is among the crucial parameters that characterise the stability of complexes.[12, 233] Investigation into Li^+ coordination with propylene carbonate glyme 1 (G1), glyme 2 (G2), glyme 3 (G3), and glyme 4 (G4) in dioxane solvent, found $K_{complex}$ increased with an increase in coordination sites of a single ligand molecule, complex cations that are stable and endure for an extended period can be formed by longer glymes.[234] The spectrum of ligands based on their chelating effect ($K_{complex}$) is depicted in **Error! Reference source not found.**.

Some limitations in the application of glyme solvents must be noted e.g., glyme solvents remain problematic for practical applications due to toxicity concerns, particularly G2 and G4 which are presently classified as reprotoxic.[163, 235] However it should be noted that the utilisation of different ligands is effective in enhancing both the stability and safety of electrolytes.[236]

Glyme-Li salt complexes (SILs) when initially introduced as a new family of ILs were investigated with different ligands. Equimolar mixtures of glyme and a Li salt, such G3, G3monoEt, G3monoBu, G3monHex, G4, G4monoEt and G4monoBu (Figure 26) with a Li^+ metal centre and $TFSI^-$ anion were investigated. They exhibit high thermal stability, ionic conductivity, and oxidative stability. The impact of modifying the structure of the glyme molecule on the physicochemical properties of SILs has been highlighted, resulting in features such as reduced melting points and enhanced conductivity.[14] The physicochemical properties and concentration dependency of [Li(G3)][TFSI] and [Li(G4)][TFSI] SILs have been investigated. It was found that viscosity and self-diffusion coefficients increase with LiTFSI concentration, while ionic conductivity peaks at approximately 1 $mol{\cdot}L^{-1}$. Additionally, the molar conductivity of LiTFSI-glyme SILs is influenced by the mole fraction of [Li(TFSI)], which affects both viscosity and ionic conductivity.[15, 237] The impact of different solvents on SILs has been extensively studied.[166, 238] G1, G2, G3, G4, G5, and THF were investigated while maintaining constant Li^+ and $TFSI^-$ ions. Concentrated solutions ($[Li(G1 \text{ or } THF)_x][TFSI]$) were differentiated from solvate ionic liquids (ILs) ($[Li(G3 \text{ or } G4)_1][TFSI]$ and $[Li(G2)_{4/3}][TFSI]$). D_{sol}/D_{Li^+} ratio analysis revealed stable SILs with a D_{sol}/D_{Li^+} of ~1, indicating long-lived complex cations.[238]

Observations of Li^+ solvation in SILs diluted with various molecular solvents indicated competitive solvation between glyme and the diluents, which affected the stability of glyme–Li complex cations.[166] Notably, dilution with nonpolar solvents was found to increase the ionic conductivity of SILs, highlighting greater dissociativity in such solvents. Overall, these findings indicate that the choice of diluting solvents significantly influences the stability and performance of SILs in Li-ion batteries.[166, 232] G3, G4 and G5 were investigated with Li, Na and K metal centres and the $TFSI^-$ anion. It was found the formation of certain complexes depended on both glyme length and M^+ ion, revealing a discernible trend in glyme complexation behaviour with various M[TFSI] complexes. Kamlet–Taft parameters and toxicity of some SILs have been determined, with investigations into [(Li-G3)TFSI] and [(Li-G4)TFSI] SILs providing valuable insights. It was found that SILs exhibit high normalised polarity and strong hydrogen bond donating properties. Additionally, these SILs are safe and suitable solvents for pharmaceutical compounds, with potential as alternatives to DMSO.[159, 163] [Li(G3)][TFSI] and [Li(G4)][TFSI] have been investigated for their lower critical solution temperature (LCST) behaviour with poly(benzyl methacrylate) (PBnMA). Findings revealed the formation of stable glyme–Li^+ complexes even in the presence of PBnMA, emphasising the coordination of Li^+ ions by glymes. The LCST phase separation process exhibited thermal stability of glyme–Li^+ complexes surpassing separation temperatures, indicating the absence of SIL decomposition during this process. The rationale for LCST behaviour was elucidated in terms of structure-forming solvation, characterised by negative ΔH_{mix} and ΔS_{mix} (negative enthalpy and negative entropy of mixing, respectively). The up field shift observed in the ^7Li NMR spectra of PBnMA/[Li(G4)][TFSI] solutions suggested cation–π interactions between $[Li(G4)]^+$ and the aromatic ring of the PBnMA side chain, where the aromatic rings coordinated perpendicularly to $[Li(G4)]^+$, serve as the underlying mechanism for the LCST behaviour.[239] Sodium bis(fluorosulphonyl)imide (NaFSI) dissolved in glymes (G1, G2 and G3) have been investigated.[240] Mixing $[Mg(G1)_3][TFSI]_2$ and $[Mg(G3)_2][TFSI]_2$ with tetrabutylammonium chloride produced highly concentrated non-volatile electrolytes, facilitating the electrodeposition and stripping of magnesium metal at elevated current densities (>1.0 A dm^{-2}). While chloride anions have no significant impact on the magnesium deposition process, they play a crucial role in the stripping process by reducing stripping overpotential and enhancing reversibility.[107] ($MgTFSI_2$)/ glymes (G3, G3Et, G3Bu, G4, G5) SIL electrolytes for magnesium batteries have been investigated.[220] Introduction of an asymmetric structure to the glyme ligand, such as substituting a terminal methyl group in G3 with alkyl groups of varying chain lengths (G3Et, G3Bu), lowered melting points, and $[Mg(G3Bu)]TFSI_2$ maintained a liquid state at room temperature. The complex exhibited higher oxidative stability compared to uncoordinated glymes, and allowed for Mg metal deposition and dissolution.[220] The transport properties of LiTFSI concentration in glyme SILs G2, G3, G4 and G5 SILs at molar ratios of 1:1 (G2 & G3), 3:4 (G3), 3:5 (G4) and 1:2 (G5) and proton conduction in hydronium (H_3O^+) G5, benzo-18-crown-6 (B18C6), 18-crown-6 (18C6) and dicyclohexano-18-crown-6 (Dh18C6) SILs with the $TFSI^-$ anion have been explore. It was found that the number of coordination sites per ligand molecule is a key factor influencing hopping conduction in glyme-based systems.[241] Proton conduction was faster when H_3O^+ was coordinated with cyclic 18C6-based ligands compared to acyclic G5 ligands. The coordination by cyclic or acyclic ligands was a crucial factor for proton conduction in hydronium SILs.[242] [Li(G3)][TFSI] and [Li(G4)][TFSI] SILs were investigated

with increased LiTFSI concentrations, greater than 1:1 stoichiometric ratios. The self-diffusion properties of [Li(G3/G4)][TFSI] were found to be dependent on temperature, Li^+-salt concentration, and viscosity. At elevated temperatures, Li^+ exhibited accelerated movement, outpacing both the glyme and anion components. Molecular dynamics simulations suggest this was due to lithium 'hopping' between glyme units, facilitated by the $TFSI^-$ anion. Acceleration of the Li^+ was greater with the G4 ligand, attributed to the looser chelation and excess Li-O ratio in G4.[183, 243] The nanostructures' development of [(Li-G3)TFSI] with increasing Li-salt concentration has been investigated utilising SAXS and Raman spectroscopy, revealing a departure from ideal SILs with increasing Li-salt concentration above equimolar ratios.[197] Higher Li-salt concentrations in [(Li-G3)TFSI] SILs has also been investigated with the key finding that the viscosity of $[Li_{1.25}(G4)_1][TFSI_{1.25}]$ was three times higher than that of $[Li_1(G4)_1][TFSI_1]$ but upon dilution with HFE (mole fractions 0.25 to 8), both SILs exhibited similar viscosity values, ensuring equal fluidity in the electrolyte solutions.[164] The transition of glyme-based lithium-ion electrolytes from regular electrolytes to SILs and high-concentration electrolytes (HCEs) has been investigated using G4, G1 and G2 ligands and LiSCN and LiTFSI salts to evaluate changes in transport properties and ionic speciation. It was found that HCEs and SILs exhibited enhanced ionicities and distinct solvation structures, facilitating a viscosity-decoupled charge transport mechanism, whereas the use of mixed glymes negatively impacts the ionicity and charge transport efficiency compared to pure glymes.[244] The speciation and dipole reorientation dynamics in glass-forming liquid electrolytes (pseudo SILs) composed of LiTFSI mixed with 1,3-propane sultone (PS) or tetrahydrothiophene-1,1-dioxide (SL) has been investigated. The findings revealed that these mixtures exhibit unique aggregate formations and dipole reorientation behaviours, with large-scale aggregate formation playing a crucial role in their high lithium-ion transference and conduction properties.[245] The properties of lithium 2,4,5-tricyanoimidazolide (LiTIM) as a fluorine-free SIL in G2 and G4 glymes has been investigated with LiTIM:tetraglyme (G4) studied between 1:1 and 1.5:1 molar ratios at salt concentrations of 4.54 M and 6.8 M, respectively. LiTIM forms highly concentrated, stable, amorphous solutions in G2 and G4, with G4-based systems exhibiting electrochemical stability up to 4.7 V vs Li/Li^+, making these electrolytes promising candidates for advanced battery applications.[246]

Modifying ligands in SIL systems is crucial for enhancing the properties and optimising the performance of SILs. Evidence from numerous studies demonstrates that changes in the chemical structure of ligands significantly impact the physicochemical properties of glyme–Li salt complexes, forming the basis of SILs. For instance, the substitution of alkyl groups in glyme leads to a reduction in melting point and glass transition temperature, expanding the liquid temperature range. Ligand modifications also affect the stability of complexes between Li^+ ions and ligands, influencing diffusion coefficients and, consequently, the lifespan of solvates in Li salt mixtures. The coordination number of metal ions with ligands plays a pivotal role, and longer glymes are associated with stable complex cations. Ligand-focused optimisation enables tailoring the properties of SILs, such as ionic conductivity, viscosity, and oxidative stability. Examples from the literature highlight the impact of ligand alterations on SIL properties, emphasising the importance of this approach in advancing the development and application of SILs in various electrochemical devices.[14, 15, 28, 159, 163, 166, 183, 220, 232, 237-242, 247-251] Despite substantial progress in understanding ligand-focused optimisation for SILs, gaps remain in fully characterising the long-term stability of complex cations, particularly when considering different glyme–metal ion combinations across a broader spectrum of coordination numbers. Furthermore, while ligand modifications have demonstrated efficacy in enhancing thermal stability and ionic conductivity, the toxicity of certain glymes and the trade-offs between enhanced performance and safety remain underexplored. Additionally, the interplay between solvent dilution and ligand stability needs further investigation to optimise practical applications in electrochemical devices.

Molecular Dynamics Simulations/Computational Characterisation

Molecular Dynamics (MD) and computational simulations in chemistry have become a cornerstone of understanding complex systems at the molecular scale. In the context of SILs, simulations have been particularly instrumental in elucidating lithium-ion transport mechanisms and interfacial stability, providing critical insights into the fundamental interactions that govern electrolyte performance. This allows researchers to track ion trajectories, conformational changes, and thermodynamic properties, offering a deeper understanding of solvation structures, ion transport pathways, and electrode-electrolyte interfaces. By employing simulations, researchers can not only study the behaviour of complex chemical systems at the atomic level but also guide the rational design of next-generation electrolytes for solid-state batteries and other energy storage applications.[252, 253] A summary of computational SIL studies focus areas and findings is included in Table 11.

When applied to SILs, the interfacial structure/behaviour of lithium-based SILs, specifically [Li(G4)][TFSI], has been explored in various studies. The interfacial structure/behaviour of SILs being the behaviour of the complete SIL at the interface with electrodes and surfaces, not just interactions between ions. Molecular dynamics simulations conducted on thin films of [Li(G4)][TFSI] at equimolar ratios revealed a unique nanostructure near the negative electrode, distinct from traditional ILs, due to the repulsion of $TFSI^-$ anions, resulting in an enrichment of neutral glyme molecules near the electrode.[210] Further investigation into the nanostructure and capacitance of a SIL–electrode interface under constant potential and inherent polarizability demonstrated that SILs exhibit a multilayer-type interfacial structure, which significantly differs from the bulk, highlighting the need to account for surface polarizability in simulations involving charge transfer at electrodes.[214]

Several studies have explored the coordination and dynamics of Li^+ ions in different SIL systems. Some studies have shown notable variations in structural organisation when comparing LiTFSI and Li 4,5-dicyano-2-(trifluoromethyl)imidazole (LiTDI)

electrolytes as they approach equimolar concentrations, with significant differences depending on the glyme-to-lithium salt ratio.[211] Investigations into equimolar SILs highlighted a strong relationship between the stability of $[Li(glyme)]^+$ complexes and enhanced ion dynamics, with Li-Glyme pair exchange likely facilitated by clusters of multiple $[Li(glyme)]^+$ pairs.[212]

Table 11 A summary table covering of SIL computational studies, highlighting focus areas and main findings.

Focus Areas	Main Findings
Interfacial interactions, MD simulations[210]	Li^+ remains within 0.5 nm of the electrode, distinct solvation structures form at different voltages, key differences from conventional ILs.
Interfacial interactions, Electrochemical properties[214]	Li^+ forms stable interfacial layers, capacitance behaviour varies with applied potential, fixed charge models underestimate interfacial structuring.
Ion transport, Anion influence[211]	$TFSI^-$ leads to SIL formation, while TDI^- promotes disproportionation and mobile Li^+ species, affecting conductivity and stability.
Bulk properties, Ion solvation[212]	Li^+ exchange in glyme occurs on ~100 ns timescales, affecting ion mobility; strong lithium-glyme binding enhances stability.
Ion transport, Conductivity[213]	Li^+ transport is dominated by translational motion, low transference numbers (~0.07), ion correlation enhances conductivity.
Computational screening, Machine learning[247]	Neural networks accelerate SIL screening, identifying high affinity glymes; trade-offs exist between Li^+ binding and oxidative stability.
Polymer-electrolyte interactions, Solvation structure[96]	Li^+ preferentially solvates ester groups in PBnMA, leading to altered ionic transport and phase behaviour in SILs.
Computational modelling, Force field development[254]	Developed a force field for glyme-based SILs that accurately predicts radial distribution functions (RDFs) solvation structures, and diffusion coefficients.
Solvation structure, Anion effects[255]	Long-chain anions induce nanoscale phase separation, affecting Li^+ solvation and transport properties.
Solvation structure, Spectroscopy[256]	Li^+ solvation shifts from solvent-separated ion pairs (SIPs) at low salt concentrations to contact ion pairs (CIPs) at high concentrations.

MD simulations have revealed that diluting [Li(G4)][TFSI] SIL with additional glyme molecules improves overall dynamics and reduces viscosity, weakening the cation–anion anticorrelation and increasing transference numbers as salt concentration decreases. This dilution leads to an increase in lithium-ion self-diffusion coefficients, as demonstrated in the study, where D_{Li+} at 303 °K (29.85 °C) rose from 4.08 x 10^{-12} m^2/s in the equimolar mixture to higher values in more diluted systems. Transference numbers, which remain low in equimolar compositions due to strong lithium–glyme complexation, show a notable increase upon dilution, reaching values closer to 0.5 as glyme concentration increases. These findings indicate that reducing the salt-to-glyme ratio enhances lithium-ion mobility while mitigating ion pairing effects, ultimately improving the electrolyte's transport properties.[213]

Further studies on equimolar [Li(G4)][TFSI] SILs under anion-blocking conditions demonstrated lower Li^+ transference numbers, suggesting that electrolyte performance could be enhanced by dilution or the use of shorter glyme molecules.[91] Deviations in Li^+ coordination were observed in equimolar mixtures of SILs, with stronger lithium–glyme coordination and weaker Li–TFSI connections.[251] Additionally, computational analyses identified complex ethers that improve SIL stability, with certain G3/4/5 chain lengths offering superior properties for Li^+, Mg^{2+}, and Na^+ metal centres.[247] The solvation structure of poly(benzyl methacrylate) (PBnMA) in [Li(G4)][TFSI] SIL has been investigated using HEXTS (high-energy x-ray total scattering) and MD simulations. It was found that the BnMA monomer repeat unit was preferentially solvated by solvate Li cations, with $TFSI^-$ anions forming a coordination layer around the $[Li(G4)]^+$ cation. The role of weak and strong interactions was highlight in determining the properties of SILs and the behaviours of thermosresponsive polymers within them.[96] A new classical, non-polarisable force field to model LiTFSI SILs with glymes of varying chain lengths and salt concentrations, based on ab initio molecular dynamics simulations was developed. The resulting model accurately reproduced radial distribution functions, coordination structures, and x-ray structure factors across glyme systems, showcasing its transferability and computational efficiency for studying glyme-based electrolytes.[254] The nanoscale structural organisation and interactions in SILs with sulphonate-based anions containing long and short perfluorinated alkyl chains has been simulated. The SILs studied included lithium nonafluoro-1-butanesulphonate and lithium trifluoromethanesulphonate, revealing that the longer fluorinated tails promote distinct polar–apolar segregation and hydrophobic domain formation, unlike the shorter tails which do not support such organisation.[255] The solvation dynamics in [Li(G3)][TFSI] SIL using far infrared spectroscopy and molecular dynamics simulations has been investigated. At low salt concentrations, lithium ions are solvated by two triglyme molecules forming solvent-separated ion pairs, while at higher salt concentrations, lithium ions are predominantly solvated by one triglyme molecule with additional contact to the anion, forming contact ion pairs.[256]

Advancements in simulations have provided deeper insights into the interfacial stability of solid polymer electrolytes (SPEs), particularly in understanding SEI formation and electrode interactions. Recent studies have demonstrated that interfacial lithium-ion transport is significantly influenced by the nanostructure of SILs near electrodes, where surface polarizability plays a crucial role in charge transfer mechanisms.[214, 247] Additionally, linking simulations with experimental electrochemical stability studies has become an emerging approach to validate theoretical predictions and refine electrolyte design. Investigations incorporating reactive

molecular dynamics and ab initio simulations have shown promise in capturing the early stages of SEI evolution and ion solvation behaviour at interfaces, providing valuable guidance for optimising lithium-ion transport in next-generation solid-state electrolytes.[254-256] Future research directions could focus on integrating simulation results with operando spectroscopic techniques to bridge the gap between computational modelling and real-world electrochemical performance, ultimately enhancing the predictive capabilities of simulation-driven electrolyte design.

MD simulations on SILs have revealed key findings about their structural and dynamic properties. Investigations into the interfacial structure of [Li(G4)][TFSI] highlighted its unique nanostructure near the negative electrode, raising questions about its suitability for battery applications. Comparisons between different lithium salt electrolytes demonstrated significant variations in structural organisation, influenced by the nature of anions. The stability of lithium-glyme complexes was linked to enhanced ion dynamics, emphasising the importance of lithium-glyme pair exchange. Further studies showed that dilution could improve lithium coordination and dynamics, while low transference numbers under specific conditions suggested potential modifications to enhance electrolyte efficiency. Additionally, research on SIL-electrode interfaces indicated that accounting for surface polarizability is critical in simulations. Coordination dynamics were found to differ notably from some previous studies, indicating a need for more accurate modelling approaches. Lastly, computational explorations identified potential ethers that could enhance SIL stability, highlighting the intricate balance between various molecular properties.[91, 196, 210-214, 247, 251-253] Despite significant advancements, key gaps remain in the exploration and understanding of MD simulations for lithium-based SIL systems, particularly in accurately modelling surface polarizability, capturing the full complexity of Li^+ coordination dynamics at different glyme-to-lithium ratios, and improving the predictive power of these simulations for electrolyte behaviour under real-world conditions.

Limiting Factors Within the Field of SILs

SILs, as chemical systems, are prone to some limitations, that in some cases exist due to their fundamental chemical nature, and sometimes due to human factors/errors.

SILs Reliance on Charge Diffuse Anions

SILs predominately rely on diffuse or 'soft' anions, which pose significant challenges in terms of purification and environmental sustainability. These diffuse anions, while beneficial for their unique solvent properties, are typically difficult to isolate through crystallisation, necessitating complicated multistep synthesis processes. In contrast, more charge-concentrated (i.e. 'harder') anions are easily purified and recrystallised using water or other environmentally benign solvents. This reliance on diffuse anions in SILs limits the potential for incorporating more environmentally friendly anionic counterparts, as many common diffuse anions include halogenated species, which are associated with environmental and health concerns. Consequently, the environmental impact of SILs could be reduced if alternative anions, more amenable to purification and less harmful, could be integrated, highlighting a significant area for future research and development in this field.

SILs Reliance on Oligoethers

The reliance of SILs on G3 and G4 ethers, as well as other oligoethers, presents significant limitations due to associated health and environmental exposure concerns. While these ethers facilitate the desirable properties of SILs, their use raises potential issues related to toxicity and environmental impact. Many of these ether compounds can pose risks through inhalation, skin contact, or environmental release, complicating their overall sustainability profile. As the demand for greener alternatives grows, it becomes crucial to explore and develop safer, more sustainable ligand options that can maintain the advantageous characteristics of SILs while minimising health and environmental risks.

SILs Terminology Inconsistency

A significant challenge to the field generally is many researchers are not aware they are working with SILs when they are working with SILs e.g. in a 2024 Masters Thesis abstract [Li(G4)][TFSI] was referred to not as a SIL, but as a "…lithium salt-based liquid electrolytes…";[257] in a 2024 paper in which [Li(G4)][TFSI] and [Li(G4)][NO_3] were used the words ionic liquid (IL) and solvate ionic liquid (SIL) were not used however the wording "…Li^+ solvated by G4 solvent…" was used,[258] so there was clearly an understanding of the chelation effect of the ether by the authors; and in another 2024 paper the solvation of G4 (1 M LiTFSI) was investigated however the words ionic liquid (IL) and solvate ionic liquid (SIL) were absent from the article abstract.[259] Similarly in a 2025 paper SILs were used in a bicontinuous SIL:epoxy resin (7:3) electrolyte system but were not referred to as ionic liquids (IL) or solvate ionic liquid (SILs) in the manuscript.[260]

The authors recommend the full words and common abbreviations of SIL terminology and SIL substituents be included within abstracts of publications on the topic to aid both search engine optimisation and the development of the SIL field broadly. If consistent terminology is used duplication of work by researchers is less likely to occur. Such terminology includes: solvate ionic liquids (SILs), ionic liquids (ILs), tetraglyme (G4), triglyme (G3), Lithium bis(trifluoromethanesulphonyl)imide (LiTFSI/LiTFSA/LiNTf_2). The LiTFSI anion is a good example of where three different acronyms and two different extended names (Lithium bis(trifluoromethanesulphonyl)imide and lithium bistriflimide) are both confusing and cumbersome to find within search engines.

SILs Reliance on Salt Solvation

SILs rely on the solvation of salts by oligoethers (e.g. G3/G4), the oligoether solvent typically coordinates with cations from the salt, stabilising the ionic structure and facilitating ion transport.

However, the effectiveness of this solvation process is highly dependent on the specific interactions between the salt and oligoether, with certain salts exhibiting inherently low or minimal solubility in oligoether solvents. This limited solubility poses a significant restriction, as salts that cannot effectively dissolve or interact within the oligoether medium are incompatible with SIL systems, limiting the range of salts that can be used in SIL-based applications. Consequently, selecting suitable salt-oligoether combinations is crucial to optimising the performance and stability of SIL systems for targeted applications.

Research Gaps and Future Prospects

Despite the significant advancements and versatility of SILs in contemporary science and technology, several research gaps and unexplored avenues warrant attention to further harness their potential.

Ligand Modification

One of the most promising yet underexplored areas in SIL research is ligand modification. While triglyme (G3) and tetraglyme (G4) paired with LiTFSI have gained prominence due to their accessibility and well-characterised nature, the potential benefits of modifying ligands, especially with the introduction of G4monoEthyl, remain largely untapped.[13] The synthesis challenges associated with G4monoEthyl notwithstanding, its superior electrochemical properties compared to its predecessor, G4, present a compelling case for dedicated exploration.[14, 39] Investigating ligand modifications could provide novel insights and pave the way for SILs with enhanced properties, thus opening new avenues for research and application.

Concentration Dependency and Physicochemical Properties

While studies have inquired into the physicochemical properties and concentration effects of glyme-LiTFSI solutions,[16237] there is a need for more comprehensive studies to understand the intricacies of concentration dependencies in SILs. Exploring the effects of varying concentrations on properties like viscosity, ionic conductivity, and molar conductivity could offer valuable insights into optimising SIL performance across different applications.

Metal Centre and Anion Impact

While SILs have been explored with different metal centres like Li^+, Na^+, and K^+,[11] further studies could focus on understanding the impact of these metal centres in conjunction with various anions on the electrochemical and thermal stabilities of SILs. Such studies could help in designing SILs tailored for specific applications and performance requirements.

Toxicity and Safety

With SILs being explored for diverse applications, including potential replacements for DMSO in pharmaceutical compounds,[29] comprehensive studies on their toxicity profiles and safety implications are crucial. Understanding potential health hazards and ensuring SILs' safe handling and disposal are essential steps towards their broader adoption.

Thermoelectrochemistry and Sustainable Energy Solutions

SILs' potential in thermoelectrochemistry for waste heat harvesting suggests a promising avenue for sustainable energy solutions. However, further research is needed to optimise SILs for this application, exploring their efficiency, stability, and compatibility with existing waste heat recovery systems.[14]

Research Gaps and Future Prospects Conclusion

In conclusion, while SILs have demonstrated remarkable versatility and potential across various scientific and technological domains, several research gaps remain. Addressing these gaps through targeted research and exploration of new avenues could unlock further advancements in SILs, shaping their trajectory and expanding their applications in the future.

Conclusions

SILs, distinguished by the presence of enduring lithium solvate cations coupled with corresponding counter anions, serve as electrolytes renowned for their exceptional attributes. These include notably high lithium-ion conductivity and inherent non-flammability, making them compelling candidates for diverse applications in electrochemical systems and energy storage devices. The enduring nature of the lithium solvate cations, combined with their compatible counter anions, underscores the potential of SILs as a reliable and safe choice for enhancing the performance and safety characteristics of electrolytes in various technological applications.

Here we embark on a thorough exploration and analysis of the current panorama within SIL research. Our objective was to present a comprehensive review that encapsulated the breadth of developments and advancements in this dynamic field. By scrutinising the current state of SIL research, we aimed to unravel the intricacies and nuances that define the present landscape. Furthermore, we explored the multifaceted applications of SILs across diverse domains, shedding light on their versatile utility in various technological and scientific realms. Through this comprehensive examination, our perspective paper seeks to contribute valuable insights and foster a deeper understanding of the pivotal role that SILs play in advancing research and applications in contemporary science and technology.

These versatile compounds serve as electrolytes in a spectrum of lithium batteries, including Li-Air, solid-state, and Li-O_2 variants, showcasing their pivotal role in advancing energy storage technologies. Furthermore, SILs contribute significantly to Li-Sulphur batteries, demonstrating their adaptability in diverse electrochemical devices. The reach of SILs extends beyond traditional battery applications, as they are employed in polymer electrolytes, electrodeposition electrolytes, and reaction media.

ARTICLE

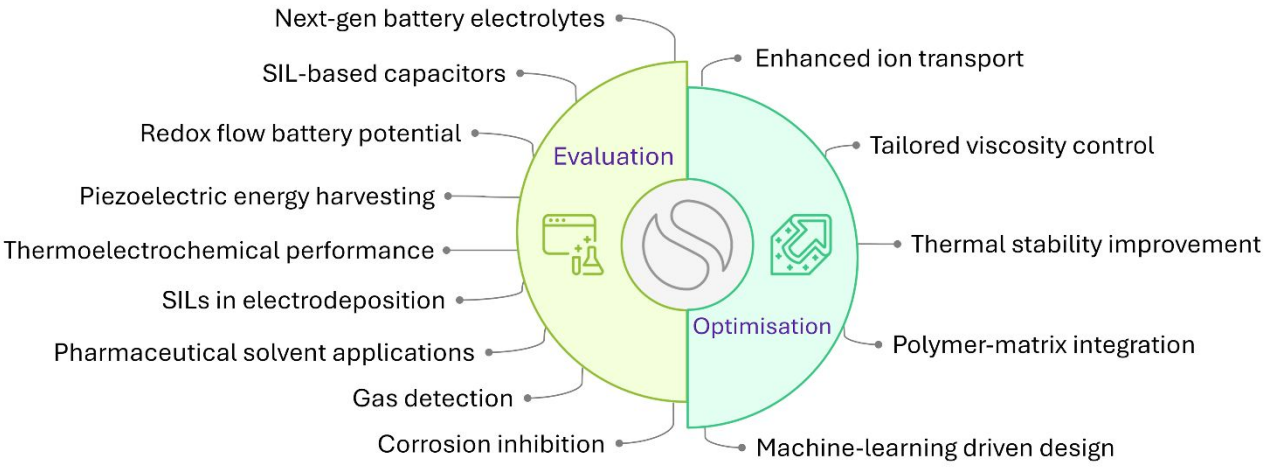

Figure 27 A graphical representation showcasing some of the promising yet underexplored future research directions in the field of SILs.

The versatility of SILs is further underscored by their application as sensors. Moreover, the application of SILs in thermoelectrochemistry for waste heat harvesting highlights their potential to contribute to sustainable energy solutions. The astonishing array of applications even extends to unconventional uses such as serving as invisible ink, showcasing the remarkable adaptability of SILs beyond traditional electrochemical domains. The multifunctionality and promising attributes of SILs in various applications emphasise their role as key players in shaping the trajectory of future research endeavours in both electrochemistry and beyond.

Implications for Future Research

The modularity of SILs as a chemical system with three interchangeable components to modularly tune the SIL properties to specific applications shines through as the resonating theme in this review. Figure 27 graphically summarises future research directions within the field of SILs.

Future research in the field of solvate ionic liquids (SILs) must address several identified gaps, particularly in understanding the structural and dynamic properties of these systems. Notably, there is a need for comprehensive studies on the coordination dynamics of Li^+ ions at varying glyme-to-lithium ratios, as well as the impacts of different anionic counterparts on SIL properties. Questions surrounding the environmental sustainability of diffuse anions used in SILs also warrant further exploration, particularly regarding the potential integration of more benign alternatives.

Emerging trends indicate a growing interest in ligand modification, particularly with novel glyme derivatives like G4monoEthyl, which may offer superior electrochemical properties. Additionally, there is a shift toward using SILs in thermoelectrochemical applications, suggesting the need for research that examines their efficiency in waste heat harvesting and other sustainable energy solutions. As technological advancements continue to evolve, incorporating innovative methodologies, such as machine learning and advanced molecular simulations, could significantly enhance our understanding of SIL behaviour.

Methodological recommendations for future studies include the adoption of interdisciplinary approaches that combine computational modelling with experimental validation. This could involve collaborations between chemists, material scientists, and environmental researchers to holistically address the challenges associated with SILs.

The implications of this research extend to real-world applications, particularly in the fields of energy storage, pharmaceuticals, and green chemistry. Understanding the toxicity profiles of SILs and their safe handling can facilitate their broader adoption, while optimised formulations could lead to improved battery technologies. Long-term research agendas should focus on building collaborative networks across institutions to pool expertise and resources, fostering innovation in SIL development.

Theoretical implications of future studies could challenge existing frameworks by offering new insights into the interactions between metal centres and various anions, potentially reshaping our understanding of SIL chemistry. Furthermore, engaging with diverse perspectives, including environmental, health, and safety considerations, will enrich

the discourse surrounding SILs, ensuring that research is aligned with societal needs. By addressing these areas, future investigations can significantly advance the field, contributing to the development of more effective and sustainable SIL systems.

Author contributions

Timothy Harte: conceptualisation, formal analysis, investigation, data curation, visualisation, writing – original draft, writing – review & editing. Bhagya Dharmasiri: project administration, supervision, writing – review & editing. Žan Simon: visualisation. David J Hayne: writing – review & editing. Daniel J. Eyckens: visualisation & supervision. Luke C. Henderson: project administration, funding acquisition, supervision, resources, writing – review & editing.

Conflicts of interest

No conflicts of interest have been reported.

Data availability

Data is included in the attached electronic supplementary information.

Acknowledgements

The authors express their gratitude to Deakin University and the Office of Naval Research Global (N62909-22-1-2052) for their vital support of this research. The study was conducted at the facilities of the Deakin University Institute for Frontier Materials and Carbon Nexus. An Australian Government Research Training Program Scholarship contributed to this work. The first author sincerely expresses their gratitude to their editing team; Luke C. Henderson, Bhagya Dharmasiri, and David J. Hayne; for their invaluable guidance, meticulous editing, and insightful contributions in refining this manuscript. The first author extends their gratitude to Žan Simon for their dedication, time, and exceptional talent in creating most of the outstanding figures in this manuscript.

Notes and references

1. K. S. Egorova, E. G. Gordeev and V. P. Ananikov, *Chem. Rev.*, 2017, **117**, 7132-7189.
2. D. J. Eyckens, M. E. Champion, B. L. Fox, P. Yoganantharajah, Y. Gibert, T. Welton and L. C. Henderson, *Eur. J. Org. Chem.*, 2016, 913–917.
3. K. Matuszek, S. L. Piper, A. Brzęczek-Szafran, B. Roy, S. Saher, J. M. Pringle and D. R. MacFarlane, *Adv. Mater.*, 2024, 2313023.
4. M. Armand, F. Endres, D. R. MacFarlane, H. Ohno and B. Scrosati, *Nat. Mater.*, 2009, **8**, 621-629.
5. J. P. Hallett and T. Welton, *Chem. Rev.*, 2011, **111**, 3508-3576.
6. H. Olivier-Bourbigou, L. Magna and D. Morvan, *Appl. Catal.*, 2010, **373**, 1-56.
7. N. V. Plechkova and K. R. Seddon, *Chem. Soc. Rev.*, 2008, **37**, 123-150.
8. H. Weingärtner, *Angew. Chem. Int. Ed. Engl.*, 2008, **47**, 654-670.
9. Q. Zhang, S. Zhang and Y. Deng, *Green Chem.*, 2011, **13**, 2619-2637.
10. C. A. Angell, Y. Ansari and Z. Zhao, *Faraday Discuss.*, 2012, **154**, 9-27.
11. T. Mandai, K. Dokko and M. Watanabe, *Chem. Rec.*, 2019, **19**, 708-722.
12. T. Mandai, K. Yoshida, K. Ueno, K. Dokko and M. Watanabe, *Phys. Chem. Chem. Phys.*, 2014, **16**, 8761-8772.
13. R. Hayes, G. G. Warr and R. Atkin, *Chem. Rev.*, 2015, **115**, 6357-6426.
14. T. Tamura, K. Yoshida, T. Hachida, M. Tsuchiya, M. Nakamura, Y. Kazue, N. Tachikawa, K. Dokko and M. Watanabe, *Chem. Lett.*, 2010, **39**, 753-755.
15. K. Yoshida, M. Tsuchiya, N. Tachikawa, K. Dokko and M. Watanabe, *J. Phys. Chem. C*, 2011, **115**, 18384-18394.
16. E. W. Castner Jr, J. F. Wishart and H. Shirota, *Acc. Chem. Res.*, 2007, **40**, 1217-1227.
17. T. Welton, *Biophys. Rev.*, 2018, **10**, 691-706.
18. T. Kawazoe, K. Hashimoto, Y. Kitazawa, H. Kokubo and M. Watanabe, *Electrochim. Acta*, 2017, **235**, 287-294.
19. R. Kido, K. Ueno, K. Iwata, Y. Kitazawa, S. Imaizumi, T. Mandai, K. Dokko and M. Watanabe, *Electrochim. Acta*, 2015, **175**, 5-12.
20. T. Nakazawa, A. Ikoma, R. Kido, K. Ueno, K. Dokko and M. Watanabe, *J. Power Sources*, 2016, **307**, 746-752.
21. K. Ueno, J.-W. Park, A. Yamazaki, T. Mandai, N. Tachikawa, K. Dokko and M. Watanabe, *J. Phys. Chem. C*, 2013, **117**, 20509-20516.
22. B. Dharmasiri, F. Stojcevski, K. A. S. Usman, S. A. Qin, J. M. Razal, E. H. Doeven, P. S. Francis, T. U. Connell, Y. Yin and G. G. Andersson, *Chem. Eng. J.*, 2023, **455**, 140778.
23. T. Harte, B. Dharmasiri, P. Coia, D. J. Eyckens and L. C. Henderson, *J. Mol. Liq.*, 2024, 124689.
24. D. J. Eyckens and L. C. Henderson, *RSC Adv.*, 2017, **7**, 27900-27904.
25. D. J. Eyckens, L. Servinis, C. Scheffler, E. Wölfel, B. Demir, T. R. Walsh and L. C. Henderson, *J. Mater. Chem. A*, 2018, **6**, 4504-4514.
26. Ž. Simon, B. Dharmasiri, T. Harte, P. C. Sherrell and L. C. Henderson, *Materials Horizons*, 2024.
27. K. Xu, *Chem. Rev.*, 2004, **104**, 4303-4418.
28. T. Mandai, K. Yoshida, S. Tsuzuki, R. Nozawa, H. Masu, K. Ueno, K. Dokko and M. Watanabe, *J. Phys. Chem. B*, 2015, **119**, 1523-1534.
29. T. Mandai, R. Nozawa, S. Tsuzuki, K. Yoshida, K. Ueno, K. Dokko and M. Watanabe, *J. Phys. Chem. B*, 2013, **117**, 15072-15085.
30. S. Terada, T. Mandai, R. Nozawa, K. Yoshida, K. Ueno, S. Tsuzuki, K. Dokko and M. Watanabe, *Phys. Chem. Chem. Phys.*, 2014, **16**, 11737-11746.
31. S. Terada, H. Susa, S. Tsuzuki, T. Mandai, K. Ueno, Y. Umebayashi, K. Dokko and M. Watanabe, *J. Phys. Chem. C*, 2016, **120**, 23339-23350.
32. S. Terada, H. Susa, S. Tsuzuki, T. Mandai, K. Ueno, K. Dokko and M. Watanabe, *J. Phys. Chem. C*, 2018, **122**, 16589-16599.

33. T. Mandai, S. Tsuzuki, K. Ueno, K. Dokko and M. Watanabe, *Phys. Chem. Chem. Phys.*, 2015, **17**, 2838-2849.
34. S. Tsuzuki, T. Mandai, S. Suzuki, W. Shinoda, T. Nakamura, T. Morishita, K. Ueno, S. Seki, Y. Umebayashi and K. Dokko, *Phys. Chem. Chem. Phys.*, 2017, **19**, 18262-18272.
35. K. Hashimoto, S. Suzuki, M. L. Thomas, T. Mandai, S. Tsuzuki, K. Dokko and M. Watanabe, *Phys. Chem. Chem. Phys.*, 2018, **20**, 7998-8007.
36. O. Kazarina, V. Agieienko, R. Nagrimanov, M. Atlaskina, A. Petukhov, A. Moskvichev, A. Nyuchev, A. Barykin and I. Vorotyntsev, *J. Mol. Liq.*, 2021, **344**, 117925.
37. M. Watanabe, K. Dokko, K. Ueno and M. L. Thomas, *Bull. Chem. Soc. Jpn.*, 2018, **91**, 1660-1682.
38. D. J. Eyckens and L. C. Henderson, *Front. Chem.*, 2019, **7**, 263.
39. T. Tamura, T. Hachida, K. Yoshida, N. Tachikawa, K. Dokko and M. Watanabe, *J. Power Sources*, 2010, **195**, 6095-6100.
40. K. Ueno, K. Yoshida, M. Tsuchiya, N. Tachikawa, K. Dokko and M. Watanabe, *J. Phys. Chem. B*, 2012, **116**, 11323-11331.
41. N. Hameed, D. J. Eyckens, B. M. Long, N. V. Salim, J. C. Capricho, L. Servinis, M. De Souza, M. D. Perus, R. J. Varley and L. C. Henderson, *ACS Appl. Polym. Mater.*, 2020, **2**, 2651-2657.
42. J. Więcławik, A. Brzęczek-Szafran, S. Jurczyk, K. Matuszek, M. Swadźba-Kwaśny and A. Chrobok, *Dalton Trans.*, 2024, **53**, 19143-19152.
43. M. K. Stanfield, F. Stojcevski, A. Hendlmeier, R. J. Varley, J. Carrascal, A. F. Osorio, D. J. Eyckens and L. C. Henderson, *Aust. J. Chem.*, 2018, **72**, 226-232.
44. M. K. Stanfield, J. Carrascal, L. C. Henderson and D. J. Eyckens, *J. Mater.*, 2021, **14**, 3230.
45. B. Dharmasiri, K. A. S. Usman, S. A. Qin, J. M. Razal, N. T. Tran, P. Coia, T. Harte and L. C. Henderson, *Chem. Eng. J.*, 2023, **476**, 146739.
46. P. Yoganantharajah, A. P. Ray, D. J. Eyckens, L. C. Henderson and Y. Gibert, *BMC Biotechnol.*, 2018, **18**, 1-7.
47. R. G. Grim, Z. Huang, M. T. Guarnieri, J. R. Ferrell, L. Tao and J. A. Schaidle, *Energy Environ. Sci.*, 2020, **13**, 472-494.
48. S. I. Wong, H. Lin, J. Sunarso, B. T. Wong and B. Jia, *Appl. Mater.*, 2020, **18**, 100522.
49. H. Sun, G. Zhu, Y. Zhu, M. C. Lin, H. Chen, Y. Y. Li, W. H. Hung, B. Zhou, X. Wang and Y. Bai, *Adv. Mater.*, 2020, **32**, 2001741.
50. K. Chatterjee, A. D. Pathak, A. Lakma, C. S. Sharma, K. K. Sahu and A. K. Singh, *Sci. Rep.*, 2020, **10**, 9606.
51. M. Watanabe, in *Functional Macromolecular Complexes*, eds. Y. Kimihisa and N. Hiroshi, 2024, vol. 1, ch. Chapter 14: Glyme-based Solvate Ionic Liquids and Their Electrolyte Properties.
52. X. Gao, W. Yuan, Y. Yang, Y. Wu, C. Wang, X. Wu, X. Zhang, Y. Yuan, Y. Tang and Y. Chen, *ACS Appl. Mater. Interfaces*, 2022, **14**, 43397-43406.
53. S. Parveen, P. Sehrawat and S. Hashmi, *Mater. Today Commun.*, 2022, **31**, 103392.
54. H. Darjazi, M. Falco, F. Colò, L. Balducci, G. Piana, F. Bella, G. Meligrana, F. Nobili, G. A. Elia and C. Gerbaldi, *Adv. Mater.*, 2024, 2313572.
55. J. H. Shin, M. B. Yi, T. H. Lee and H. J. Kim, *Adv. Funct. Mater.*, 2022, **32**, 2207329.
56. X. Zhong, Z. Zheng, J. Xu, X. Xiao, C. Sun, M. Zhang, J. Ma, B. Xu, K. Yu and X. Zhang, *Adv. Mater.*, 2023, **35**, 2209980.
57. L. Wichmann, J. P. Brinkmann, M. Luo, Y. Yang, M. Winter, R. Schmuch, T. Placke and A. Gomez-Martin, *Batteries Supercaps*, 2022, **5**, e202200075.
58. S. Lu, J. Cai, W. Zheng, Z. Lai, B. Xie, Z. Ding and H. He, *J. Mater. Sci. Mater. Electron.*, 2022, **33**, 18621-18631.
59. T. Hirano, R. Kizu, J. Hashimoto, N. Munekane, Y. Miwa, M. Oshimura and K. Ute, *Polym. Chem.*, 2018, **9**, 1421-1429.
60. T. Hirano, T. Yuki, R. Kizu, R. Kamiike, M. Oshimura and K. Ute, *Polym. J.*, 2022, **246**, 124780.
61. A. Liu, M. Guo, Y. Liu, F. Liu, X. Hu and Z. Shi, *Electrochemistry (Tokyo)*, 2022, **90**, 027006-027006.
62. P. Kumari, S. Parveen and S. Hashmi, *ACS Appl. Energy Mater.*, 2023.
63. K. Dokko, N. Tachikawa, K. Yamauchi, M. Tsuchiya, A. Yamazaki, E. Takashima, J.-W. Park, K. Ueno, S. Seki and N. Serizawa, *J. Electrochem. Soc.*, 2013, **160**, A1304.
64. R. Tatara, N. Tachikawa, H.-M. Kwon, K. Ueno, K. Dokko and M. Watanabe, *Chem. Lett.*, 2013, **42**, 1053-1055.
65. Y. Kitazawa, K. Iwata, S. Imaizumi, H. Ahn, S. Y. Kim, K. Ueno, M. J. Park and M. Watanabe, *Macromol.*, 2014, **47**, 6009-6016.
66. H. Moon, R. Tatara, T. Mandai, K. Ueno, K. Yoshida, N. Tachikawa, T. Yasuda, K. Dokko and M. Watanabe, *J. Phys. Chem. C*, 2014, **118**, 20246-20256.
67. C. Zhang, A. Yamazaki, J. Murai, J.-W. Park, T. Mandai, K. Ueno, K. Dokko and M. Watanabe, *J. Phys. Chem. C*, 2014, **118**, 17362-17373.
68. K. Takechi, Y. Kato and Y. Hase, *Adv. Mater.*, 2015, **27**, 2501-2506.
69. D. Y. Oh, Y. J. Nam, K. H. Park, S. H. Jung, S. J. Cho, Y. K. Kim, Y. G. Lee, S. Y. Lee and Y. S. Jung, *Adv. Energy Mater.*, 2015, **5**, 1500865.
70. H. Wang, S. Sunahiro, M. Matsui, P. Zhang, Y. Takeda, O. Yamamoto and N. Imanishi, *ChemElectroChem*, 2015, **2**, 1144-1151.
71. Z. Chen, P. A. FitzGerald, G. G. Warr and R. Atkin, *Phys. Chem. Chem. Phys.*, 2015, **17**, 14872-14878.
72. K. Ikeda, S. Terada, T. Mandai, K. Ueno, K. Dokko and M. Watanabe, *Electrochemistry (Tokyo)*, 2015, **83**, 914-917.
73. N. Tachikawa, R. Furuya, K. Yoshii, M. Watanabe and Y. Katayama, *Electrochemistry (Tokyo)*, 2015, **83**, 846-848.
74. S. Saito, H. Watanabe, K. Ueno, T. Mandai, S. Seki, S. Tsuzuki, Y. Kameda, K. Dokko, M. Watanabe and Y. Umebayashi, *J. Phys. Chem. B*, 2016, **120**, 3378-3387.
75. Z. Li, S. Zhang, S. Terada, X. Ma, K. Ikeda, Y. Kamei, C. Zhang, K. Dokko and M. Watanabe, *ACS Appl. Mater. Interfaces*, 2016, **8**, 16053-16062.
76. Z. Li, Y. Kamei, M. Haruta, T. Takenaka, A. Tomita, T. Doi, S. Zhang, K. Dokko, M. Inaba and M. Watanabe, *Electrochemistry (Tokyo)*, 2016, **84**, 887-890.
77. H. Lu, Y. Yuan, Z. Hou, Y. Lai, K. Zhang and Y. Liu, *RSC Adv.*, 2016, **6**, 18186-18190.
78. J. J. Black, T. Murphy, R. Atkin, A. Dolan and L. Aldous, *Phys. Chem. Chem. Phys.*, 2016, **18**, 20768-20777.
79. S. Zhang, A. Ikoma, Z. Li, K. Ueno, X. Ma, K. Dokko and M. Watanabe, *ACS Appl. Mater. Interfaces*, 2016, **8**, 27803-27813.
80. Z. Chen, S. McDonald, P. A. Fitzgerald, G. G. Warr and R. Atkin, *Phys. Chem. Chem. Phys.*, 2016, **18**, 14894-14903.
81. S. Seki, N. Serizawa, K. Takei, S. Tsuzuki, Y. Umebayashi, Y. Katayama, T. Miura, K. Dokko and M. Watanabe, *RSC Adv.*, 2016, **6**, 33043-33047.

82. A. Ando, A. Ikoma, K. Obata, Y. Kamei, K. Dokko and M. Watanabe, 2016.
83. M. Sugiyama, N. Tachikawa, K. Yoshii and Y. Katayama, 2016.
84. H.-M. Kwon, M. L. Thomas, R. Tatara, Y. Oda, Y. Kobayashi, A. Nakanishi, K. Ueno, K. Dokko and M. Watanabe, *ACS Appl. Mater. Interfaces*, 2017, **9**, 6014-6021.
85. A. Obregón-Zúñiga, M. Milán and E. Juaristi, *Org. Lett.*, 2017, **19**, 1108-1111.
86. S. Seki, N. Serizawa, K. Takei, Y. Umebayashi, S. Tsuzuki and M. Watanabe, *Electrochemistry (Tokyo)*, 2017, **85**, 680-682.
87. Y. Wang, M. C. Turk, M. Sankarasubramanian, A. Srivatsa, D. Roy and S. Krishnan, *J. Mater. Sci.*, 2017, **52**, 3719-3740.
88. H.-Y. Li and Y.-H. Chu, *Anal. Chem.*, 2017, **89**, 5186-5192.
89. N. Tachikawa, R. Kasai, K. Yoshii, M. Watanabe and Y. Katayama, *Electrochemistry (Tokyo)*, 2017, **85**, 667-670.
90. Y. Kitazawa, K. Iwata, R. Kido, S. Imaizumi, S. Tsuzuki, W. Shinoda, K. Ueno, T. Mandai, H. Kokubo and K. Dokko, *Chem. Mater.*, 2018, **30**, 252-261.
91. D. Dong, F. Sälzer, B. Roling and D. Bedrov, *Phys. Chem. Chem. Phys.*, 2018, **20**, 29174-29183.
92. Z. Yu, C. Fang, J. Huang, B. G. Sumpter and R. Qiao, *ACS Appl. Mater. Interfaces*, 2018, **10**, 32151-32161.
93. B. Zhang, Z. Shi, L. Shen, A. Liu, J. Xu and X. Hu, *J. Electrochem. Soc.*, 2018, **165**, D321.
94. B. Zhang, Y. Yao, Z. Shi, J. Xu and Z. Wang, *ChemElectroChem*, 2018, **5**, 3368-3372.
95. M. Haruta, T. Moriyasu, A. Tomita, T. Takenaka, T. Doi and M. Inaba, *J. Electrochem. Soc.*, 2018, **165**, A1874.
96. K. Hashimoto, Y. Kobayashi, H. Kokubo, T. Ueki, K. Ohara, K. Fujii and M. Watanabe, *J. Phys. Chem. B*, 2019, **123**, 4098-4107.
97. A. J. D'Angelo and M. J. Panzer, *Chem. Mater.*, 2019, **31**, 2913-2922.
98. S. Chereddy, J. Aguirre, D. Dikin, S. L. Wunder and P. R. Chinnam, *ACS Appl. Energy Mater.*, 2019, **3**, 279-289.
99. K. S. S. McHale, M. J. Wong, A. K. Evans, A. Gilbert, R. S. Haines and J. B. Harper, *Org. Biomol. Chem.*, 2019, **17**, 9243-9250.
100. Y. Matsumae, K. Obata, A. Ando, M. Yanagi, Y. Kamei, K. Ueno, K. Dokko and M. Watanabe, *Electrochemistry (Tokyo)*, 2019, **87**, 254-259.
101. B. Zhang, Z. Shi, L. Shen, X. Liu, J. Xu and Z. Wang, *J. Solid State Electrochem.*, 2019, **23**, 1903-1909.
102. S. Di Pietro, V. Bordoni, A. Mezzetta, C. Chiappe, G. Signore, L. Guazzelli and V. Di Bussolo, *Molecules*, 2019, **24**, 2946.
103. N. Togasaki, T. Naruse, T. Momma and T. Osaka, *J. Electrochem. Soc.*, 2019, **166**, A3391.
104. Y. Cao, S. Lou, Z. Sun, W. Tang, Y. Ma, P. Zuo, J. Wang, C. Du, Y. Gao and G. Yin, *Chem. Eng. J.*, 2020, **382**, 123046.
105. H. Shobukawa, K. Shigenobu, S. Terada, S. Kondou, K. Ueno, K. Dokko and M. Watanabe, *Electrochim. Acta*, 2020, **353**, 136559.
106. J. Kawaji, A. Unemoto, T. Hirano, D. Takamatsu, E. Seki, M. Morishima and T. Okumura, *J. Electrochem. Soc.*, 2020, **167**, 140525.
107. P. Geysens, J. Fransaer and K. Binnemans, *RSC Adv.*, 2020, **10**, 42021-42029.
108. N. Serizawa, K. Kitta, N. Tachikawa and Y. Katayama, *J. Electrochem. Soc.*, 2020, **167**, 110560.
109. A.-m. Liu, M.-x. Guo, Z.-y. LÜ, B.-g. Zhang, F.-g. Liu, W.-j. Tao, Y.-j. Yang, X.-w. Hu, Z.-w. Wang and Y.-b. Liu, *T. NONFERR. METAL SOC.*, 2020, **30**, 2283-2292.
110. Y. Kemmizaki, Y. Katayama, H. Tsutsumi and K. Ueno, *RSC Adv.*, 2020, **10**, 4129-4136.
111. T. Mori, N. Tsuchida, A. Kitada, K. Fukami and K. Murase, 2020.
112. A. Unemoto, M. Hirooka, E. Seki, J. Kawaji and T. Okumura, *Electrochemistry (Tokyo)*, 2020, **88**, 321-324.
113. S. Saito, R. Tamate, K. Miwa, S. Shimizu, T. Horii, K. Ueno, S. Ono and M. Watanabe, *Jpn. J. Appl. Phys.*, 2020, **59**, 030901.
114. M. S. Grewal, K. Kisu, S.-i. Orimo and H. Yabu, *Chem. Lett.*, 2020, **49**, 1465-1469.
115. W. Zhang, S. Feng, M. Huang, B. Qiao, K. Shigenobu, L. Giordano, J. Lopez, R. Tatara, K. Ueno and K. Dokko, *Chem. Mater.*, 2021, **33**, 524-534.
116. X. Zhang, A. Liu, F. Liu, Z. Shi, B. Zhang and X. Wang, *Electrochem. Commun.*, 2021, **133**, 107160.
117. B. Zhang, L. Wang, K. Pan, W. Zhang, Y. Liu, Y. Zhang, L. Zhang and Z. Shi, *J. Phys. Chem. C*, 2021, **125**, 20798-20805.
118. K. Motobayashi, K. Matsumoto, S. Tsuzuki and K. Ikeda, *ELSA*, 2022, **2**, e2100150.
119. Y. Xu, X. Jiang, Z. Liu, Z. Chen, S. Zhang and Y. Zhang, *J. Power Sources*, 2022, **546**, 231952.
120. M. Haruta, H. Konaga, T. Doi and M. Inaba, *J. Electrochem. Soc.*, 2022, **169**, 020519.
121. W. Lei, C. Zhang, R. Qiao, M. Ravivarma, H. Chen, F. B. Ajdari, M. Salavati-Niasari and J. Song, *ACS Appl. Energy Mater.*, 2023, **6**, 4363-4371.
122. H. Watanabe, Y. Sugiura, S. Seki, J. Han, I. Shitanda, M. Itagaki and Y. Umebayashi, *J. Phys. Chem. C*, 2023, **127**, 6645-6654.
123. J. Yi, C. Yan, D. Zhou and L.-Z. Fan, *Nano Res.*, 2023, **16**, 8411-8416.
124. G. Kamesui, K. Nishikawa, M. Ueda and H. Matsushima, *Electrochem. Commun.*, 2023, **151**, 107506.
125. D. Y. Oh, Y. J. Nam, K. H. Park, S. H. Jung, K. T. Kim, A. R. Ha and Y. S. Jung, *Adv. Energy Mater.*, 2019, **9**, 1802927.
126. A. Adamson, K. Tuul, T. Bötticher, S. Azam, M. D. Garayt and M. Metzger, *Nat. Mater.*, 2023, **22**, 1380-1386.
127. S. Stuckenberg, M. M. Bela, C. T. Lechtenfeld, M. Mense, V. Küpers, T. T. K. Ingber, M. Winter and M. C. Stan, *Small*, 2024, **20**, 2305203.
128. T. A. Yersak, Y. Zhang, H. Hafiz, N. P. Pieczonka, H. J. G. Malabet, H. Cunningham and M. Cai, *J. Electrochem. Soc.*, 2024, **171**, 070529.
129. H. Watanabe, Y. Sugiura, I. Shitanda and M. Itagaki, 2024.
130. E. V. Kuzmina, A. R. Yusupova, E. V. Karaseva, X. Chen, Q. Zhang and V. S. Kolosnitsyn, *J. Phys. Chem. B*, 2024, **128**, 7833-7847.
131. S. Oho, Y. SHIMBORI and K. Kanamura, *Electrochemistry (Tokyo)*, 2024, **92**, 017001-017001.
132. Y. Zhen, Z. Qin, Z. Jia, H. Geng, Y. Feng, Z. Yang, X. Jiang, W. Yang, Y. Qie and Q. Xue, *J. Mater. Sci. Eng., B*, 2024, **301**, 117105.
133. G. Lingua, G. Depraetère, J. Wang, J. E. Bara, M. Forsyth and D. Mecerreyes, *J. Power Sources*, 2024, DOI: https://doi.org/10.1016/j.jpowsour.2024.235535.
134. Y. Matsuda, K. Tanaka, M. Okada, Y. Takasu, M. Morita and T. Matsumura-Inoue, *J. Appl. Electrochem.*, 1988, **18**, 909-914.

135. Y. Katayama, M. Yoshihara and T. Miura, *J. Electrochem. Soc.*, 2015, **162**, H501.
136. F. R. Brushett, J. T. Vaughey and A. N. Jansen, *Adv. Energy Mater.*, 2012, **2**, 1390-1396.
137. C. Sun, J. Liu, Y. Gong, D. P. Wilkinson and J. Zhang, *Nano Energy*, 2017, **33**, 363-386.
138. D. Lee and A. Manthiram, *J. Mater. Chem. A*, 2024, **12**, 3323-3330.
139. Z. Wei, S. Zhu, X. Zhu, L. Yu, Z. Jiang, X. Tang, X. Qu, Y. Wang, H. Tang and X. Liu, *Energy & Fuels*, 2024, **38**, 8296-8305.
140. C. luo, G. Zhao, M. Zhang, B. Wu, Y. Sun and Q. Hua, *SSRN (Elsevier)*, 2024, DOI: http://dx.doi.org/10.2139/ssrn.4719385.
141. X.-T. Yin, W.-W. Wang, Z. Tan, Y. Ding, B.-W. Mao and J.-W. Yan, *Curr. Opin. Electrochem.*, 2024, 101563.
142. J. Anurangi, M. Herath, D. T. Galhena and J. Epaarachchi, *Adv. Compos. Mater.*, 2023, 1-45.
143. H. D. Asfaw, A. Kucernak, E. S. Greenhalgh and M. S. Shaffer, *Compos. Sci. Technol.*, 2023, **238**, 110042.
144. T. Carlson, D. Ordéus, M. Wysocki and L. E. Asp, *Compos. Sci. Technol.*, 2010, **70**, 1135-1140.
145. E. S. Greenhalgh, S. Nguyen, M. Valkova, N. Shirshova, M. S. Shaffer and A. Kucernak, *Compos. Sci. Technol.*, 2023, DOI: https://doi.org/10.1016/j.compscitech.2023.109968, 109968.
146. X.-T. Yin, E.-M. You, R.-Y. Zhou, L.-H. Zhu, W.-W. Wang, K.-X. Li, D.-Y. Wu, Y. Gu, J.-F. Li and B.-W. Mao, *Nat. Commun.*, 2024, **15**, 5624.
147. H. Du, X. Lin, Z. Xu and D. Chu, *J. Mater. Sci.*, 2015, **50**, 5641-5673.
148. Y. He, Y. Yang, S. Nie, R. Liu and Q. Wan, *J. Mater. Chem. C*, 2018, **6**, 5336-5352.
149. M. I. Hossain and G. J. Blanchard, *J. Phys. Chem. Lett.*, 2023, **14**, 2731-2735.
150. M. I. Hossain, H. Wang, L. Adhikari, G. A. Baker, A. Mezzetta, L. Guazzelli, P. Mussini, W. Xie and G. J. Blanchard, *J. Phys. Chem. B*, 2024, **128**, 1495-1505.
151. R. AliAkbari, Y. Marfavi, E. Kowsari and S. Ramakrishna, *Mater. Circ. Econ.*, 2020, **2**, 1-27.
152. G. Vanhoutte, N. R. Brooks, S. Schaltin, B. Opperdoes, L. Van Meervelt, J.-P. Locquet, P. M. Vereecken, J. Fransaer and K. Binnemans, *J. Phys. Chem. C*, 2014, **118**, 20152-20162.
153. A. Miki, K. Nishikawa, G. Kamesui, H. Matsushima, M. Ueda and M. Rosso, *J. Mater. Chem. A*, 2021, **9**, 14700-14709.
154. R. Tatara, K. Ikeda, K. Ueno, M. Watanabe and K. Dokko, *J. Solid State Electrochem.*, 2024, 1-7.
155. C. Andrew and J. Mani, *Pure Appl. Chem.*, 2024.
156. G. Kamesui, K. Nishikawa, M. Ueda and H. Matsushima, *J. Electrochem. Soc.*, 2024, **171**, 100507.
157. X. Zhang, S. Li, J. Yuan and Z. Shi, *J. Electroanal. Chem.*, 2024, **957**, 118131.
158. G. Gamboa-Velázquez, I. J. Arroyo-Córdoba, C. G. Ávila-Ortiz, C. Naranjo-Castañeda and E. Juaristi, *Eur. J. Org. Chem.*, 2024, **27**, e202400167.
159. D. J. Eyckens, B. Demir, T. R. Walsh, T. Welton and L. C. Henderson, *Phys. Chem. Chem. Phys.*, 2016, **18**, 13153-13157.
160. C. Reichardt, *Green Chem.*, 2005, **7**, 339-351.
161. L. Crowhurst, R. Falcone, N. L. Lancaster, V. Llopis-Mestre and T. Welton, *J. Org. Chem.*, 2006, **71**, 8847-8853.
162. T. Ur-Rehman, S. Tavelin and G. Gröbner, *Int. J. Pharm.*, 2010, **394**, 92-98.
163. P. Yoganantharajah, D. J. Eyckens, J. L. Pedrina, L. C. Henderson and Y. Gibert, *New J. Chem.*, 2016, **40**, 6599-6603.
164. K. Takahashi, Y. Ishino, W. Murata, Y. Umebayashi, S. Tsuzuki, M. Watanabe, H. Takaba and S. Seki, *RSC Adv.*, 2019, **9**, 24922-24927.
165. T. Sudoh, K. Shigenobu, K. Dokko, M. Watanabe and K. Ueno, *Phys. Chem. Chem. Phys.*, 2022, **24**, 14269-14276.
166. K. Ueno, J. Murai, H. Moon, K. Dokko and M. Watanabe, *J. Electrochem. Soc.*, 2016, **164**, A6088.
167. H. K. Bergstrom and B. D. McCloskey, *ACS Energy Lett.*, 2024, **9**, 373-380.
168. S. L. Piper, C. M. Forsyth, M. Kar, C. Gassner, R. Vijayaraghavan, S. Mahadevan, K. Matuszek, J. M. Pringle and D. R. MacFarlane, *RSC Sustain.*, 2023, **1**, 470-480.
169. X. Cheng, J. Pan, Y. Zhao, M. Liao and H. Peng, *Adv. Energy Mater.*, 2018, **8**, 1702184.
170. J. Le Bideau, L. Viau and A. Vioux, *Chem. Soc. Rev.*, 2011, **40**, 907-925.
171. X. Zhong, J. Tang, L. Cao, W. Kong, Z. Sun, H. Cheng, Z. Lu, H. Pan and B. Xu, *Electrochim. Acta*, 2017, **244**, 112-118.
172. Y. Maeyoshi, in *Interface Ionics: For All-Solid-State Batteries and Solid State Ionics Devices*, eds. I. Yasutoshi, A. Koji, T. Yoshitaka and Y. Naoaki, Springer, 1 edn., 2024, DOI: https://doi.org/10.1007/978-981-97-6039-8, pp. 117-125.
173. S. S. More, R. B. Kale, P. J. Ambekar, N. D. Khupse, R. S. Kalubarme, M. V. Kulkarni and B. B. Kale, *ACS Appl. Polym. Mater.*, 2024, **6**, 11953-11963.
174. Y. Yuan, Y. Kong, X. Peng, L. Zhang, Z. Li and H. Lu, *Sustainable Energy & Fuels*, 2025, DOI: 10.1039/D4SE01381F.
175. Y. Dong, X. Qi, M. Tanaka and H. Kawakami, *Electrochim. Acta*, 2025, 145661.
176. S. Parveen, A. Kumar and S. Hashmi, *ACS Appl. Energy Mater.*, 2024, **7**, 10441-10453.
177. J. Zhang, J. Zhu, R. Zhao, J. Liu, X. Song, N. Xu, Y. Liu, H. Zhang, X. Wan and Y. Ma, *Energy Environ. Sci.*, 2024, **17**, 7119-7128.
178. D. Lee, M. Yang, U. H. Choi and J. Kim, *Small*, 2024, DOI: https://doi.org/10.1002/smll.202308821, 2308821.
179. R. Liu, L. Jin, D. Lu, G. Hu, L. He and J. Shan, *Electrochim. Acta*, 2013, **114**, 372-378.
180. N. Shirshova, A. Bismarck, S. Carreyette, Q. P. Fontana, E. S. Greenhalgh, P. Jacobsson, P. Johansson, M. J. Marczewski, G. Kalinka and A. R. Kucernak, *J. Mater. Chem. A*, 2013, **1**, 15300-15309.
181. B. Dharmasiri, *Mater. Horizons*, 2024, **11**, 4237-4238.
182. T. Harte, B. Dharmasiri, D. J. Eyckens and L. C. Henderson, *ACS Sustain. Chem. Eng.*, 2024.
183. T. Harte, B. Dharmasiri, G. S. DOBHAL, T. R. Walsh and L. C. Henderson, *Phys. Chem. Chem. Phys.*, 2023, **25**, 29614-29623.
184. X. Wang, Y. Chi and T. Mu, *J. Mol. Liq.*, 2014, **193**, 262-266.
185. S. Zhang, N. Sun, X. He, X. Lu and X. Zhang, *J. Phys. Chem. Ref. Data*, 2006, **35**, 1475-1517.
186. D. Rooney, J. Jacquemin and R. Gardas, *J. Ion. Liq.*, 2010, 185-212.
187. J. O. Valderrama and R. E. Rojas, *Eng. Chem. Res.*, 2009, **48**, 6890-6900.

188. S. M. Murray, R. A. O'Brien, K. M. Mattson, C. Ceccarelli, R. E. Sykora, K. N. West and J. H. Davis Jr, *Angew. Chem. Int. Ed. Engl.*, 2010, **49**, 2755-2758.
189. T. Mandai, A. Matsumura, M. Imanari and K. Nishikawa, *J. Phys. Chem. B*, 2012, **116**, 2090-2095.
190. R. A. Patil, M. Talebi, C. Xu, S. S. Bhawal and D. W. Armstrong, *Chem. Mater.*, 2016, **28**, 4315-4323.
191. H. Matsumoto, H. Kageyama and Y. Miyazaki, *Chem. Lett.*, 2001, **30**, 182-183.
192. H. Tokuda, K. Hayamizu, K. Ishii, M. A. B. H. Susan and M. Watanabe, *J. Phys. Chem. B*, 2005, **109**, 6103-6110.
193. H. Matsumoto, H. Sakaebe and K. Tatsumi, *J. Power Sources*, 2005, **146**, 45-50.
194. S. Tang and H. Zhao, *RSC Adv.*, 2014, **4**, 11251-11287.
195. B. McLean, H. Li, R. Stefanovic, R. J. Wood, G. B. Webber, K. Ueno, M. Watanabe, G. G. Warr, A. Page and R. Atkin, *Phys. Chem. Chem. Phys.*, 2015, **17**, 325-333.
196. K. Shimizu, A. A. Freitas, R. Atkin, G. G. Warr, P. A. FitzGerald, H. Doi, S. Saito, K. Ueno, Y. Umebayashi and M. Watanabe, *Phys. Chem. Chem. Phys.*, 2015, **17**, 22321-22335.
197. L. Aguilera, S. Xiong, J. Scheers and A. Matic, *J. Mol. Liq.*, 2015, **210**, 238-242.
198. K. Ueno, R. Tatara, S. Tsuzuki, S. Saito, H. Doi, K. Yoshida, T. Mandai, M. Matsugami, Y. Umebayashi and K. Dokko, *Phys. Chem. Chem. Phys.*, 2015, **17**, 8248-8257.
199. S. Saito, H. Watanabe, Y. Hayashi, M. Matsugami, S. Tsuzuki, S. Seki, J. N. Canongia Lopes, R. Atkin, K. Ueno and K. Dokko, *J. Phys. Chem. Lett.*, 2016, **7**, 2832-2837.
200. D. A. Dolan, D. A. Sherman, R. Atkin and G. G. Warr, *ChemPhysChem*, 2016, **17**, 3096-3101.
201. A. Cook, K. Ueno, M. Watanabe, R. Atkin and H. Li, *J. Phys. Chem. C*, 2017, **121**, 15728-15734.
202. Z. Chen, Y. Tonouchi, K. Matsumoto, M. Saimura, R. Atkin, T. Nagata, M. Katahira and R. Hagiwara, *J. Phys. Chem. Lett.*, 2018, **9**, 6662-6667.
203. A. Kitada, S. Takeoka, K. Kintsu, K. Fukami, M. Saimura, T. Nagata, M. Katahira and K. Murase, *J. Electrochem. Soc.*, 2018, **165**, H121.
204. A. Kitada, K. Kintsu, S. Takeoka, K. Fukami, M. Saimura, T. Nagata, M. Katahira and K. Murase, *J. Electrochem. Soc.*, 2018, **165**, H496.
205. K. Kawata, A. Kitada, N. Tsuchida, M. Saimura, T. Nagata, M. Katahira, K. Fukami and K. Murase, *J. Electrochem. Soc.*, 2020, **167**, 046508.
206. Y. Kemmizaki, H. Tsutsumi and K. Ueno, *Electrochemistry (Tokyo)*, 2018, **86**, 46-51.
207. H. Li, M. W. Rutland, M. Watanabe and R. Atkin, *Faraday Discuss.*, 2017, **199**, 311-322.
208. M. Huang, S. Feng, W. Zhang, J. Lopez, B. Qiao, R. Tatara, L. Giordano, Y. Shao-Horn and J. A. Johnson, *Chem. Mater.*, 2019, **31**, 7558-7564.
209. T. Murphy, S. K. Callear, N. Yepuri, K. Shimizu, M. Watanabe, J. N. C. Lopes, T. Darwish, G. G. Warr and R. Atkin, *Phys. Chem. Chem. Phys.*, 2016, **18**, 17224-17236.
210. S. W. Coles, M. Mishin, S. Perkin, M. V. Fedorov and V. B. Ivaništšev, *Phys. Chem. Chem. Phys.*, 2017, **19**, 11004-11010.
211. P. Jankowski, M. Dranka, W. Wieczorek and P. Johansson, *J. Phys. Chem. Lett.*, 2017, **8**, 3678-3682.
212. W. Shinoda, Y. Hatanaka, M. Hirakawa, S. Okazaki, S. Tsuzuki, K. Ueno and M. Watanabe, *J. Chem. Phys.*, 2018, **148**, 193809.
213. D. Dong and D. Bedrov, *J. Phys. Chem. B*, 2018, **122**, 9994-10004.
214. S. W. Coles and V. B. Ivaništšev, *J. Phys. Chem. C*, 2019, **123**, 3935-3943.
215. F. Schmidt and M. Schönhoff, *J. Phys. Chem. B*, 2020, **124**, 1245-1252.
216. M. Potangale and S. Tiwari, *J. Mol. Liq.*, 2020, **297**, 111882.
217. K. Kawata, A. Kitada, K. Fukami, M. Saimura, T. Nagata, M. Katahira and K. Murase, *J. Electrochem. Soc.*, 2021, **168**, 026515.
218. C. M. Burba, K. Feightner, M. Liu and A. Hawari, *ChemPhysChem*, 2022, **23**, e202100548.
219. S. Terada, T. Mandai, S. Suzuki, S. Tsuzuki, K. Watanabe, Y. Kamei, K. Ueno, K. Dokko and M. Watanabe, *J. Phys. Chem. C*, 2016, **120**, 1353-1365.
220. K. Dokko, S. Suzuki, S. Terada, K. Hashimoto, S. Tsuzuki, M. L. Thomas, T. Mandai and M. Watanabe, 2019.
221. N. N. Rajput, X. Qu, N. Sa, A. K. Burrell and K. A. Persson, *J. Am. Chem. Soc.*, 2015, **137**, 3411-3420.
222. C. Mönich, R. Andersson, G. Hernández, J. Mindemark and M. Schönhoff, *J. Am. Chem. Soc.*, 2024, **146**, 11105-11114.
223. R. F. Pereira, K. Zehbe, S. Krüger, M. M. Silva, A. Salama, P. Hesemann, V. de Zea Bermudez and A. Taubert, *Ionic liquids for the synthesis and design of hybrid biomaterials and interfaces*, 2018.
224. H. Tokuda, K. Hayamizu, K. Ishii, M. A. B. H. Susan and M. Watanabe, *J. Phys. Chem. B*, 2004, **108**, 16593-16600.
225. P. Bonhote, A.-P. Dias, N. Papageorgiou, K. Kalyanasundaram and M. Grätzel, *Inorg. Chem.*, 1996, **35**, 1168-1178.
226. Y. Kameda, Y. Umebayashi, M. Takeuchi, M. A. Wahab, S. Fukuda, S.-i. Ishiguro, M. Sasaki, Y. Amo and T. Usuki, *J. Phys. Chem. B*, 2007, **111**, 6104-6109.
227. W. A. Henderson, F. McKenna, M. A. Khan, N. R. Brooks, V. G. Young Jr and R. Frech, *Chem. Mater.*, 2005, **17**, 2284-2289.
228. C. S. Kim and S. M. Oh, *Electrochim. Acta*, 2000, **45**, 2101-2109.
229. I. A. Guzei, L. C. Spencer, J. W. Su and R. R. Burnette, *Acta. Crystallogr. B. Struct. Sci. Cryst. Eng. Mater.*, 2007, **63**, 93-100.
230. K. Izod, E. R. Clark, W. Clegg and R. W. Harrington, *Organometallics*, 2012, **31**, 246-255.
231. D. Brouillette, D. Irish and N. Taylor, *Phys. Chem. Chem. Phys*, 2002, **4**, 6063-6071.
232. K. Ueno, J. Murai, K. Ikeda, S. Tsuzuki, M. Tsuchiya, R. Tatara, T. Mandai, Y. Umebayashi, K. Dokko and M. Watanabe, *J. Phys. Chem. C*, 2016, **120**, 15792-15802.
233. K. Shigehara, A. Yamada, H. Sano and E. Tsuchida, *Macromol. Chem. Phys.*, 1980, **181**, 1823-1840.
234. C. B. Tsvetanov, E. Petrova, D. Dimov, I. Panayotov and J. Smid, *J. Solution Chem.*, 1990, **19**, 425-436.
235. M. M. Archuleta, *J. Power Sources*, 1995, **54**, 138-142.
236. K. Takada, Y. Yamada, E. Watanabe, J. Wang, K. Sodeyama, Y. Tateyama, K. Hirata, T. Kawase and A. Yamada, *ACS Appl. Mater. Interfaces*, 2017, **9**, 33802-33809.
237. H. Hirayama, N. Tachikawa, K. Yoshii, M. Watanabe and Y. Katayama, *Electrochemistry (Tokyo)*, 2015, **83**, 824-827.

238. C. Zhang, K. Ueno, A. Yamazaki, K. Yoshida, H. Moon, T. Mandai, Y. Umebayashi, K. Dokko and M. Watanabe, *J. Phys. Chem. B*, 2014, **118**, 5144-5153.
239. Y. Kobayashi, Y. Kitazawa, K. Hashimoto, T. Ueki, H. Kokubo and M. Watanabe, *Langmuir*, 2017, **33**, 14105-14114.
240. P. Geysens, V. S. Rangasamy, S. Thayumanasundaram, K. Robeyns, L. Van Meervelt, J.-P. Locquet, J. Fransaer and K. Binnemans, *J. Phys. Chem. B*, 2018, **122**, 275-289.
241. A. Kitada, Y. Koujin, M. Shimizu, K. Kawata, C. Yoshinaka, M. Saimura, T. Nagata, M. Katahira, K. Fukami and K. Murase, *J. Electrochem. Soc.*, 2021, **168**, 090521.
242. K. Kawata, A. Kitada, N. Tsuchida, M. Saimura, T. Nagata, M. Katahira, K. Fukami and K. Murase, *Phys. Chem. Chem. Phys.*, 2021, **23**, 449-456.
243. T. Harte, B. Dharmasiri, G. S. Dobhal, T. R. Walsh and L. C. Henderson, *Phys. Chem. Chem. Phys.*, 2025, **27**, 5932-5932.
244. E. O. Nachaki and D. G. Kuroda, *J. Phys. Chem. C*, 2024, **128**, 11522-11533.
245. Y. Umebayashi, E. Otani, H. Watanabe and J. Han, *Faraday Discuss.*, 2024.
246. G. Z. Żukowska, M. Piszcz, K. Gańko, M. Więckowski, M. Królikowski, M. Poterała and M. Dranka, *Mater. Chem. Phys.*, 2024, **315**, 128999.
247. W. Wang, T. Yang, W. H. Harris and R. Gómez-Bombarelli, *Chem. Commun.*, 2020, **56**, 8920-8923.
248. N. Arai, H. Watanabe, T. Yamaguchi, S. Seki, K. Ueno, K. Dokko, M. Watanabe, Y. Kameda, R. Buchner and Y. Umebayashi, *J. Phys. Chem. C*, 2019, **123**, 30228-30233.
249. J. J. Black, A. Dolan, J. B. Harper and L. Aldous, *Phys. Chem. Chem. Phys.*, 2018, **20**, 16558-16567.
250. S. Terada, K. Ikeda, K. Ueno, K. Dokko and M. Watanabe, *Aust. J. Chem.*, 2018, **72**, 70-80.
251. A. Thum, A. Heuer, K. Shimizu and J. N. C. Lopes, *Phys. Chem. Chem. Phys.*, 2020, **22**, 525-535.
252. Q. Xie and R. Tinker, *J. Chem. Educ.*, 2006, **83**, 77.
253. J. R. Gissinger, B. D. Jensen and K. E. Wise, *Polym. J.*, 2017, **128**, 211-217.
254. O. Carrillo-Bohórquez, D. G. Kuroda and R. Kumar, *J. Chem. Phys.*, 2024, **161**.
255. K. Shimizu, A. A. de Freitas, J. T. Allred and C. M. Burba, *Molecules*, 2024, **29**, 2071.
256. J. K. Philipp, K. Fumino, A. Appelhagen, D. Paschek and R. Ludwig, *ChemPhysChem*, 2025, e202400991.
257. C. Nicotri, *Masters Thesis JAGIELLONIAN UNIVERSITY*, 2024.
258. F. OZAWA, K. KOYAMA, D. IWASAKI, S. AZUMA, A. NOMURA and M. SAITO, *Electrochemistry*, 2024, **92**, 047003-047003.
259. Q. Han, S. Jiao, X. Liu, T. Bian and Y. Zhao, *J. Mater. Chem. A*, 2024, **12**, 14679-14687.
260. P. Coia, B. Dharmasiri, D. J. Hayne, T. Harte, S. Dann, B. Newman, E. Austria, B. Akhavan, M. A. N. Judicpa, K. P. Marquez, K. A. S. Usman, J. Zhang, J. Razal and L. C. Henderson, *J. Chem. Eng.*, 2025, 160502.

No primary research results, software or code have been included and no new data were generated or analysed as part of this review.